Universidade de Aveiro Departamento de Química
Ano 2020

Andreia Alexandra Farinha Lopes

Ensaio de quantificação da viabilidade do *Plasmodium falciparum*: uma abordagem mitocondrial

Plasmodium falciparum viability quantification assay: a mitochondrial approach

Universidade de Aveiro Departamento de Química
Ano 2020

ANDREIA ALEXANDRA FARINHA LOPES

Ensaio de quantificação da viabilidade do *Plasmodium falciparum*: uma abordagem mitocondrial

Plasmodium falciparum viability quantification assay: a mitochondrial approach

Tese apresentada à Universidade de Aveiro para cumprimento dos requisitos necessários à obtenção do grau de Mestre em Bioquímica, Especialização em Métodos Biomoleculares, realizada sob a orientação científica da Doutora Fátima Nogueira, Investigadora Auxiliar da Unidade de Ensino e Investigação de Parasitologia Médica do Instituto de Higiene e Medicina Tropical, Universidade Nova de Lisboa, da Doutora Catarina Almeida, Professora Auxiliar do Departamento de Ciências Médicas da Universidade de Aveiro, e da Doutora Rita Ferreira, Professora Auxiliar do Departamento de Química da Universidade de Aveiro.

Esta dissertação teve o apoio da UIE de Parasitologia Médica do IHMT, UNL.

This dissertation was supported by UEI of Medical Parasitology at IHMT, UNL

DESDE 1902
INSTITUTO DE HIGIENE E MEDICINA TROPICAL
UNIVERSIDADE NOVA DE LISBOA

UNIVERSIDADE NOVA DE LISBOA

Dedico este trabalho aos meus pais, por me darem as oportunidades que nunca tiveram.

o júri

Presidente

Prof. Doutor Mário Manuel Quialheiro Simões
Professor Auxiliar da Universidade de Aveiro

Doutora Susana Filipa Garcia Ramos
Investigadora Pós-Doc do Instituto Gulbenkian de Ciência

Doutora Maria de Fátima Carvalho Nogueira
Investigadora Auxiliar do Instituo de Higiene e Medicina Tropical – Universidade Nova de Lisboa

agradecimentos

Às minhas orientadoras, Professora Doutora Fátima Nogueira, Professora Doutora Catarina Almeida e Professora Doutora Rita Ferreira, agradeço a orientação científica que me proporcionaram, pela disponibilidade que me prestaram e a confiança que depositaram em mim. Em especial, à Professora Doutora Fátima Nogueira por me ter recebido no seu laboratório com tanta prontidão, por todos os conhecimentos que me transmitiu, por todas as aprendizagens que me proporcionou, por toda a paciência, ajuda e incentivo, pela disponibilidade dentro e fora de horas, e por todas as palavras amigáveis e ensinamentos de vida. À Professora Doutora Catarina Almeida, agradeço especialmente por todas as tardes de esclarecimentos e introdução à citometria de fluxo. À Professora Doutora Rita Ferreira, agradeço especialmente por toda atenção com que me cuidou, mesmo à distância, e por me ter facilitado tão prontamente a oportunidade de voltar a casa.

À Doutora Lis Lobo, agradeço a simpatia e disponibilidade para me acompanhar e ensinar.

Ao Doutor Pedro Florindo e seus restantes colaboradores, agradeço pelo trabalho publicado com minha co-autoria.

Agradeço também à Unidade de Ensino e Investigação (UEI) de Parasitologia Médica do IHMT, onde foi desenvolvida o trabalho experimental. Agradeço a todos os Doutores, Mestres e Licenciados que comigo partilharam os escritórios e laboratórios do IHMT pelo companheirismo, amizade, momentos de descontração, palavras de apoio e motivação, por me trocarem o meio das culturas quando não podia e por me fazerem sentir que estávamos todos no mesmo barco.

Agradeço à Universidade de Aveiro, em especial a todos os professores do Mestrado de Bioquímica pela excelente formação académica e pessoal que me proporcionaram, e a todos os colegas com que partilhei o primeiro ano de mestrado pela forma como me acolheram na vossa cidade.

Agradeço a todos os meus mais próximos que me ouviram e consolaram quando as coisas corriam menos bem. Agradeço principalmente aos meus pais por fazerem o possível e o impossível para que tudo fosse mais fácil, e à minha irmã e aos seus pequenotes por serem a razão de muitas alegrias.

palavras-chave

Plasmodium falciparum, viabilidade, Mitotracker™ Deep Red FM, SYBR™ Green, citometria de fluxo

resumo

O tratamento recomendado para *Plasmodium falciparum* malaria é a Terapia Combinada de Artemisininas (ACT). Desde 2008, as estirpes de *P. falciparum* resistentes estão a propagar-se em regiões endémicas de malária. O fenótipo resistente a derivados de Artemisinina é caracterizado por um padrão de dormência que se assemelha morfologicamente a parasitas mortos. Este fenótipo inviabiliza a implementação dos testes de suscetibilidade a drogas antimaláricas baseados em ensaios de viabilidade atualmente em uso. Neste sentido, novas abordagens são necessárias de forma a diferenciar parasitas vivos de parasitas mortos de forma inequívoca, fácil e rápida. A presente dissertação teve como objetivo implementar um novo protocolo de avaliação da viabilidade, de forma a auxiliar na identificação de parasitas resistentes a antimaláricos e caracterizar o impacto de novos antimaláricos na viabilidade do parasita. Consequentemente, sondas fluorescentes com alvo no ΔΨm e DNA do parasita (Mitotracker™ Deep Red FM e SYBR™ Green I, respetivamente) foram utilizadas e as suas emissões de fluorescências lidas por citometria de fluxo. Cada passo do protocolo foi optimizado, sendo que no final o ensaio foi testado na sua eficácia em detetar variações no ΔΨm. O ensaio final foi aplicado ao estudo de novos compostos, de forma a contribuir para a elucidação do seu mecanismo de ação. O ensaio de viabilidade, com base na integridade da mitocôndria, desenvolvido e implementado no âmbito da presente dissertação provou ser uma ferramenta importante para uma avaliação rápida e fidedigna da viabilidade de parasitas sujeitos a tratamento por antimaláricos. Foi igualmente possível determinar o estadio intra-eritrocitário através da aplicação desta nova metodologia. A adaptação para condições de campo, através da introdução do passo de fixação no protocolo do ensaio, não foi possível de alcançar sem que se comprometesse a eficácia do método desenvolvido. Ainda assim, o composto de organoruthenium (Ru2) foi devidamente avaliado na sua capacidade de condicionar a viabilidade do parasita e, consequentemente, reduzir a sua sobrevivência. Com base nos resultados obtidos pelo ensaio de dupla-sonda, outros estudos se seguiram de forma a compreender a farmacodinâmica do Ru2. Estes estudos demonstraram que o Ru2 é um antimalárico de ação rápida, com a capacidade de afetar igualmente parasitas em estádios jovens e maduros. No futuro, espera-se ainda avaliar o stress oxidativo no parasita induzido por este tratamento, bem como estudar processos de fixação que sejam compatíveis com a deteção do comprometimento do ΔΨm em diferentes tipos de amostras.

keywords

Plasmodium falciparum, viability, Mitotracker™ Deep Red FM, SYBR™ Green, flow cytometry

abstract

The recommended treatment for *Plasmodium falciparum* malaria is the Artemisinin Combination Therapy (ACT) treatment. Since 2008, resistant *P. falciparum* strains are spreading in malaria-endemic regions. Artemisinin derivatives resistant phenotype is characterized by a dormancy pattern in the parasites that morphologically resembles dead parasites. This phenotype creates a problem in current viability assays employed in antimalarial drug susceptibility tests. New approaches are needed to more easily differentiate dead from live parasites, in a shorter period. The present thesis aims to implement a new viability assessment, to help identify drug-resistant parasites and characterize the impact of newly synthesized antimalarials in parasite viability. Hence, fluorescent probes targeting the parasite $\Delta\Psi m$ and DNA, with Mitotracker™ Deep Red FM and SYBR™ Green I, respectively, were applied, and the fluorescence emission recorded by flow cytometry. Each step of the protocol was optimized, and in the end, the assay efficacy in detecting variations of $\Delta\Psi m$ was tested. As a proof-of-concept, one assay was applied to analyze new compounds and contribute to the clarification of its mechanism of action. The developed and implemented viability assay, based on mitochondrial integrity, proved to be a resourceful tool for a fast and reliable viability assessment of parasites submitted to antimalarial treatment. It was also possible to determine stage-specific events with the application of this methodology. As an adaptation for field condition, a fixation step was added to the protocol, but unfortunately, this comprised the method efficacy. Even so, the organoruthenium compound (Ru2) was accurately assessed on its ability to constrain parasite viability, hence repressing its survival. Based on the dual-probe assay findings, other studies on Ru2 followed to understand its pharmacodynamics. These studies showed that Ru2 is a fast-acting drug, with the capability of similarly affecting younger, and mature intra-RBC stages. In the future, the study of Ru2 should be correctly complemented with the evaluation of the oxidative stress-induced in parasites. Besides, the implemented technique would gain with further testing of alternative fixation methodologies compatible with detection of the $\Delta\Psi m$ collapse, and also with its implementation on different types of samples.

Publications from this thesis:

Milheiro, S. A., Gonçalves, J., Lopes, R. M. R. M., Madureira, M., Lobo, L., Lopes, A., Nogueira, F., Fontinha, D., Prudêncio, M., Piedade, M. F. M., Pinto, S. N., Florindo, P. R. & Moreira, R. Half-Sandwich Cyclopentadienylruthenium(II) Complexes: A New Antimalarial Chemotype. Inorg. Chem. (2020). doi:10.1021/acs.inorgchem.0c01795

TABLE OF CONTENTS

LIST OF FIGURES

LIST OF TABLES

CHAPTER I

ABBREVIATIONS

ΔΨm – mitochondrial membrane potential

ACT – Artemisinin Combination Therapies

APC – Allophycocyanin

ATP – Adenosine triphosphate

ATQ – Atovaquone

CoA – Coenzyme A

CoQ – Coenzyme Q

Cyt c – Cytochrome *c*

DHA – Dihydroartemisinin

DHODH – Dihydroorotate dehydrogenase

DMSO - Dimethyl sulfoxide

DNA – Deoxyribonucleic acid

DNA-IFD – DNA-intercalating fluorescent dyes

EDTA – Ethylenediaminetetraacetic acid

EF1 – Elongation factor 1

ELISA – Enzyme-Linked Immunosorbent Assay

ETC – Electron transport chain

FITC – Fluorescein isothiocyanate

FSC – Forward scatter

G3PDH – glycerol-3-phosphate dehydrogenase

GA – Glutaraldehyde

GFP – Green fluorescent protein

GM – Geometric mean

HEPES - 4-(2-hydroxyethyl)-1-piperazineethanesulfonic acid

hpi – hours post-invasion

HRP2 – Histidine-rich protein 2

IC_{50} – Half (50%) maximal inhibitory concentration

IHMT – Instituto de Higiene e Medicina Tropical/ Institute of Hygiene and Tropical Medicine

IPTi – Intermittent preventive treatment in infants

IPTp – Intermittent preventive treatment in pregnancy

iRBC – infected Red blood cells

LDH – lactate dehydrogenase

MQO – malate-quinone oxidoreductase

MTDR – Mitotracker™ Deep Red FM

NADH – Reduced nicotinamide adenine dinucleotide

PBS – Phosphate buffer saline

PCR – Polymerase chain reaction

PE – Phycoerythrin

PES – Polyethersulfone

PFA – Paraformaldehyde

PfCRT – Plasmodium falciparum chloroquine resistance transporter

PfDHFR – Plasmodium falciparum dihydrofolate reductase

PfDHPS - Plasmodium falciparum dihydropteroate synthetase

PfK13 – Plasmodium falciparum Kelch13

PfMDR – Plasmodium falciparum multidrug resistance transporter

PVM – Parasitophorous vacuole membrane

Q – ubiquinone

QH_2 – ubiquinol

RBC – Red blood cell

RFU – Relative fluorescent units

Rho123 – Rhodamine123

RPMI - Roswell Park Memorial Institute growth medium

RPMIc – RPMI complete medium

rRNA – ribosomal Ribonucleic acid

SD – Standard deviation

SEM – Standard error of the mean

SG – SYBR™ Green I

SMC – Seasonal malaria chemoprevention

SNP – Single nucleotide polymorphism

SSC – Side scatter

T - time

TCA – Tricarboxylic acid

TMRE – Tetramethylrhodamine ethyl ester

TMRM – Tetramethylrhodamine methyl ester

tRNA – transfer Ribonucleic acid

UEI – Unidade de Ensino e Investigação

uRBC – uninfected Red blood cells

WHO – World Health Organization

CHAPTER I

Introduction
Literature Review

Introduction

Plasmodium falciparum malaria is an endemic disease[1] which has been responsible for numerous deaths along the years[2]. Public health control efforts have been successful and managed to reduce infection incidence and death rates globally. However, drug-resistant strains have become more and more prevalent in some endemic regions, compromising the progress done so far[3]. Such strains enter dormancy when subjected to drug pressure. This phenomenon creates a problem in diagnostic and in drug susceptibility tests, because of the morphological and metabolic resemblances of dead and dormant parasites[4–6].

Most of the drug susceptibility tests make use of viability assays. These assays intend to assess progression on the parasite life cycle, and metabolic activity, such as DNA synthesis or protein presence[7]. All these parameters can be misrepresented in dormant resistant parasites or became very time-consuming to give a reliable result. Thus, it is mandatory to create a less demanding and quicker alternative to the currently used viability methods, like a mitochondrial integrity-based viability assay. Such assay lays down on the detection of the few metabolic processes still maintain by resistant strains[4], and capable of distinguishing viable from death parasites earlier than other methodologies[8].

The use of fluorophores is a more manageable and adequate assessment of viability[9,10], based on mitochondrial integrity. A DNA probe will synergistically identify *P. falciparum* parasites to add more precision to the development technique. Combining both detection methodologies, the use of a flow cytometer will allow a faster and more accurate assessment based on mitochondrial integrity. In this way, the result of the present work will be the implementation of a new flow cytometry viability assessment protocol in the UEI Malaria Laboratory, Institute of Hygiene and Tropical Medicine (IHMT), to help identify drug-resistant parasites and characterize the impact of newly synthesized antimalarials in parasite viability.

This dissertation opens with a state of the art analysis of viability methods for *P. falciparum*. From which it is carried the posterior development of the viability assay based on mitochondrial membrane potential ($\Delta\Psi m$) and DNA presence. In the end, the optimized assay serves to complete the characterization of an antimalarial candidate.

Literature Review

I.1. MALARIA

I.1.1. Clinical aspects of the disease

Malaria is a febrile hemolytic disease caused by a protozoan infection of the host red blood cells (RBC). The infection starts with the bite of a female *Anopheles spp.* mosquito[1], which injects the parasite into the host skin and bloodstream[11]. The parasite acts, by cycling destroying the RBCs in its continuous multiplication and invasion of these cells, which triggers a series of events in the host organism[12]. The parasite responsible for the illness belongs to the genus *Plasmodium*[1]. *P. falciparum* belongs to the group of five human-infecting *Plasmodium*, and it is responsible for the most severe forms of the disease, including death[1,13].

P. falciparum malaria can have different scales of complications: uncomplicated malaria and severe malaria[14]. Each one characterized by the severity of symptoms. In uncomplicated malaria, the most common syndrome is a febrile illness[11], with headaches, fatigue, abdominal discomfort, and muscle aches[12]. On the other hand, severe malaria defines a more aggravated clinical condition in the presence of a positive parasitological test[14]. Some of the symptoms of severe malaria include impaired consciousness, prostration, multiple convulsions, acidosis, hypoglycemia, severe anemia, renal impairment, jaundice, pulmonary edema, enlargement of the spleen, coagulopathy, significant bleeding, and cerebral malaria, with non-awakening coma leading to death or leaving the patient with persistent neurologic deficits[1,12,14]. This non-specificity of *P. falciparum* malaria symptoms results in a delay in diagnosis, which may lead to death. That said, the parasitological test is essential for the disease diagnosis.

I.1.2. Epidemiology of *Plasmodium falciparum* malaria worldwide

Malaria is an infectious disease most common in the tropical region of the globe[1], such as Southeast Asia, Latin America, and sub-Saharan Africa[1] (as illustrated in Figure I.1). Since 2004, public health efforts have paid off, and the number of fatalities has reached lower

and lower numbers[2]. Even so, the number of deaths due to malaria is still very high (435 000 globally in 2017)[3], and most of them occur in children under the age of 5 (61% of all malaria deaths worldwide)[3].

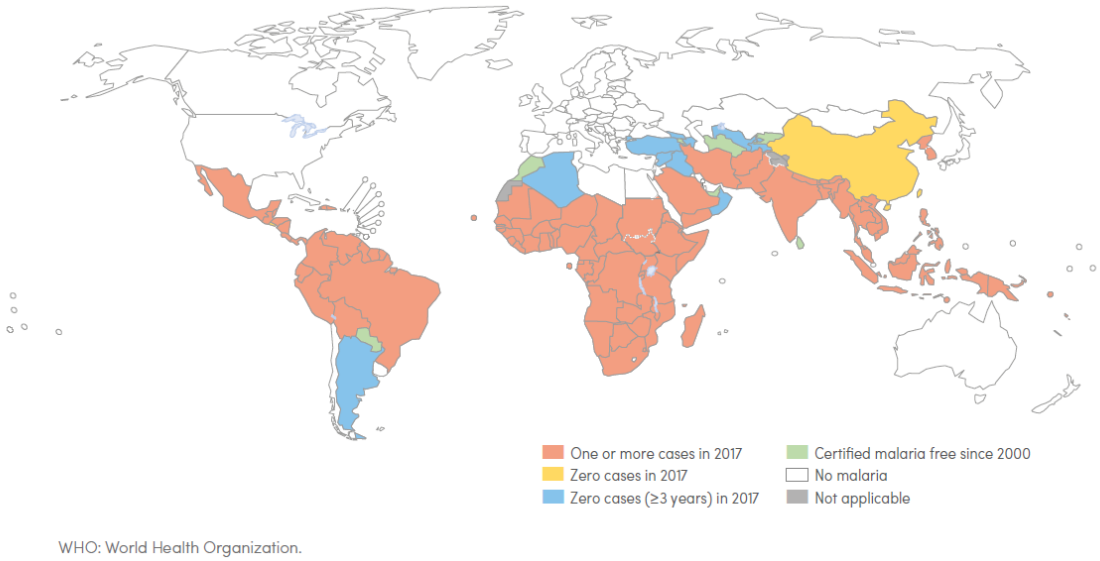

Figure I.1 – Endemic regions of *Plasmodium falciparum* malaria. World map showing countries with indigenous cases in 2000 and their status by 2017. Adapted from World Malaria Report of 2018[3].

Malaria is still on the top 10 of the leading causes of early death[15]. Globally, the malaria incidence rate has been following mortality, with a decrease in infected patients since 2010. However, from 2014 to 2017, the rate has flattened. In fact, during this period, in the WHO Region of Americas (especially in Brazil, Nicaragua, and Venezuela), the incidence has even increased[3]. Besides this local rise in incidence, global statistics are indicative of good prospects, as a result of the increasing number of countries that are progressing to the definitive elimination of malaria[3].

I.2. *PLASMODIUM FALCIPARUM*

I.2.1. *Plasmodium falciparum* life cycle

P. falciparum belongs to the phylum Apicomplexa. This phylum shares the presence of a specialized apical complex, that is relevant in the invasion process. Its life cycle involves an arthropod vector that feeds[16] on the blood of both vertebrate and invertebrate hosts[7],

transmitting the parasite through them. The arthropod vector in mammalian hosts is the female *Anopheles spp.* mosquito[7,16]. Mosquitoes ingest sexual stages of *Plasmodium*, called gametocytes, in a blood meal from an infected host. Inside the vector, gametocytes develop into infectious forms (sporozoites)[7], which are injected later to a new host in the following blood meal[16].

In the inoculation of the *P. falciparum* parasite into the human host, the mosquito deposits sporozoites under the skin[17]. Once inside the bloodstream, sporozoites migrate to the liver. In the liver, sporozoites transmigrate various hepatocytes[16,18] and eventually, initiate schizogony[7], which is a state where they develop and multiply into new liver merozoites[11], in an intracellular asexual division[7]. Thousands of merozoites, found in merossomes[18], are then released from each infected hepatocytes, ready to invade RBC[7,16]. RBCs became the new host cell of the parasites, that will start to feed on its hemoglobin[11].

Inside RBCs, *P. falciparum* starts its asexual division, developing through the stages of ring, trophozoite, and schizont. A mature schizont is formed by 8 to 22 merozoites[19], which are released from the RBC host cell by lysis of the schizont, in a process designated egress. Once out of the RBC, merozoites reinvade other uninfected RBCs. The new cycle of invasion can lead to the development of merozoites into asexual stage forms (asexual division) or, a small proportion of merozoites, transform into male and female gametocytes (sexual division)[7]. The ring stage takes place until 22h post-invasion (hpi), the trophozoite stage is observed between 22 and 38hpi and the schizont stage happens between 38 and 48hpi, during which merozoites maturate, just before the next cycle of invasion[20]. The asexual division results in a rapid expansion and sustained cycling of the parasite population[11], whereas sexual division results in gametocytes that can be ingested by a female mosquito during a blood meal, reinitiating the full cycle[7] (Figure I.2).

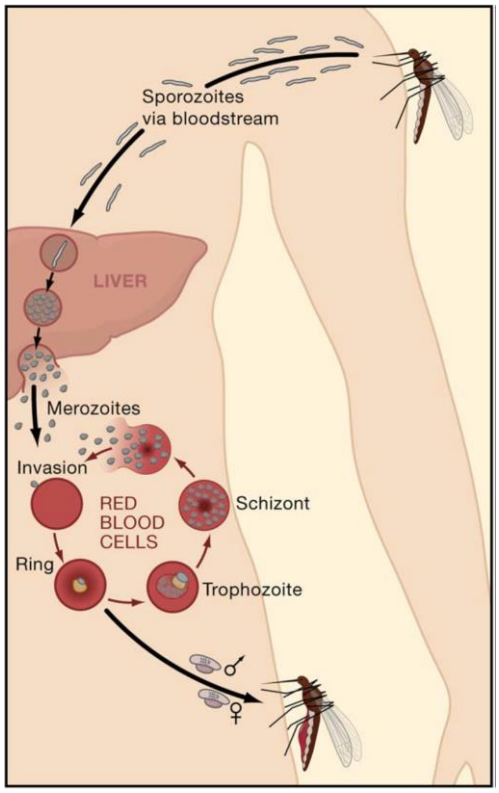

Figure I.2 – *Plasmodium falciparum* life cycle in a human host. (Adapted from[16]).

I.2.2. Blood stage development and morphology features of *Plasmodium falciparum*

P. falciparum blood stages are composed of numerous organellar structures hold by a plasma membrane and the parasitophorous vacuole membrane (Figure I.3). In the parasite cytoplasm, there are secretory vesicles, ribosomes, a single mitochondrion, and a single plastid[21]. The mitochondrion and the plastid maintain a tight spatial relationship throughout all parasite stages of development[22–24]. There is also a nucleus, an endoplasmic reticulum, and a Golgi complex[23,24]. There is also the cytostome, a structure that works as a vehicle to the parasite RBC hemoglobin feeding, associated with vesicles containing hemozoin cristals[21], sometimes called the food vacuole[23].

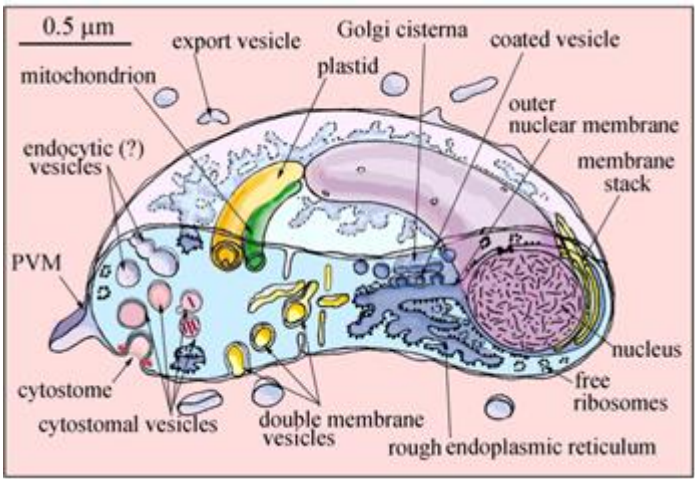

Figure I.3 – Parasite organellar and morphology features. Ring stage of *P. falciparum* portraying its general organelle organization within the cytoplasm (Adapted from[24]).

During its 48h asexual cycle of development, *P. falciparum* invades the RBC, matures from a merozoite to a ring-stage parasite, develops continuously, until it becomes a multinucleated schizont (Figure I.4). Merozoite parasites have a drop-like shape, with a basal placed nucleus and an apex structure on the opposite side. In the apex, the parasite contains secretory vesicles meant for the invasion process of the RBC[21]. Once inside the RBC, parasite starts to feed on the RBC hemoglobin, growing in size and changing its morphological shape to a ring-stage parasite[25]. Ring-stage parasites resemble a flattened biconcave disc[24]. Inside the RBC, the parasite develops from ring-stage, from 6h to 18hpi (Figure I.4, first row), to trophozoite, from 22 to 34hpi (Figure I.4, second row), and schizont, from 38h to 46hpi (Figure I.4, third row). At 48hpi, egress occurs, and merozoites are set free to reinvade new RBCs.

The ring-stage parasite nucleus (6h to 18h in Figure I.4) resembles a rounded-shaped mass, and cytoplasm changes from a densely staining and narrow rim feature[24] to an increasingly thick mass. Other sub-cellular structures like free ribosomes and the rough endoplasmic reticulum start gradually to dominate the cytoplasm[24]. When *P. falciparum* reaches the trophozoite stage (22h to 34h in Figure I.4), it appears ellipsoidal and with regular, smooth boundaries[25], occupying 10 to 20% of the host cell volume[25] but maintaining a single nucleus. During this stage, the parasite goes into profound metabolic and morphological changes until reaching the schizont stage (34h to 48h in Figure I.4). During schizogony, the nucleus goes into successive mitotic divisions, originating up to 15 nuclei in late schizogony[23], forming the schizont.

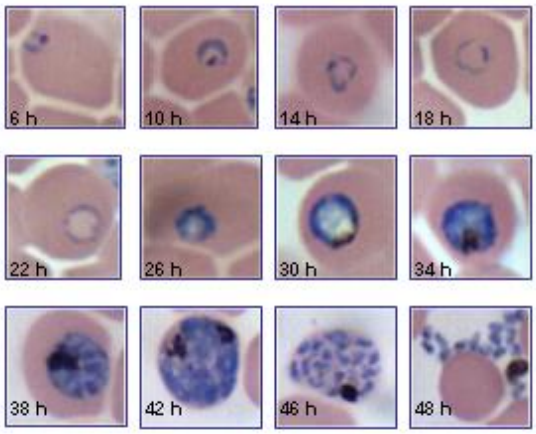

Figure I.4 –Blood stages of *Plasmodium falciparum.* Photomicrography of a Giemsa stained smear of infected RBCs (Adapted from[26]). The first row (from 6h to 18h) consists of ring-stage parasites, the second row (from 22 h to 34h) there are only trophozoite-stage parasites, and in the third row (from 38 to 46h) is shown schizont-stage parasites and free merozoites (48h).

I.2.2.1. *Plasmodium falciparum* mitochondrion

Asexual *P. falciparum* mitochondrion is a double-membrane organelle with only one or two tubular-like cristae[27,28] frequently called an acristate structure[29]. It is a dynamic organelle, undergoing numerous morphologic changes during the parasite blood cycle. Mitochondrion starts as an elongated (during ring stage) or branched organelle, in trophozoite stage, and progressively becomes more and more branched as schizogony starts, until it breaks in shorter mitochondria in late schizogony[23,30] (Figure I.5).

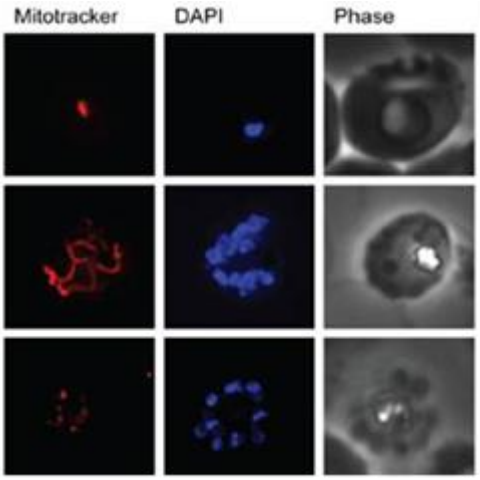

Figure I.5 – *Plasmodium falciparum* mitochondrion morphology in different life cycle stages. *P. falciparum* blood-stage parasites stained with Mitotracker® to identify mitochondria and DAPI to identify nuclei, showing mitochondria's morphological changes through the parasite life cycle. Top panel

corresponds to a late ring parasite (elongated mitochondrion organelle), middle panel to a later trophozoite, or early schizont (branched mitochondrion organelle), and bottom panel to a schizont parasite (multiple mitochondria) (Adapted from[30]).

This single mitochondrion maintains the mitochondrial electron flow, the tricarboxylic acid (TCA) cycle, and the acetyl-CoA production. The mitochondrial electron flow in the blood stages of the malaria parasite renders more consuming than producing ATP mitochondrion to the malaria parasite. The five enzymes that participate in this process are NADH dehydrogenase (complex I), succinate dehydrogenase (complex II), ubiquinol-cytochrome *c* oxidoreductase (complex III), cytochrome *c* oxidase (complex IV), and ATP synthase (complex V). These five complexes, shown in Figure I.6, form the respiratory chain of the mitochondrion and work simultaneously with two-electron shuttles between them: ubiquinone (coenzyme Q - CoQ) and cytochrome *c* (Cyt c). Complexes III and IV form the proton pump of the electron transport chain[29]. Together, they establish the mitochondrial membrane potential or proton motive force, by pumping protons from the mitochondrial matrix to the intermembrane space, which will re-enter the matrix space via ATP synthase (Complex V)[31]. In this way, while creating a mitochondrial membrane potential, the proton pump also works as a driving force for complex V[29], promoting the synthesis of ATP[31]. Despite ATP synthase playing a central role in the blood stages of the parasites, the most significant function of the parasite mitochondrial electron flow is the regeneration of CoQ as a cosubstrate of dihydroorotate dehydrogenase (DHODH)[31], that will serve in the critical pyrimidine biosynthetic pathway[32].

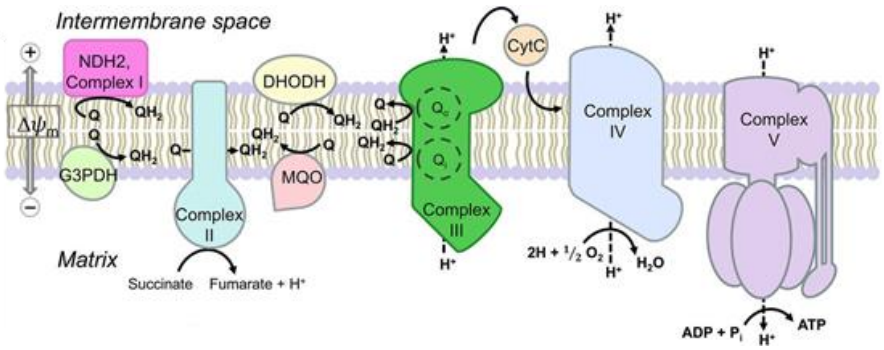

Figure I.6 – Components of *Plasmodium falciparum* oxidative phosphorylation. (Adapted from[33]). CytC, soluble cytochrome C; G3PDH, glycerol-3-phosphate dehydrogenase; MQO, malate-quinone oxidoreductase; Q, ubiquinone; QH_2, ubiquinol; $\Delta\psi m$, mitochondrial membrane potential.

I.3. CURRENTLY AVAILABLE ANTIMALARIAL DRUGS TO TREAT UNCOMPLICATED *PLASMODIUM FALCIPARUM* MALARIA

P. falciparum malaria has been treated with several different drugs throughout the years[34,35] (described in Table 1). Unfortunately, most of these drugs have gone out of use due to the emergence of drug resistance. Currently, *P. falciparum* has developed resistance to virtually all antimalarial drugs in use. Hence a new strategy was applied: the introduction of artemisinin-based combination therapies (ACTs)[36] and abolishment of monotherapies. ACTs have become the first-line treatment for uncomplicated *P. falciparum* malaria recommended by the WHO, since 2006[14,36].

Table I.1 – Antimalarial drugs for the treatment of *Plasmodium falciparum* malaria.

Antimalarial drug class	Antimalarial drugs	Mechanism of action	Mechanism of resistance	Current use[14]
Antifolates	Pyrimethamine Proguanil Sulfadoxine	Inhibits the folate biosynthetic pathway[37].	Mutations in *PfDHFR* and *PfDHPS*[38].	ACTs. IPTp. IPTi. SMC.
Naphtoquinones	Atovaquone	Ubiquinone analog (bc1 inhibition of the ETC)[39].	Mutations in cytochrome b[40].	Prophylaxis. Treatment of uncomplicated malaria outside malaria-endemic areas.
Aryl-amino alcohols	Lumefantrine Quinine Mefloquine	Inhibits haem detoxification[41].	Mutations in *PfMDR*[42].	ACTs. Treatment of severe malaria. Treatment during 1st trimester of pregnancy. Prophylaxis.
4-aminoquinolines	Chloroquine* Amodiaquine Piperaquine	Inhibits haem detoxification[43].	Mutations in *PfCRT* and *PfMDR*[43].	ACTs. SMC.
8-aminoquinolines	Primaquine	Interferes with mitochondria integrity[44].	Unknown[34].	Reduction of transmission. Prophylaxis.
Antibiotics	Clindamycin Doxycycline	Inhibits protein synthesis[45].	Mutations in apicoplast rRNA[46].	Prophylaxis. Treatment during 1st trimester of pregnancy.
Endoperoxides	Artemether Artesunate DHA	Induces oxidative stress[47].	Mutations in the *PfK13*[38].	ACTs Treatment of severe malaria. Reduction of transmission.

IPTp – intermittent preventive treatment in pregnancy

IPTi – intermittent preventive treatment in infants

SMC – seasonal malaria chemoprevention

* out of use for *P. falciparum* malaria (except in some parts of Central America)

Artemisinin or qinghaosu is the active component of a sweet wormwood plant extract (*Artemisia annua* or qinghao) discovered in the 1970s[36]. A great variety of lipid and water-soluble artemisinin derivatives have been synthesized[36]. The most used semi-synthetic derivatives are artesunate, artemether, and dihydroartemisinin (DHA). DHA is the metabolite responsible for the majority of parasiticidal activity[48]. All these compounds have shown to produce a rapid reduction of parasite biomass at nanomolar concentrations, even against multi-drug resistant *P. falciparum*, with the great advantage of acting on ring stage *P. falciparum* parasites. Moreover, they have a gametocidal effect, which is very helpful for parasite transmission reduction[36].

Combining two different antimalarial drugs improves treatment efficacy. Such a combination also delays the selection of resistance to each drug. In this way, ACTs are a combination of an artemisinin analog with another antimalarial partner drug with a longer half-live, reducing the duration of the treatment to 3 days[36]. The ACTs recommended for uncomplicated *P. falciparum* malaria are artemether and lumefantrine; artesunate and amodiaquine; artesunate and mefloquine; dihydroartemisinin and piperaquine; and artesunate and sulfadoxine-pyrimethamine[14]. With the use of artemisinin derivatives, ACTs can rapidly remove parasites from the blood and kill sexual stages, while the longer-acting partner drug clears the remaining parasites, avoiding the development of resistance[14].

I.4. PARASITE RESISTANCE TO ARTEMISININ DERIVATES

I.4.1. *Plasmodium falciparum* drug resistance to artemisinin derivatives

Antimalarial drug resistance is the property of the parasite strain to survive and/or multiply in the presence of an equal or higher drug quantity administration, with a recommended time of drug exposure[14]. In the case of the artemisinin resistance, this definition translates into a delay in parasite clearance following treatment with artesunate monotherapy or ACT. This phenomenon does not necessarily lead to treatment failure but can place a higher demand on the partner drug, jeopardizing its future efficacy.

Despite ACTs being a combination of two drugs, the selection of resistant *P. falciparum* strains as already occur in Southeast Asia[49], probably caused by the widespread availability of artemisinin monotherapies in the past[49]. These occurrences arise from the selection of parasites with genetic changes that provide them with reduced susceptibility to the drug[14]. Multiple Single Nucleotide Polymorphisms (SNPs) in the gene (*pfK13*) coding for the protein Kelch13, have been highly predictive of slow parasite clearance and associated with more than double the parasite clearance half-life. The geographic distribution of such SNPs in the gene parasite strains is concurrent with the emergence and spread of artemisinin resistance in Southeast Asia[50].

Artemisinin resistance in *P. falciparum* is currently present in China (Yunnan province), Cambodia, Lao People's Democratic Republic, Myanmar, Thailand, and Viet Nam[3], as shown in Figure I.7. The emergence of these strains is a threat to the progress achieved in malaria control and has significant implications in global public health[3,50]. The main concern, currently, is not *if*, but *when* will it spread to Africa[51,52]. Thus, the development of new drugs against artemisinin-resistant malaria is critical.

Figure I.7 – Geographic distribution of artemisinin-resistant *Plasmodium falciparum* strains. Graphical representation of the World Malaria Report of 2018 conducted by the World Health Organization (WHO)[3] showing the number of ACTs with high failure rates in the treatment of *P. falciparum* infections.

I.4.2. Dormancy of *Plasmodium falciparum* - a feature of resistance to artemisinin

Dormancy is a mechanism used by resistant strains to cope with environmental conditions that threaten their survival. In this way, parasites enter a dormant state after drug pressure. This strategy is adopted to avoid exposure of metabolic pathways targeted by the drugs, to decrease drug uptake, or to prioritize repair and recovery over replication[53].

I.4.2.1. Morphological characteristics

The dormant state occurs in early ring-stage (0-3hpi) *P. falciparum* drug-resistant strains exposed to artemisinin derivatives[4,5]. These dormant parasites are smaller and persist viable in time until parasite recovery[5,54]. Their morphological appearance is characterized by a blue cytoplasm and condensed red chromatin (Giemsa stained), in opposition to dead ring-stage parasites which show a collapsed nucleus without cytoplasm[4,6] (Figure I.8). Nevertheless, the recognition of a dormant morphology is subjective and depends greatly on the observer, staining of the parasites, among others.

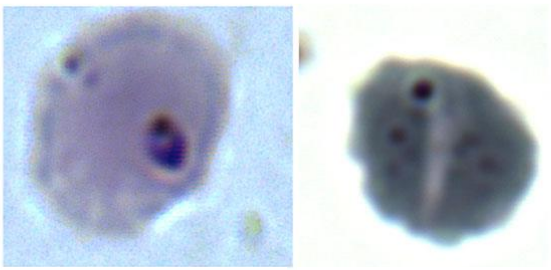

Dormant parasite Dead parasite

Figure I.8 – Dormant forms of *Plasmodium falciparum* artemisinin-resistant strains. Micographs of giemsa-stained dormant parasite morphology (left) in comparison with giemsa-stained dead parasite appearance (right). Showing the close resemblances between the two occurrences. (Adpated from [4]).

I.4.2.2. Metabolic signs

When entering dormancy, parasites adjust their metabolism to surpass the drug pressure and assure its later recovery. The strategy consists mainly of down-regulating housekeeping genes[55] and simultaneously maintaining or up-regulating genes that become necessary to its ultimate survival and later recovery[5]. Dormant rings keep active some of

its cell functions and up-regulate others. Glycolysis, DNA synthesis, tRNA synthesis, folate synthesis, and protein synthesis[5,56] are some of the metabolic pathways that are turned down in dormant ring-stage parasites. However, dormant rings maintain up-regulated metabolic activities in two organelles, apicoplast, and mitochondria.

The single mitochondrion of the dormant parasite maintains its membrane potential[4]. High rates of transcription of the nuclear genes that code mitochondrial localized enzymes during dormancy (namely complexes II, III, and IV) are responsible for the maintenance of the mitochondrial membrane potential ($\Delta\Psi m$)[4,5]. The temporary inhibition of the electron-shuttle CoQ was proven to induce a delayed recovery in dormant parasites[56], which reinsures the importance of this organelle in growth development after dormancy and its maintenance during this period. Regarding the apicoplast metabolic activity of the dormant rings, two metabolic pathways are more active in dormant than in healthy parasites (not subjected to drug pressure): the fatty acid synthesis[4,5] and the pyruvate metabolism[5].

Both mitochondrion and apicoplast metabolic activity could be useful markers in the detection of artemisinin-resistant/dormant parasites after drug pressure. However, apicoplast metabolic activity detection is not easily trackable, because it requires either mass spectrometry[57], PCR[5], GFP gene fusion[57,58], or fluorescent antibodies targeting[57], methods not easily implemented as routine assays. On the other hand, mitochondrial membrane potential has several commercialized dyes to its detection (see below I.5.3.2.). Such dyes already have been studied in its reliability and application in *P. falciparum* isolates and cultures. Such a fact leads to the fostering of the mitochondrial membrane potential as a more fit marker to the study of artemisinin-resistant strains.

I.5. VIABILITY ASSESSMENT ASSAYS

P. falciparum viability assessment assays are used mainly for *in vitro* drug susceptibility evaluation. Drug susceptibility assays based on the parasite viability aim to discover new antimalarial compounds or monitor the emergence of drug resistance[59]. Viability can be assessed generally through parasite metabolic activity (LDH and HRP2-ELISA), mitotic activity (isotopic assay, schizont maturation assay, and permeable DNA intercalating fluorescent dyes), and mitochondrial activity (fluorophores targeting mitochondrial

membrane potential). All these cellular markers can indicate if the parasite is viable after the limited time of drug exposure, hence measuring the antimalarial potential of numerous drugs.

I.5.1. LDH and HRP2-ELISA assay

P. falciparum histidine-rich protein 2 (HRP2) and lactate dehydrogenase (LDH) are two parasite proteins that correlate with metabolic activity. Their levels translate the metabolic state of the parasite[59,60]. For this reason, both proteins are markers of parasite viability in ELISA assays[59].

HRP2 is a protein involved in hemozoin formation. HRP2 presence is concurrent with a healthy feeding parasite, being in this way a viability marker of *P. falciparum*. Although being expressed in all parasite stages, HRP2 based assays require a minimum incubation time of 48h (to cover a full life cycle)[61–63] to produce detectable levels of the protein. A serious drawback to the general implementation of this method is the fact that there are some reports of *P. falciparum* strains lacking HRP2 gene[64], making it unusable for field conditions.

LDH ELISA assay has shown some disadvantages. For a start, LDH only accounts for the viability of trophozoite and schizont stages, because this enzyme is not expressed in ring-stage parasites[65]. Also, ELISA assays based on the presence of *P. falciparum* LDH reported to depend on the drug under study[66], producing substantially higher IC_{50} than microscopy or flow cytometry (particularly, artemisinin derivates and chloroquine). Such dependency may be due to the lack of LDH production during the ring-stage parasites and poses a problem in the application of this assay to test new drugs. All these factors prevent LDH-ELISA to be used transversally in different study conditions, which is a considerable limitation for a viability assay.

I.5.2. Isotopic assay

The isotopic assay refers to the method that employs radioactive isotope [^{3}H]-hypoxanthine. The isotopic assay relies on the assessment of DNA synthesis during

schizogony. Hypoxanthine is a DNA precursor, that can cross the malaria parasite membrane[67] and incorporate into nucleic acids. After drug exposure to parasites, radioactive hypoxanthine incorporation signals for the occurrence of DNA synthesis and is a target of measure as counts per minute. These results can be correlated to parasite growth or inhibition, hence assess drug efficacy[68].

Radioactive hypoxanthine assay is easy and fast to perform[69] and gives reliable antimalarial activity quantification. Its results are independent of the compound and its mechanism of action[59], which is also another great advantage. Nevertheless, it has some disadvantages like i) the equipment required is very expensive; ii) presents considerable difficulties and limitations related to radioactive compounds management[69]; and iii) because it is based only on hypoxanthine uptake and incorporation it does not differentiate the invasion process (schizont to ring-stage phase), hence leading to misinterpretation of stage-specific events.[69,70]

I.5.3. Schizont maturation assay

Schizont maturation assay is the standard assay recommended by the WHO[71,72]. It starts with the incubation of infected RBCs (iRBC) with a specific drug concentration. The effects caused by the drug on parasite viability are measured through the assessment of mitotic activity, specifically the schizogony process. The number of schizonts is estimated using a Giemsa-stained smear of a 48h drug-exposed iRBCs[73,74]. Specialized microscopists record the number of schizonts with three or more nuclei, in 200 asexual parasites found in each smear[71]. The number of mature parasites will, in this way, correlate with drug efficacy.

Schizont maturation assay can reliably correlate with clinical findings, and it is still applied in multiple *P. falciparum* drug susceptibility studies. However, efforts have been made to reduce the schizont maturation assay's time. One of the proposals is a modified 24h trophozoite maturation inhibition assay. This alternative method suggests a 24h reduction in the assessment time, evaluating the progression from ring to trophozoite, instead of counting the number of schizonts in a smear. This modification bears some flaws and owns the same disadvantages that the previous method. Schizont maturation assay or the newly

proposed trophozoite inhibition assay, although being conceptually simple, it is very time-consuming and demands specialized or trained techniques in microscopy[72].

I.5.4. Methods based on fluorophores

I.5.4.1. DNA intercalating fluorescent-dyes

Fluorescent dyes are molecules that provide high sensitivity in detecting an array of microorganisms. During the symptomatic phase of the disease, the blood-stage, *P. falciparum* infects RBCs, a cell that does not have nucleus nor mitochondria, hence the only DNA present in the host cell is parasite DNA. Several DNA-intercalating fluorescent dyes (DNA-IFD) have been used to detect malaria parasites (Table 2), among these, the most frequently used is SYBR™ Green I [8,69,75–79].

SYBR™ Green I (SG) is a membrane-permeable probe that rapidly[10] stains specifically double-stranded DNA[80]. This DNA-IFD presents high resolution between infected and uninfected RBCs[81], and it does not depend on the integrity of the membrane[65,82,83]. SG fluorescence intensity pattern on malaria parasites has a linear relationship with parasitemia[82,83] and increases with parasite maturation[84]. SG fluorescence on iRBCs features a great variety of intensity scales. The broad spectrum of fluorescence intensities depicted by SG, when linked to intra-RBC *P. falciparum* DNA, can sometimes be an obstacle in data interpretation. Nevertheless, comparing with the other DNA-IFD, SG is, frequently, the best option to scale-up antimalarial drugs testing[59]. Besides, SG is far less expensive than the isotopic assay and gives similar or better results than microscopy[82].

Table I.2 – DNA-intercalating fluorescent dyes used in *Plasmodium falciparum*.

DNA fluorescent probe	Target	Excitation maximum	Emission maximum	Permeability	*P. falciparum* assay application
SYTOX Green	Nucleic acids. Double-stranded DNA.	504nm	523nm	impermeable	Parasite viability[85].
YOYO-1	Nucleic acids	491nm	509nm	impermeable	Drug susceptibility[86]. Egress and invasion[87]. Life cycle staging[75]. Parasite burden[88]. Diagnosis[89].
SYTO-16	DNA RNA	488nm 494nm	518nm 525nm	permeable	Apoptosis assessment[90]. Parasitemia measurement[91].
SYTO-61	Nucleic acids.	628nm	645nm	permeable	Growth analysis[92].
Acridine orange	DNA RNA	503nm 503nm	530nm 640nm	impermeable	Diagnosis[93,94].
SYBR™ Green I	DNA	488nm	522nm	permeable	Drug susceptibility[95,96].
Hoechst 33258	DNA	345nm	478nm	permeable	Drug susceptibility[97]. Diagnosis and parasitemia measurement[98]. Life cycle staging[99].
Hoechst 33342	DNA	355nm	465nm	permeable	Parasite quantification and staging[100].

I.5.4.2. Fluorophores targeting ΔΨm

Cell death and/or irreversible damage correlates with the collapse of ΔΨm[101,102]. In this way, the assessment of ΔΨm integrity became a target in viability assays. Because human RBCs lack mitochondria, the ΔΨm signal can only come from parasite mitochondrion[10]. In malaria-infected RBCs, fluorescent dyes are used frequently to monitor ΔΨm, evaluating mitochondrial viability and function. After parasite irreversible injury, SG fluorescence declines 24h later than Rhodamine123 fluorescence (ΔΨm dye)[4]. Because the collapse of ΔΨm, precedes the plasmatic membrane disintegration or DNA disintegration, fluorophores that target the ΔΨm can provide an earlier assessment of cell viability.

Fluorophores used to monitor ΔΨm are normally cations, that became attracted to the negative potential across the inner mitochondrial membrane (Figure I.9). Fluorophores targeting ΔΨm accumulate within the cell because of its capability in crossing hydrophobic membranes and are localized in the mitochondrial matrix (Figure I.9). Some of these dyes have the property of persisting at the mitochondrial linkage, even after fixation.

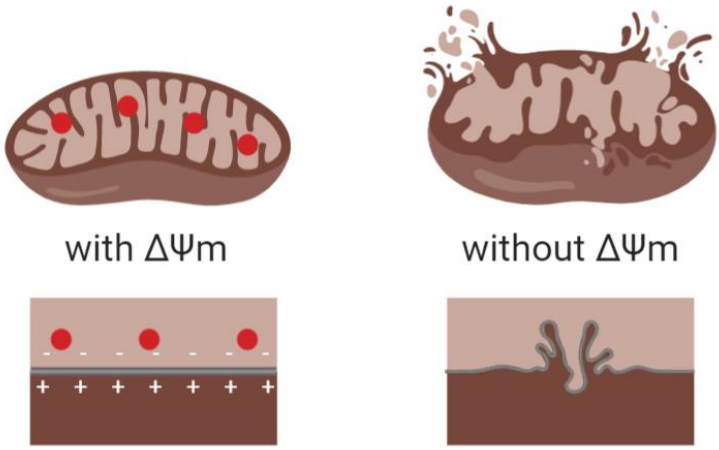

Figure I.9 – Specificity of the ΔΨm dye. Schematic representation of the ΔΨm dye (red circle) specific linkage to the inner membrane of viable mitochondria (left) and the absence of the same fluorophore connection in the presence of a nonviable mitochondrion (right). Created with Biorender.

The most used ΔΨm dyes divide into three families: rhodamine, carbocyanine, and rosamine[31]. All three family dyes are described below and summarized in Table 3:

a) Rhodamine dyes

Rhodamine dyes include Rhodamine123 (Rho123), Tetramethylrhodamine methyl ester (TMRM), and Tetramethylrhodamine ethyl ester (TMRE). Rho123 is a widely used probe but is not well retained by the mitochondria. However, Rho123 linkage is not affected by a mitochondrial membrane potential disruptor, which reveals its inability to evaluate the collapse of mitochondrial membrane potential[103]. As for TMRM and TMRE, they both are highly fluorescent, non-toxic stains that do not form aggregates and emit in an orange spectrum of fluorescence. Upon the collapse of the mitochondrial membrane potential, the decrease of TMRM fluorescence can be easily quantified[104], which is a great advantage for some viability assays applications. In contrast with Rho123, TMRM and TMRE have a low propensity to bind with other sub-organelles or macromolecules. Both

Tetramethylrhodamine stains are an effortless method to apply in simple laboratory facilities and are very low-priced[31]. From all rhodamine dyes, TMRM is probably the more suitable for a reliable viability assay.

b) Carbocyanine dyes

Regarding the carbocyanine dyes, the two most frequently used to monitor ΔΨm are JC-1 and $DiOC_6(3)$[31]. JC-1 has a polychromatic fluorescence emission, it can emit fluorescence in two colors: green – in a monomeric state (without membrane potential) and red – in an aggregate state (in the presence of membrane potential)[31,101]. These dual-emission allows for a differentiation of membrane potential loss by changing its color of emission, which makes JC-1 a very widely used ΔΨm probe[103]. On the other hand, $DiOC_6(3)$ also can be used to monitor cell death[104], but it fails to detect the collapse of ΔΨm[103]. It also binds to other organelle membranes in an unspecific-manner and is affected by numerous factors, such as cell/dye ratio and size[31].

c) Rosamine dyes

Rosamine dyes are a class of fluorophores that are related to rhodamine but lack a carboxylic acid. The loss of carboxylic acid allows for a more flexible structure. This flexibility translates in fluorescence with a more flexible response to environmental changes[105]. Rosamine dyes include tetramethylrosamine and its reduced form dihydrotetramethylrosamine[106]. From these fluorescent compounds, the most recognizable commercial brand is Mitotracker® [31]. Mitotracker®, as opposed to JC-1, does not connect with mitochondrial membrane potential qualitatively (change in colors) but in a quantitative way (increase or decrease in fluorescence emission)[31]. Mitotracker™ Deep Red FM (MTDR) is one of the Mitotracker® dyes and has been used widely for malaria viability assays[9,10]. MTDR emits at 665nm when excited at 644nm. Once linked to the mitochondrial membrane, the MTDR becomes permanently retained. Its retention allows for its persistence even after permeabilization and fixation[31,80]. Such property is due to their thiol-reactive chloromethyl moiety[31].

Table I.3 – Fluorescent dyes used to monitor ΔΨm in *Plasmodium falciparum*.

ΔΨm fluorescent probe	Family dye	Excitation maximum	Emission maximum	ΔΨm collapse detection	Retention after fixation
Rho123	Rhodamine	507nm	529nm	No	No
TMRM	Rhodamine	548nm	574nm	Yes	No
TMRE	Rhodamine	549nm	574nm	Yes	No
JC-1	Carbocyanine	514nm[a] 585nm[b]	529nm[a] 590nm[b]	Yes	No
$DiOC_6(3)$	Carbocyanine	482nm	504nm	No	No
MTDR	Rosamine	644nm	665nm	Yes	Yes

a – monomer form
b – aggregate form

I.5.4.3. Fluorescence detection methods applied to parasite viability quantification

The most widely used methods to detect and quantify fluorophores for parasite viability assessment are based on fluorescence microscopy, fluorometry, and flow cytometry methodologies. Their numerous advantages make them very attractive to reduce intense labor, inter- and intra-assay variability, and save founds. Flow cytometry is in good agreement with microscopy and fluorimetry methodologies[66,69,107]. Among all, flow cytometry has several advantages: its speed of measurement, accuracy, reproducibility, the use of smaller sample volumes, the combination of multiple parameters in the same analysis, results in quantitative information, easily automation and standardization, the possibility of reexamination, and equal sensitivities in laboratory and field conditions[78].

Flow cytometry assays that call upon fluorescent DNA and ΔΨm probes, as SG and MTDR, respectively, became a faster and easier to perform methodology, to assess the viability of malaria parasites. SG dye can distinguish infected from uninfected RBCs (uRBC). However, with only an SG stain, pyknotic* parasites are still accounted for as viable parasites. These pyknotic-like forms can either be dead parasites or dormant forms (see above I.4.2.) of the artemisinin-resistant strains. As MTDR stains functional mitochondria, it labels the viable (dormant) but not the dead (pyknotic) parasites[9,10]. Also, MTDR detects apoptotic events earlier than SG, which can be a way to reduce the experimental time in malaria viability assays from 48h to 24h or less[8].

* Pyknotic parasites are parasites that have suffered irreversible condensation of chromatin in the nucleus of a cell undergoing necrosis or apoptosis.

MTDR permeates and stains very rapidly[10], giving it a well-resolved fluorescence from the green fluorescent of other dyes[108]. This dye, when tested with SG allows for a simple, medium-throughput flow cytometry-based assay to distinguish viable from nonviable parasites[10]. That said, although JC-1 is considered the most reliable mitochondrial membrane potential probe, MTDR is more suitable for experimental conditions that require fixation, hence allowing possible application in field conditions.

SG coupled with MTDR in flow cytometry assays seems the most suitable viability assay to evaluate artemisinin-resistant strains' susceptibility. This methodology can reliably distinguish viable from non-viable parasites, in the presence of dormant rings. Also, MTDR retention allows for a field condition application of such an assay. From this conclusion, a simplistic and fast method, such as the one previously described, can be hereafter employed in earlier detection of dormant parasites from field-collected samples, as well as serve as a complementary characterization technique of the newly synthesized drugs and their targeted pathways.

CHAPTER II

Aims

Aims

P. falciparum viability assays applied either on the diagnosis of resistant-strains or for research purposes, especially for the study of antimalarial therapeutics, have stayed beyond its purposes, mostly due to the new challenges introduced by drug-resistance. Currently used viability assays are challenging, time-consuming, and prone to bias their results in the presence of dormant parasites. The present thesis aims to **develop and optimize a mitochondrion integrity-dependent viability assay**, providing a more reliable and fast methodology to complement studies of new antimalarial drugs. For this, we outlined the following specific objectives:

II.1 – Optimization of a viability quantification assay based on mitochondrial membrane potential.

a) Optimization of the staining conditions for the Mitotracker™ Deep Red and SYBR™ Green I: concentration of dyes and incubation time.

b) Validation of the viability assay.

c) Adaptation to field conditions (fixation).

II.2 – Characterization of the activity of a newly synthesized antimalarial candidate molecule (Ru2).

a) Determine the effect of Ru2 on the *Plasmodium falciparum* mitochondrial membrane potential ($\Delta\Psi m$).

b) Characterize the stage-specific activity of the new compound using the developed viability assay.

c) Evaluation of the cytocidal activity of Ru2 against *Plasmodium falciparum.*

CHAPTER III

Methods

Methods

III.1. DESCRIPTION OF TECHNIQUES

III.1.1. Thawing of cryopreserved *Plasmodium falciparum* samples

The vial was thawed with 0.2mL of 12% NaCl solution (see Annex I), during homogenization with this solution. The mixture was left to rest at room temperature for 3min. Then, the sample mix was added to 10mL of 1.6% NaCl solution (see Annex I) in a falcon tube. The mixture was homogenized and centrifuged at 2,000rpm for 5min. The supernatant was rejected, followed by the addition of 10mL of salt-dextrose solution (see Annex I) to the pellet. The solution was homogenized and centrifuged at 2,000rpm for 5min. Finally, the pellet was resuspended in RPMIc medium (see Annex I) and transferred to a culture flask. The culture maintenance occurred at 37°C, with 5% CO_2. When thawing cryopreserved *P. falciparum*-infected RBCs, time and temperature become critical for optimal recovery of the sample. It is advisable to proceed with speed and to maintain all solutions at the same temperature. If needed, an adjustment of the culture hematocrit is done, with the addition of uRBC (see Annex II). The protocol used is in agreement with [109].

III.1.2. *Plasmodium falciparum* cell culture

The continuous cell culture maintenance demanded to an RPMI 1640 complete medium formulation that includes Hepes buffer, Albumax, hypoxanthine, and $NaHCO_3$ (see Annex I), and to an atmosphere of 5% CO_2, 5% O_2, and 90% N_2 at 37 ºC, in an incubator. A daily change in medium was performed, as also the addition of fresh RBCs (see Annex II) every 3-4 days. Parasitemia (see III.1.4.) was assessed daily from a Giemsa-stained smear[110] (see III.1.3.) to keep parasitemia below 5%. The method was previously described by[110] and applied with modifications.

III.1.2.1. Cell culture maintenance

In an identified 50mL culture flask, it was added 3mL of pre-warmed at 37°C RPMIc medium (see Annex I) with 75µl of iRBCs and 150µl of 50% uRBCs (see Annex II), to a final hematocrit of 5%. The culture flask incubated at 37°C, with 5% CO_2. At the end of a 24h period, the medium was discarded and replaced with the same amount of fresh medium. When the parasitemia reached 5%, the culture was reconstituted, with the disposal of a culture portion and the addition of medium and uRBC, to a final hematocrit of 5%.

III.1.3. Giemsa-stained smear

Small samples of the settled RBCs, in culture flask, were taken with a capillary pipette and deposited in a cleaned and labeled glass microscope slide, to perform a blood smear. The dried blood smear was fixated with a wash of 100% methanol (the smear must be well dried from the methanol bath to avoid further precipitates). The blood smear was covered with a filtered solution of Giemsa at 20% (see Annex I) in for 15min. The smear was washed with tap water and left to dry.

III.1.4. Parasitemia assessment

The parasitemia was assessed by a microscopical observation of a Giemsa-stained smear (see III.1.3.), with a 1,000x magnification in an oil-immersion objective. The number of iRBCs was registered in 10 microscopical fields in proportion to the total number of RBCs found in these fields. This parameter was presented as a percentage, multiplying the registered value for 100, as shown in the following equation:

$$Parasitemia\ (\%) = \frac{\tilde{x}\ (number\ of\ parasitized\ erythrocytes\ in\ 10\ fields)}{\tilde{x}\ (number\ of\ erythrocytes\ in\ 10\ fields)} \times 100$$

III.1.5. *Plasmodium falciparum* culture synchronization

The synchronization process of a *P. falciparum* culture allows the retrieval of only ring-stage parasites[111]. Due to the increased uptake of substrates by the infected RBC membrane

pores, sorbitol (substrate) treatment-induced on these cells destroys the parasites through osmotic lysis[111–113]. Ring-stage parasites that induce lower uptakes on the RBC membrane pores can resist the lysis better than the more maturated stages[111]. Hence, the culture was maintained until it reached 5-10%, with a prevalence of ring-stage parasites. At this level, the culture centrifuged at 2 500rpm for 5min. After supernatant removal, it was added to the pellet 10x its volume of D-sorbitol 5% (see Annex I). The mixture incubated at 37°C for 10min, with vigorous mixing at half-time, and vortex for 5 seconds at the end. Then, the mixture centrifuged at 2,500rpm for 5min. Its supernatant was discarded and replaced with sterile PBS (see Annex I). A second and third centrifugations were perfomed at 2,500rpm for 5min, with two more identical PBS wash steps. The pellet was reconstituted in RPMIc (see Annex I), with the addition of uRBC (see Annex II) to complete a final hematocrit of 5%. The cell culture was submitted to three sorbitol treatments to narrow the age of the ring-stage parasite. The Sorbitol treatment schedule portrays below, Figure III.1. The following protocol is described by[111], and here applied with modifications.

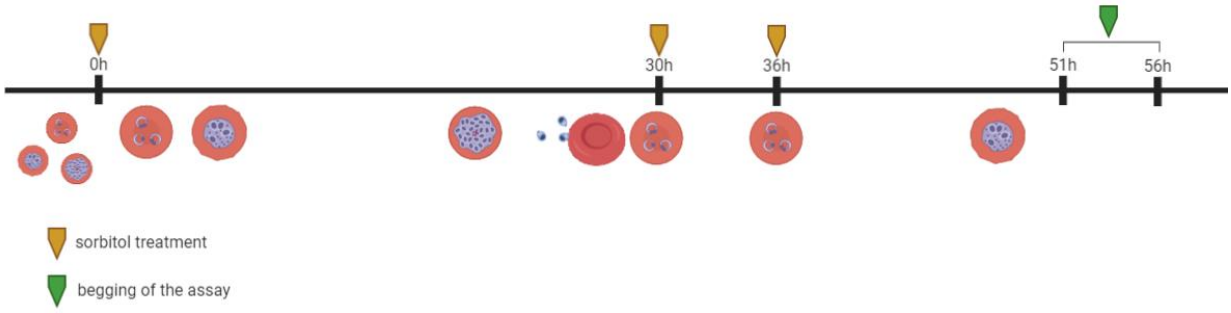

Figure III.1 – Time-lapse of the sorbitol treatment schedule. Timing of the sorbitol treatments (yellow arrows) and begging of the assay for 20-24hhpi trophozoite stage (green arrow) overlaid with *P. falciparum* culture life cycle stages. Created with Biorender.

III.2. METHODOLOGY

III.2.1. Viability quantification of *Plasmodium falciparum* after exposure to antimalarials

III.2.1.1. Induction of the ΔΨm collapse

3D7 cultures incubated with atovaquone (ATQ; 500nM, 5µM, and 10 µM, equivalent to 100x, 1,000x, and 2,000x IC_{50})[39,114], and 80nM, 800nM and 8 µM of Ru2, equivalent to its 10x, 100x, and 1,000x IC_{50} (37°C, 5% CO_2). At the same time and in the same conditions, a 3D7 culture incubated with RPMI (negative control). After treatment, cells were washed with PBS (see Annex I) for three times (2,500rpm for 1min).

III.2.1.2. ΔΨm assay

III.2.1.2.1. Fluorescent probe staining

III.2.1.2.1.1. Mitotracker™ Deep Red FM

Before the MTDR staining procedure, cell suspensions were washed three times with PBS at 2,500rpm for 1min. Then, 3% hematocrit and 3% parasitemia cell suspensions were stained with MTDR (concentrations tested ranged between 100nM and 600nM) (see Annex I) at 37°C. Finished incubation time, three wash steps were performed with the addition of 500µl of PBS (see Annex I) and centrifugations of 2,500rpm for 1min. The protocol is in agreement with [9,108].

III.2.1.2.1.2. SYBR™ Green I

Before the SG staining procedure, cell suspensions were washed three times with PBS at 2,500rpm for 1min. Then 3% hematocrit and 3% parasitemia cell suspensions stained with SG^9 (concentrations tested ranged between 0.03125x and 2x) at 37°C. (Optional: Three wash with the addition of 500µl of PBS and centrifugations of 2,500rpm for 1min follow the staining.) The protocol is in agreement with [9,80,108].

III.2.1.2.2. Fixation

Fixations were performed in MTDR-stained 3D7 cultures at 0.3% hematocrit and 1% parasitemia and incubated in the fixation solutions (0.025% glutaraldehyde, 4% paraformaldehyde with 0.0075% glutaraldehyde, and 2% paraformaldehyde with 0.06% glutaraldehyde) for 20min at RT. At the same time and in the same conditions, an MTDR-stained 3D7 culture was incubated with PBS (negative control). This fixation step took place between the MTDR stain and SG stain in the ΔΨm assay.

III.2.1.2.3. Flow cytometry

All previously stained samples and controls were submitted to a 0.3% hematocrit reduction. Then, 200µl of all cell suspensions were transferred to a 96-well plate. Cell suspensions were examined using a 488nm and a 633nm laser on a CytoFLEX V0-B4-R2 Flow Cytometer (Beckman-Coulter), collecting data from 10,000-100,000 events. CYTOFLEX and Flowjo™ for Windows, version X 10.07r2 (Becton, Dickinson, and Company), was used to collect, analyze, and represent all cytometric data. The geometric mean (GM) of fluorescence and percentage of green fluorescence emitting events within RBC population was retrieved.

III.2.1.2.3.1. Gating strategy for 3D7HT-GFP cell suspensions

The first gate (Figure III.2, Gate I) targeted single events. The exclusion of doublets from this gate subtracted abnormal fluorescence emission, which could cause a misinterpretation of the results. The second gate (Figure III.2, Gate II) defined cell morphology, eliminating cellular debris and other events that could emit fluorescence and skew further plots. Finally, the infected RBC (iRBC; RBCs infected with 3D7HT-GFP parasites) population (Figure III.2, Gate III) was identified by GFP green fluorescence emission from 3D7HT-GFP parasites, on a FITC-H/PE-H[†] plot[115]. The iRBC population is defined by events emitting higher intensities of green fluorescence than yellow fluorescence. The presented flow cytometric gating strategy was based on [100,116].

[†] FITC channel measures the GFP signal emitted by iRBCs (510nm, green), and PE channel measures the background fluorescence (585/42nm, yellow).

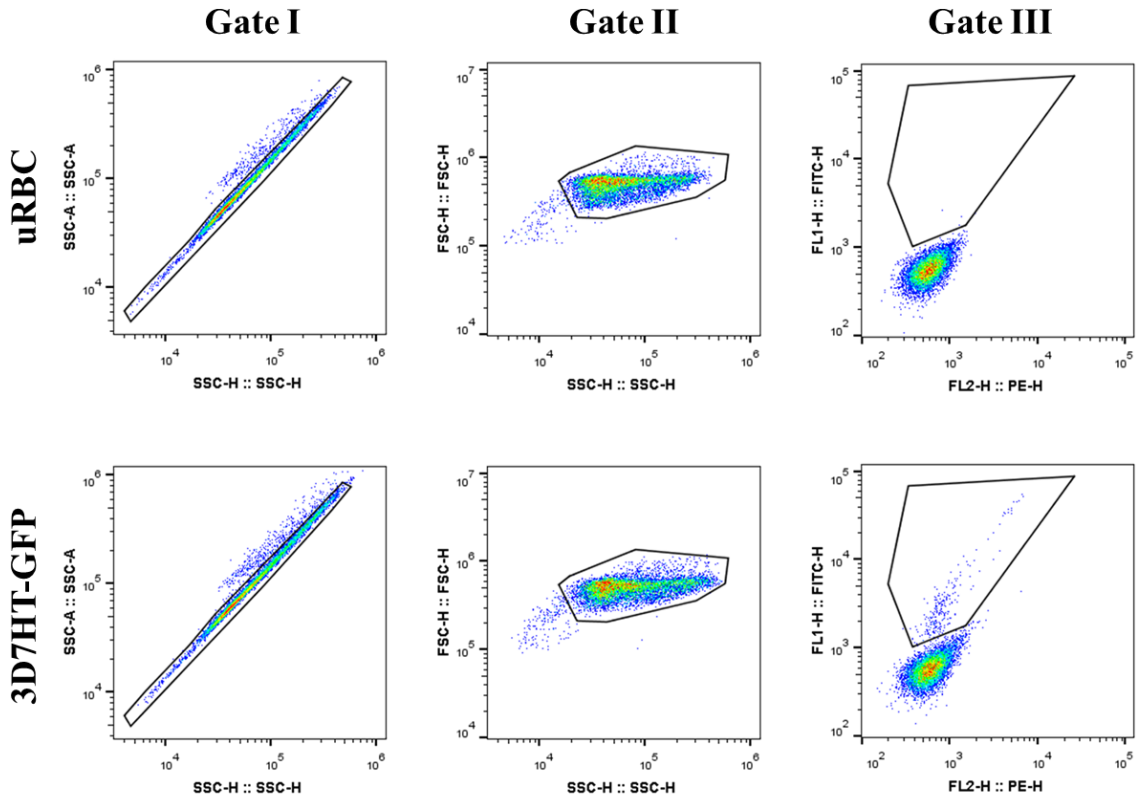

Figure III.2 – Gating strategy for the detection of 3D7HT-GFP infected RBCs. Gate I: single events. Gate II: RBC. Gate III: RBC infected with a 3D7HT-GFP strain (10,000 recorded events). uRBC, uninfected RBC. SSC-A, side scatter – area. SSC-H, side scatter – height. FSC, forward scatter. FL, fluorescence channel. FITC, fluorescein isothiocyanate (green). PE, phycoerythrin (yellow).

III.2.1.2.3.2. Gating strategy for 3D7 cell suspensions stained with SYBR™ Green I

Similarly, to the previous gating strategy (see III.4.1.2.3.1), a gate of single events was defined (Figure III.3, Gate I). Then, single-cell events were gated according to the RBC morphology (Figure III.3, Gate II). Finally, SG stained iRBCs were retrieved from a population emitting fluorescence in a green spectrum (Figure III.3, Gate III).

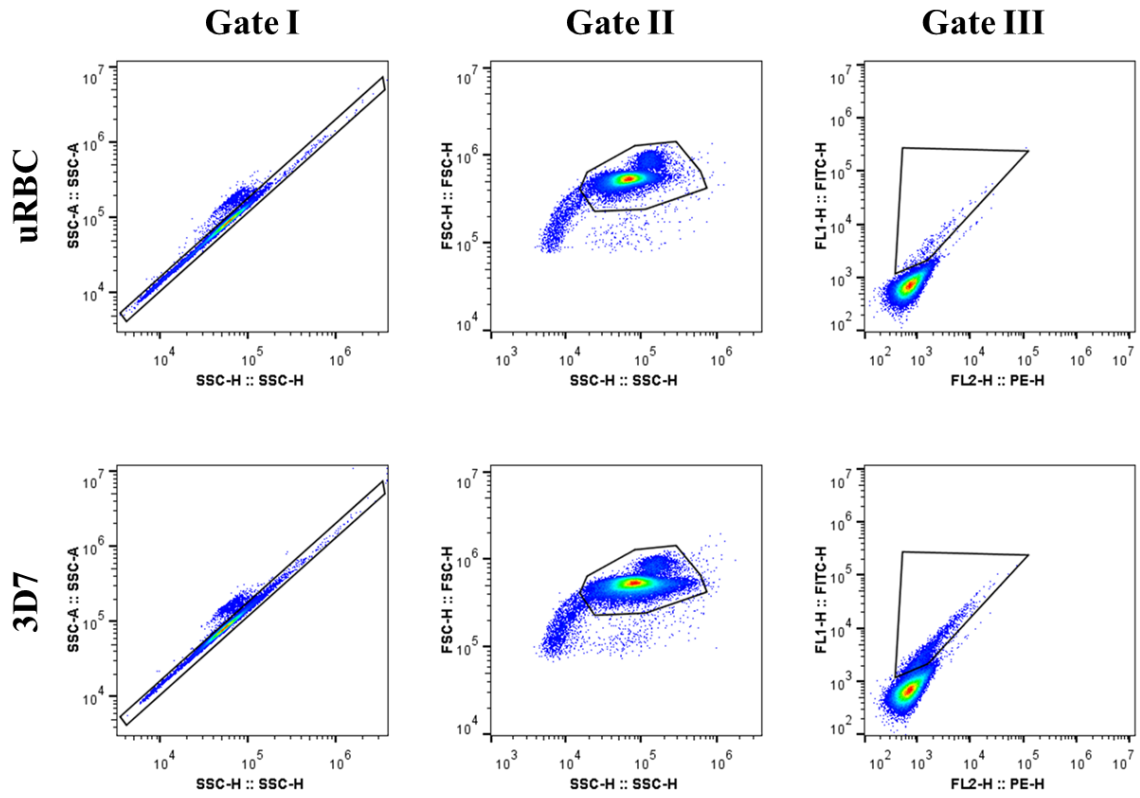

Figure III.3 – Gating strategy for SYBR Green I-stained 3D7. Gate I: single events. Gate II: RBC. Gate III: RBC infected with a 3D7 strain (100,000 recorded events). uRBC, uninfected RBC. SSC-A, side scatter – area. SSC-H, side scatter – height. FSC, forward scatter. FL, fluorescence channel. FITC, fluorescein isothiocyanate (green). PE, phycoerythrin (yellow).

III.2.1.2.3.3. Gating strategy for 3D7 cell suspensions stained with SYBR™ Green I and Mitotracker™ Deep Red FM

Adapting the previous gating strategy (see III.4.1.2.3.2.) to the addition of a far-red fluorescent probe, events were firstly treated with single event identification (Figure III.4, Gate I). Later, the RBC morphology was defined (Figure III.4, Gate II). At the end, iRBC population was retrieved from a population emitting both green and red fluorescence (Figure III.4, Gate III).

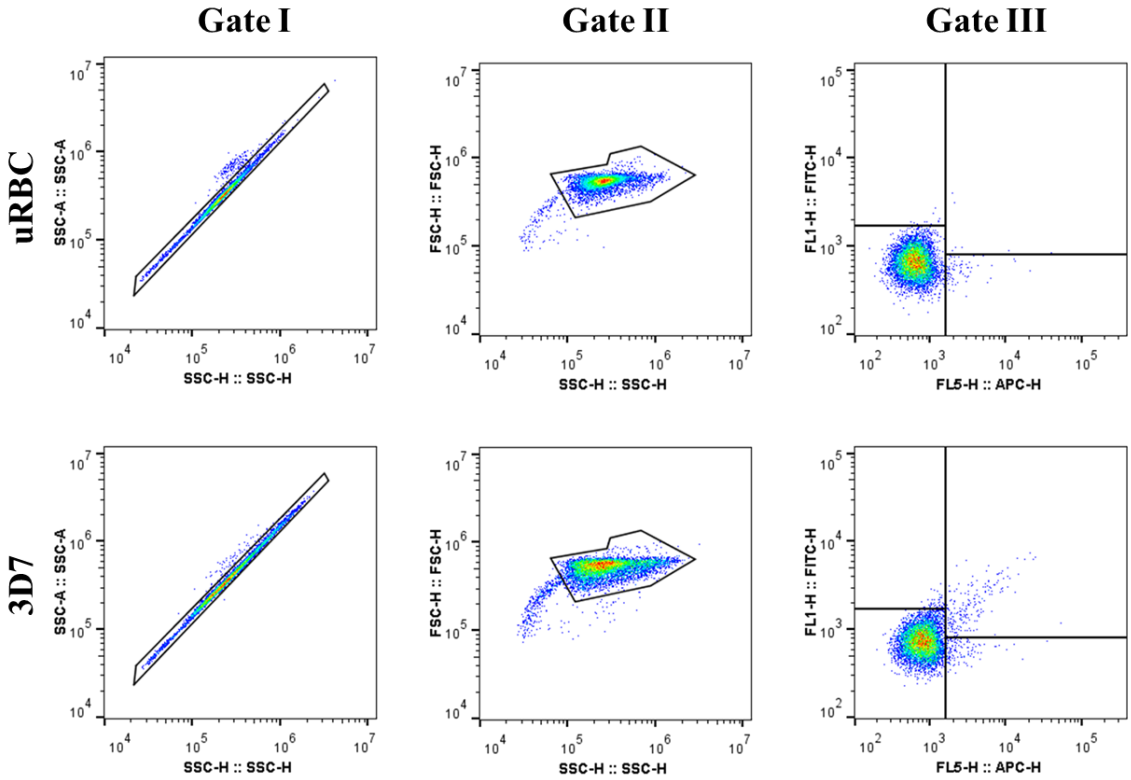

Figure III.4 – Gating strategy for Mitotracker™ Deep Red FM and SYBR™ Green I-stained 3D7. Gate I: single events. Gate II: RBC. Gate III: RBC infected with a 3D7 strain (10,000 recorded events). uRBC, uninfected RBC. SSC-A, side scatter – area. SSC-H, side scatter – height. FSC, forward scatter. FL, fluorescence channel. FITC, fluorescein isothiocyanate (green). APC, allophycocyanin (red).

III.2.1.2.4. Microscopy

For microscopical observations, 10µl of each stained sample were transferred to an identified glass slide. The suspension was carefully covered with a coverslip and sealed with nail polish to prevent liquid escape. Glass slides were examined on a bright-field microscope and/or fluorescence microscope recording pictures of sample representative parasites. ImageJ 1.52 (National Institutes of Health, USA) was used to process all images collected.

III.2.1.2.5. Statistical analysis

GraphPad Prism version 6.01, 2012 (GraphPad Inc.) was used to perform the Mann-Whitney test. The non-parametric Mann-Whitney test detects differences between the two analyzed groups. A significant difference is assumed when $p < 0.05$.

III.2.2. Determination of the Cytocidal activity of compounds

III.2.2.1. Cell treatment:

3D7 synchronized culture with 22-28hpi trophozoites and 3-9hpi rings (3% hematocrit and 1% parasitemia) incubated with 10x IC_{50} (80nM) for 3h and 6h (37°C, 5% CO_2) in a 96-well plate. Cells also incubated with RPMI for a negative control. After 3h and 6h of treatment, all cells underwent PBS washing.

III.2.2.2. Growth assessment after 48h by flow cytometry:

Cells incubated with RPMI for 48h (37°C, 5% CO_2). Then, they were stained with 0.5x SG in PBS. Hematocrit was reduced to 0.3% and parasitemia was quantified using a 488nm and a 633nm laser on a Beckman-Coulter CYTOFLEX flow cytometer, collecting data from 100,000 cells. The percentage of green fluorescence emitting events within RBC population was retrieved to calculate parasitemia

III.2.2.3. Growth assessment after 96h by flow cytometry:

Samples were diluted 1:16 and allow to grow for an additional two cell cycles (4 days – 96h). Cells were stained with 0.5x SG in PBS and underwent a hematocrit reduction to 0.3%. Parasitemia was quantified using a 488nm and a 633nm laser on a Beckman-Coulter CYTOFLEX flow cytometer, collecting data from 100,000 cells. The percentage of green fluorescence emitting events within RBC population was retrieved to calculate parasitemia.

III.2.2.4. Morphological characterization by Giemsa-stained smears:

Cell suspensions after the 48h and 96h of growth were used to perform Giemsa-stained smears (see III.1.3.). Images were analyzed in a bright-field microscope, with an oil

immersion objective, at 1,000x magnification. ImageJ 1.52 (National Institutes of Health, USA) were used to process all images collected.

III.2.2.5. Statistical analysis

GraphPad Prism version 6.01, 2012 (GraphPad Inc. All rights reserved) was used to perform the Mann-Whitney test. The non-parametric Mann-Whitney test detects differences between the two analyzed groups. A significant difference is assumed when $p < 0.05$.

CHAPTER IV

Results and Discussion

Results and Discussion

IV.1. PARASITE VIABILITY ASSAY BASED IN FLOW CYTOMETRY EVALUATION OF MITOCHONDRIAL MEMBRANE POTENTIAL

Artemisinin-resistant *P. falciparum* strains can enter a dormant form. This phenotype includes growth arrest at ring-stage and morphological resemblance with dead/pyknotic parasites, reducing metabolic activity to minimal functions such as apicoplast metabolism or mitochondrial membrane potential[5,54]. Morphologically, it is virtually impossible to distinguish viable from arrested/dormant parasites. Hence a more sensible and reproducible method is needed.

Mitochondrial membrane potential ($\Delta\Psi m$) is an important indicator of mitochondrial function and dysfunction. Fluorescent dyes accumulation in mitochondria can be optically detected by flow cytometry. We chose Mitotracker™ Deep Red FM (MTDR; a far red-fluorescent dye) to stain active mitochondria in live parasite cells. MTDR's well-resolved fluorescence from the green fluorescence of other probes (like SYBR™ Green I), allows for a dual stain approach[108]. MTDR provides rapid staining; it is well-retained after fixation and/or permeabilization with detergents, hence allowing quantitative measurement of $\Delta\Psi m$[31,108] in future field adapted assays (in conditions where flow cytometry is not readily available). In combination with SYBR™ Green I, it has been tested in flow cytometry viability assays (of malaria parasites)[9], demonstrating good resolution between viable and non-viable parasites. Hence, the MTDR staining specificity for viable *P. falciparum* was put to test. Its retention within intact mitochondria and the flow cytometry quantification of its fluorescence was evaluated.

The microscopical observation of MTDR stained samples granted a visual confirmation of the parasite mitochondria specific staining by MTDR. GFP showed the cytosol dimension of the trophozoite-stage parasite, whereas MTDR identified the parasite mitochondrion (Figure IV.1). The merge of both emissions revealed the position of the mitochondrion within the cytosol. The pattern of the MTDR red fluorescence emission on the trophozoite-

stage parasite agrees with mitochondrial targeting fluorescent probes emission[114,117,118] and with the morphological characterization of the parasite mitochondria in this intra-RBC life cycle stage[23,30]. *P. falciparum* mitochondria are described as a tubular-like organelle, that grows in size, by elongation and branching, in the trophozoite stage, appearing to fuse back on itself[23].

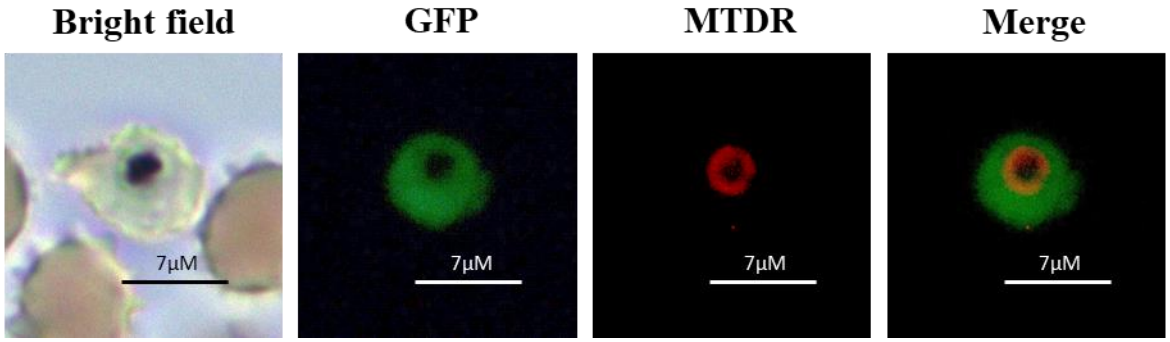

Figure IV.1 – *Plasmodium falciparum* 3D7HT-GFP strain stained with Mitotracker™ Deep Red FM. From left to right: bright-field image, GFP, and MTDR fluorescence emission, and both emissions merged on a trophozoite-stage parasite (3D7HT-GFP, 250nM MTDR, 1,000x magnification under oil immersion objective). GFP, green fluorescence protein; MTDR, Mitotracker™ Deep Red FM.

Flow cytometry analysis of MTDR-stained parasites allowed us to quantify the result obtained by fluorescence microscopy. GFP fluorescence emission was analyzed in a green fluorescence[‡] channel and MTDR fluorescence emission was analyzed in a red fluorescence channel[§]. A red and green fluorescence group of events (iRBC) detached from the major population (uRBC), Figure IV.2. The green fluorescence is indicative of the presence of cytoplasmatic GFP produced by 3D7HT-GFP strains. The set of green fluorescent events is also emitting red fluorescence from MTDR accumulated within viable mitochondria. As expected[9], flow cytometry of MTDR stained *P. falciparum* granted a discriminative and quantitative method for the identification of parasites.

[‡] GFP fluorescence emitted by 3D7HT-GFP strains: 510nm, green.
[§] MTDR fluorescence emitted by stained iRBCs: 665nm, red.

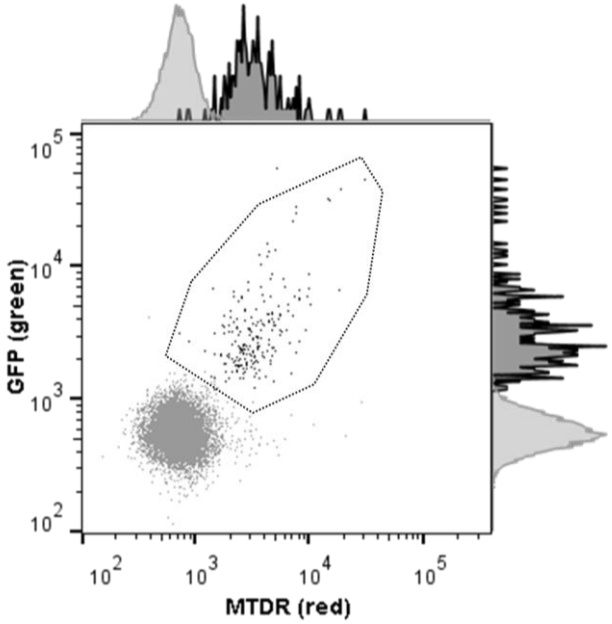

Figure IV.2 – Flow cytometry detection of viable parasites by GFP and Mitotracker™ Deep Red FM. Green and red fluorescence plot with adjunct histograms, corresponding to the GFP and MTDR fluorescence emission (3D7HT-GFP, 250nM MTDR; 10,000 recorded events). Gray – uninfected RBCs (from a gate II). Black, gated – infected RBCs (from a gate III). GFP, green fluorescent protein. MTDR, Mitotracker™ Deep Red FM.

To develop a methodology based in flow cytometry for the discrimination of viable *vs* unviable *P. falciparum* parasites several steps were taken: i) optimization of staining conditions (time and concentration); ii) evaluation of its discrimination power between intact and collapsed mitochondrial membrane potential (ΔΨm); iii) adaptation to field conditions.

IV.1.1. Optimization of Mitotracker™ Deep Red FM concentrations

In this optimization step, the 3D7HT-GFP strain expressing GFP was used (see III.2.1.). The intrinsic green fluorescence of the GFP strain circumvents the need for a second fluorescent probe (samples were stained and processed as in III.4.1.2.1.1.).

Three MTDR concentrations were tested (100nM, 250nM, and 600nM, chosen according to [9,108]) to distinguish viable parasites. Three independent assays were performed, each with one or two biological replicas and six technical replicas. Representative results are shown in Figure IV.3. All 3 MTDR concentrations were capable of staining iRBCs and a higher red fluorescence emission than uRBCs can be observed in all 3 tested concentrations. However, 600nM of MTDR indices very high red fluorescence emission from the uRBC, without conferring higher resolution between iRBCs *vs* uRBCs. Parasitemia values were estimated by flow cytometry-based in red (MTDR) and green (GFP) fluorescence. When compared to 100nM and 600nM, staining with 250nM of MTDR gave closer red/green-parasitemia values (Figure IV.3).

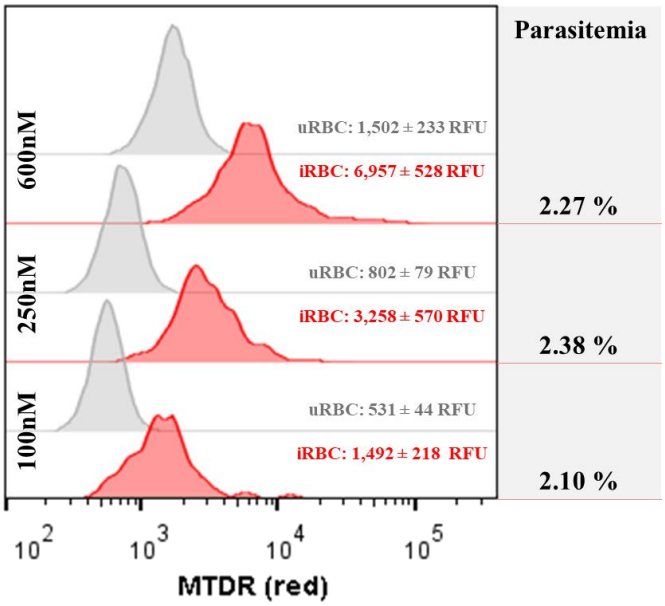

Figure IV.3 – Mitotracker™ Deep Red FM Red fluorescence emission at different concentrations. MTDR fluorescence histograms for the 600nM, 250nM, and 100nM concentrations (3D7HT-GFP; 10,000 recorded events), followed by the geometric mean (GM) of fluorescence (GM ± standard deviation, RFU), and parasitemia (percentage of events emitting both green and red fluorescence). uRBC, uninfected RBC (gray line histogram, from a gate II). iRBC, infected RBC (red line histogram, from a gate III). RFU, relative fluorescence units.

The 250nM concentration did not interfere with the second fluorescence probe GFP, nor cause morphologically evident damage to iRBCs or uRBCs (Annex I and II). Hence the 250nM of MTDR concentration was chosen to implement further optimization steps.

IV.1.2. Optimization of Mitotracker™ Deep Red FM incubation time

Two periods were chosen, 15min and 30min (according to [108]), corresponding to the minimum and medium time required for the specific staining of ΔΨm, respectively. RBCs infected with a 3D7HT-GFP (iRBCs) were stained with 250nM of MTDR (as in III.4.1.2.1.1.) and gated as described in Figure III.2. The results are presented in Figure IV.4. Samples stained during 15min achieved similar resolution as those stained for 30min. Therefore, the shortest incubation time (15min) was adopted during further optimization steps.

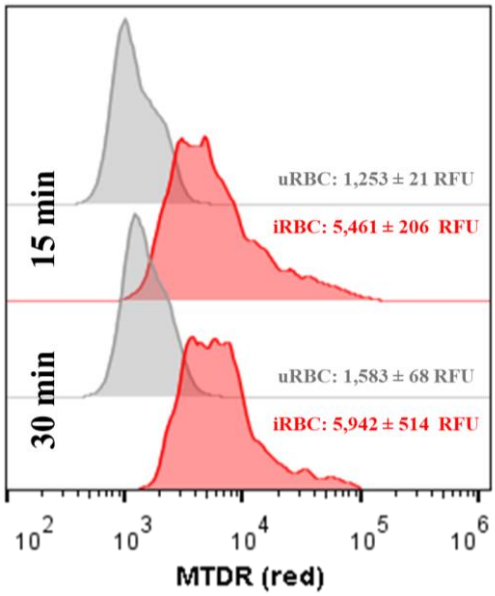

Figure IV.4 – Mitotracker™ Deep Red FM Red fluorescence emission after different incubation times. MTDR fluorescence histograms for the 15min and 30min incubation times (3D7HT-GFP; 100,000 recorded events), followed by the geometric mean (GM) of fluorescence (GM ± standard deviation, RFU). uRBC, uninfected RBC (gray line histogram, from a gate II). iRBC, infected RBC (red line histogram, from a gate III). RFU, relative fluorescence units. MTDR, Mitotracker™ Deep Red FM.

IV.1.3. Optimization of a differential staining with SYBR™ Green I

Our aims included the optimization of the ΔΨm assay to be used not only with 3D7-GFP but with other *P. falciparum* parasites in particular strains with different drug-resistance phenotypes and to be used for *ex vivo* assays (with infected RBCs withdrawal directly from patients). These adaptations require the addition of a second fluorescent probe (to

discriminate the parasite) such as SYBR™ Green I. SYBR™ Green I (SG) is a membrane-permeable DNA intercalating green fluorescent dye[10,80] that discriminates iRBCs (infected RBCs) from uRBCs[**] (uninfected RBCs). In combination with MTDR (fluoresces red with sustained $\Delta\Psi m$) it allows the resolution of the viable from unviable parasites using flow cytometry[9,10]. To optimize SG staining conditions, the 3D7 strain (see III.2.1.) was used.

Three SG concentrations were tested (0.5x, 1x, and 2x, chosen according to [80], with 15min of incubation) to distinguish iRBC from the uRBC population within the sample. Washing after staining was also analyzed to assess the impact in SG staining. One independent assay was performed, with one biological replica and two technical replicas for each SG concentration and washing conditions. Resolution improved as the SG concentration increased (Figure IV.5-A, iRBC fluorescence increase). The gain in resolution with higher SG concentration benefited from washing after staining. Particularly in green fluorescence emission decrease of 2x SG stained uRBC, probably due to unspecific staining caused by 2x SG. All 3 SG concentrations gave concordant values with the parasitemia[††] calculated from microscopy (Figure IV.5-B). Nonetheless, although not statistically significant, washing steps resulted in slightly lower parasitemia percentages.

[**]Human RBCs are anucleate cells. The absence of a nucleus, and therefore DNA molecules, allows the discrimination of uRBC from a parasitized sample, by the lack of fluorescence emitted from DNA specific dyes in these cells.

[††] Parasitemia of cell suspensions submitted to a flow cytometry reading was obtained from the 'percentage of green fluorescence emitting events within RBC population (see Gate II and III, Figure III.3).

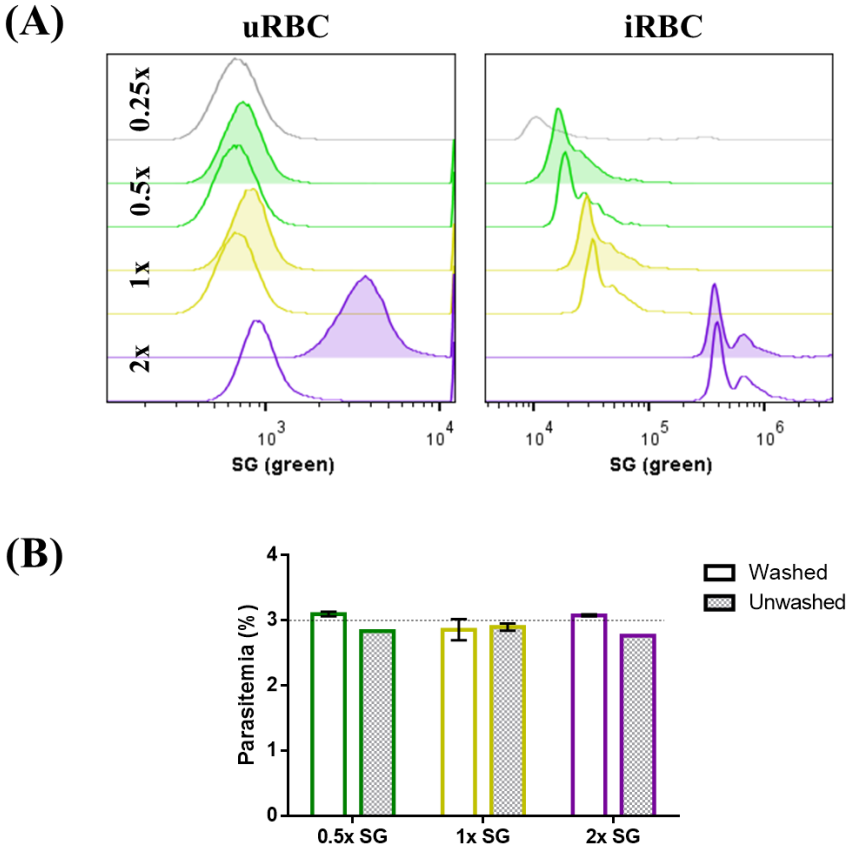

Figure IV.5 – SYBR™ Green I fluorescence emission after different concentrations and wash procedures. (A) SG fluorescence histograms for the uRBC (top, left) and iRBC (top, right) stained with 0.25x, 0.5x, 1x and 2x concentrations, with a posterior wash step or its absence (3D7, events retrieved from Gate II for uRBC and III for iRBC, within 100,000 events recorded). uRBC, uninfected RBC. iRBC, infected RBC. 0.25x SG, gray line histogram. 0.5x SG, green line histogram. 1x SG, yellow line histograms. 2x SG, purple line histograms. Washed samples, uncolored histograms. Unwashed samples, colored histograms. (B) Parasitemia obtained from the 0.5x, 1x, and 2x SG concentrations with or without the wash step after stain ($p > 0.05$ between wash and unwashed conditions). The dotted line stands for the parasitemia calculated from microscopical observation of Giemsa-stained smears. Error bars represent SEM.

Staining with 0.5x SG, allows the detection of iRBC as accurately as, with higher concentrations. Introducing a wash step, although beneficial, was not critical for the accurate quantification of iRBC. Hence, the lower concentration (0.5x) and the fastest approach (without a posterior wash step) was adopted in further optimization steps.

IV.1.4. Mitochondrial membrane potential (ΔΨm) evaluation using Mitotracker™ Deep Red FM assay

P. falciparum-infected RBCs were treated with atovaquone (as in III.4.1.1.) as a control for the method reliability in the identification of a ΔΨm breakdown. The ΔΨm of the *P. falciparum* is created by complexes III and IV of the mitochondrial inner membrane when pumping protons from the matrix to the intermembrane space[31]. Atovaquone is a known antimalarial drug as a bc1 (complex III) inhibitor[39], therefore capable of inducing a decrease in ΔΨm dependent fluorescence[39,114], due to membrane collapse[119]. Samples were stained as optimized, according to III.4.1.2.

IV.1.4.1. Impact of ATQ treatment in the viability of an asynchronous *Plasmodium falciparum* cell culture

To determine the impact of ATQ treatment in the viability of the parasites, asynchronous *P. falciparum* cultures were treated during 6h with two different concentrations, 500nM and 5μM, corresponding to the 100x $IC_{50,}$ and 1,000x IC_{50}, respectively (conditions chosen according to [39,114]). One independent assay with two biological replicas and 6 technical replicas each was performed. ATQ impact was evaluated using the ΔΨm assay (III.4.1.2., adding optimized conditions established in IV.1.1.-IV.1.3.) and the results are presented in Figure IV.9. Red fluorescence emission was only detected in MTDR stained parasites[‡‡], corroborating the efficiency of our assay. However, it was not possible to detect a significant difference in red fluorescence emission (ΔΨm quantitative parameter) between treated and untreated cultures, with either of the two ATQ tested concentrations (Figure IV.6).

[‡‡] Geometric mean of fluorescence was only counted on samples with more than 10 events collected in the red fluorescence channel, within the iRBC spectrum range.

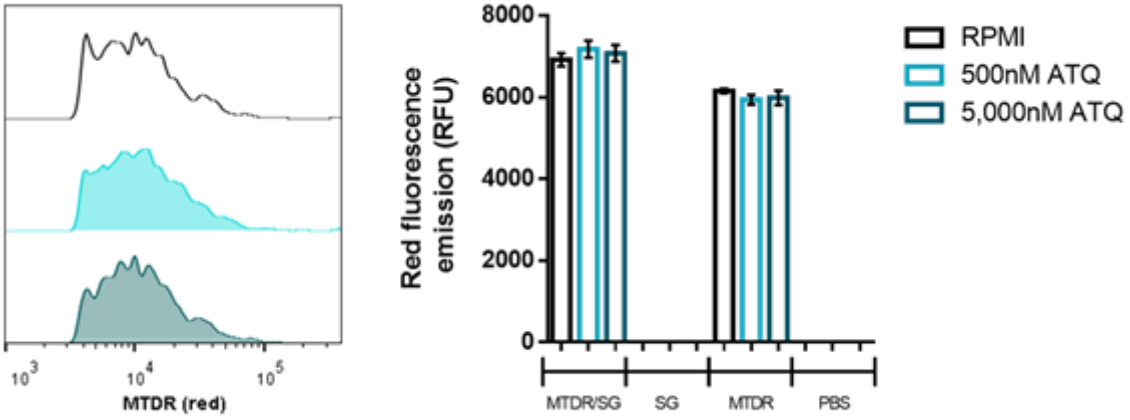

Figure IV.6 – ΔΨm variation in *P. falciparum* asynchronous-cultures treated with ATQ. Geometric mean (GM) of the red fluorescence emission obtained from the following treatments: RPMI, 500nM ATQ, and 5µM ATQ. Samples incubated with MTDR and SG, SG only, MTDR only, and PBS after ATQ treatment (3D7, 250nM MTDR, 0.5x SG, events retrieved from Gate III, within 100,000 events recorded). $p > 0.05$ between ATQ-treated and RPMI-treated conditions. Error bars represent SEM. ΔΨm, mitochondrial membrane potential. RFU, relative fluorescent units. MTDR, Mitotracker™ Deep Red FM. SG, SYBR™ Green I. PBS, phosphate buffer saline. ATQ, atovaquone.

ATQ exerts greater effect on trophozoite-stage parasites[32,120]. Culture asynchrony widens samples MTDR fluorescence emission spectrum, due to the different ΔΨm owed by distinct stage parasites[23,30,121]. The ΔΨm collapse in trophozoites within an asynchronous culture can be masked by equal intensities of MTDR fluorescence emitted by other stages.

a) Stage-specific fluorescence emission of Mitotracker™ Deep Red FM

To evaluate the possible interference of the parasite-stage in the assessment of ΔΨm in asynchronous cultures, MTDR stage-specific fluorescence emission was evaluated on rings and trophozoites. *P. falciparum* (strain 3D7) cultures were synchronized with sorbitol (as in III.3.5.) and level of synchrony confirmed by Giemsa-stained smears (as in III.3.3.). Rings (15-20hpi) and trophozoites (30-36hpi) were double-stained with MTDR and SG (as in III.4.1.2.), two independent assays were performed with 2-6 technical replicas and representative results are shown in Figure IV.7. MTDR fluorescence reveals different intensities between rings and trophozoites, proportional to the SG fluorescence emitted by the same stages. Trophozoites bear the higher red fluorescence emission, as opposed to rings that emit in between uRBCs and trophozoites fluorescence.

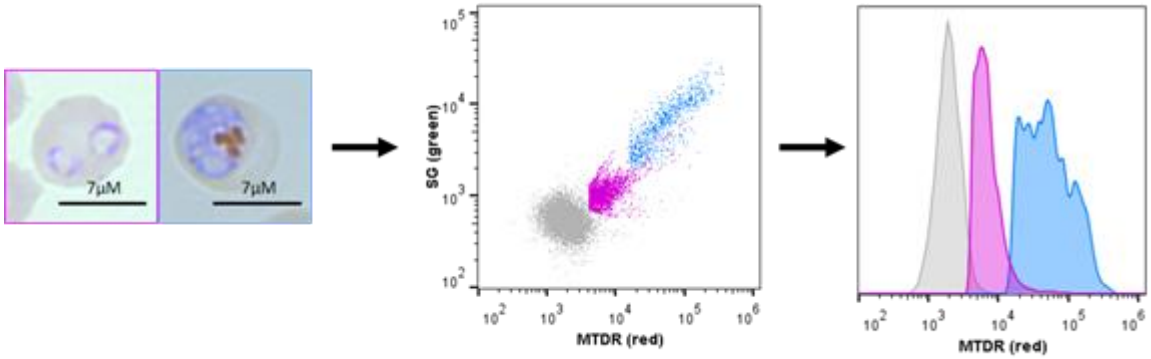

Figure IV.7 – Mitrotracker Deep Red FM fluorescence emission of synchronized *Plasmodium falciparum* on rings and trophozoites. Giemsa-stained smears (1,000x magnification) of rings (15-20hpi) and trophozoites (30-36hpi), and their corresponding SG and MTDR fluorescence emission, and MTDR fluorescence emission only (3D7, 250nM MTDR, 0.5x SG, events retrieved from Gate II for uRBC and III for rings and trophozoites, within 100,000 events recorded). Rings, pink. Trophozoites, blue. uRBC, gray. SG, SYBR™ Green I. MTDR, Mitotracker™ Deep Red FM.

MTDR fluorescence emission of stage-specific parasites is proportional to the expected extension of its mitochondrial membrane[23,30,121]. Ring-stage parasites usually contain a single small mitochondrion, contrasting with trophozoite-stage where mitochondrion morphology progressively develops in size and complexity[23], being capable of retaining a higher number of fluorescent probes. Previous stage-specific identification assays with Mitotracker® probes have also reported the same fluorescence emission pattern[122,123].

b) Implementation of the viability assay (ΔΨm assay)

MTDR-stained trophozoites emit higher intensities of red fluorescence. Any difference in the trophozoite ΔΨm will be visible in a fluorescence intensity range detached from the other populations (e.g. uRBC). Hence, trophozoite-stage *P. falciparum* culture was treated during 6h with three different concentrations, 500nM, 5µM, and 10µM, corresponding to the 100x IC_{50}, 1,000x IC_{50}, and 2,000x IC_{50}, respectively. ATQ treatment was evaluated by the ΔΨm assay (III.4.1.2., adding optimized conditions). Results of three independent assays, each with four technical replicas are presented in Figure IV.8. As expected, all ATQ tested concentrations induced a significant decrease (between 20-30%, $p < 0.05$

between ATQ-treated and RPMI-treated) in ΔΨm[§§] , and the collapse of ΔΨm [***] was proportional to the concentration of the drug. Our observations are in agreement with previously described values[39,114].

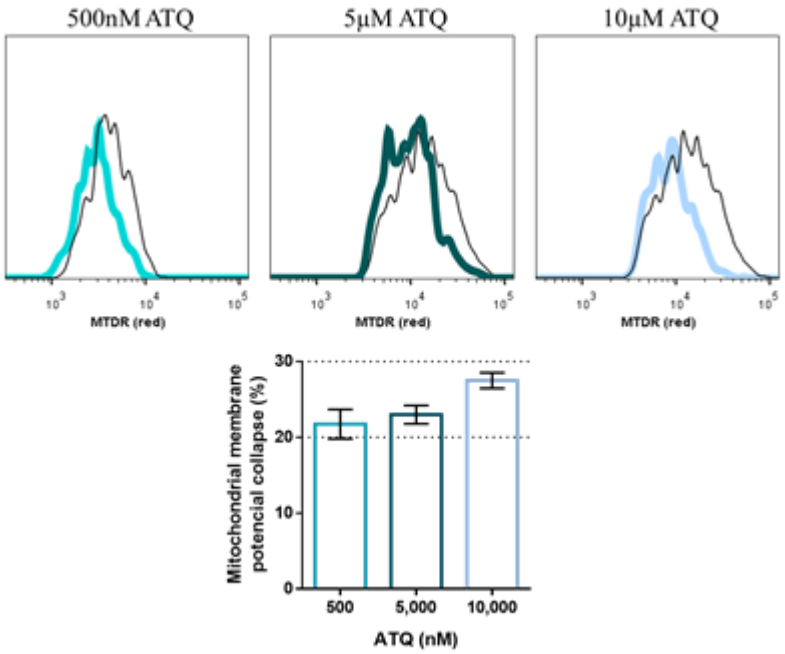

Figure IV.8 – ΔΨm collapse detection in trophozoite-stage 3D7 parasites submitted to ATQ. Red fluorescence emission obtained from the following treatments: 500nM ATQ, 5µM ATQ, and 10µM ATQ overlaid with RPMI-treated samples (3D7, events retrieved from Gate III, within 100,000 events recorded). ΔΨm collapse induced by the three ATQ concentration treatments, with the 20-30% interval ($p < 0.05$ between ATQ-treated and RPMI-treated) marked by dotted lines. Error bars represent SEM. ΔΨm, mitochondrial membrane potential. MTDR, Mitotracker™ Deep Red FM. ATQ, atovaquone. 500nM ATQ, turquoise histogram, and graph bar. 5µM ATQ, dark turquoise histogram, and graph bar. 10µM ATQ, light blue histogram, and graph bar. Negative control (RPMI-treated), thin black line histogram.

IV.1.4.2. Adaptation of the ΔΨm assay to fixation conditions

Our aims included the optimization of the ΔΨm assay to be used not only with 3D7-GFP but with other *P. falciparum* parasites: i) in particular strains with different drug-resistance phenotypes and ii) to be used for *ex vivo* assays (with infected RBCs withdrawal directly from patients) under field conditions. These adaptations require the addition of a second fluorescent probe (to discriminate the parasite) as well as, the use of fixatives, to preserve

[§§] Measured by the geometric mean (GM) of red fluorescence (MTDR).

tested parasites for later reading of the assay if necessary (e.g. a facility equipped with a flow cytometer).

The adaptation to field conditions of the developed assay was attempted by the introduction of a fixation step in between the dual fluorescent probe staining. For this, samples were submitted to three different fixation processes (as in III.4.1.2.2.), namely: 4% paraformaldehyde (PFA) with 0.0075% glutaraldehyde (GA), 2% PFA with 0.06% GA, and 0.025% GA and stained with MTDR and SG (as in III.4.1.2.).

a) Establishing fixation conditions

The ΔΨm assay was performed including each one of the fixation procedures in between the MTDR and SG staining (as in III.4.1.2.). Fixation conditions were evaluated in one assay with two technical replicas and results are presented in Figure IV.9. The dual fluorescence emission of fixed samples within 0.025% GA, reveals an aberrancy; an isolated grey population is seen in the cytometry dot-plot image, absent from the samples fixated with PFA containing solutions (Figure IV.9-A). All fixation solutions render identical parasitemia[†††] between them and to unfixed control (PBS), with an overestimation of iRBC in the 4% PFA + 0.075% GA fixation procedure ($p < 0.05$). When compared to unfixed control (PBS), only the cultures fixed with 4% PFA-containing solution, follow an identical green (from SG) fluorescence pattern (Figure IV.9-B. On the other hand, red fluorescence (from MTDR) emission follows an identical pattern for both PFA-containing solutions, and in comparison, to unfixed control (Figure IV.9-C).

[***] Percentage of the lost red fluorescence emission calculated by subtracting the ATQ-treated sample GM of red fluorescence to the RPMI-treated samples mean of GM of red fluorescence.
[†††] Parasitemia was calculated for each fixation condition by retrieving the percentage of green fluorescence emitting events within the RBC population (see Gate III and II, respectively, from Figure III.4).

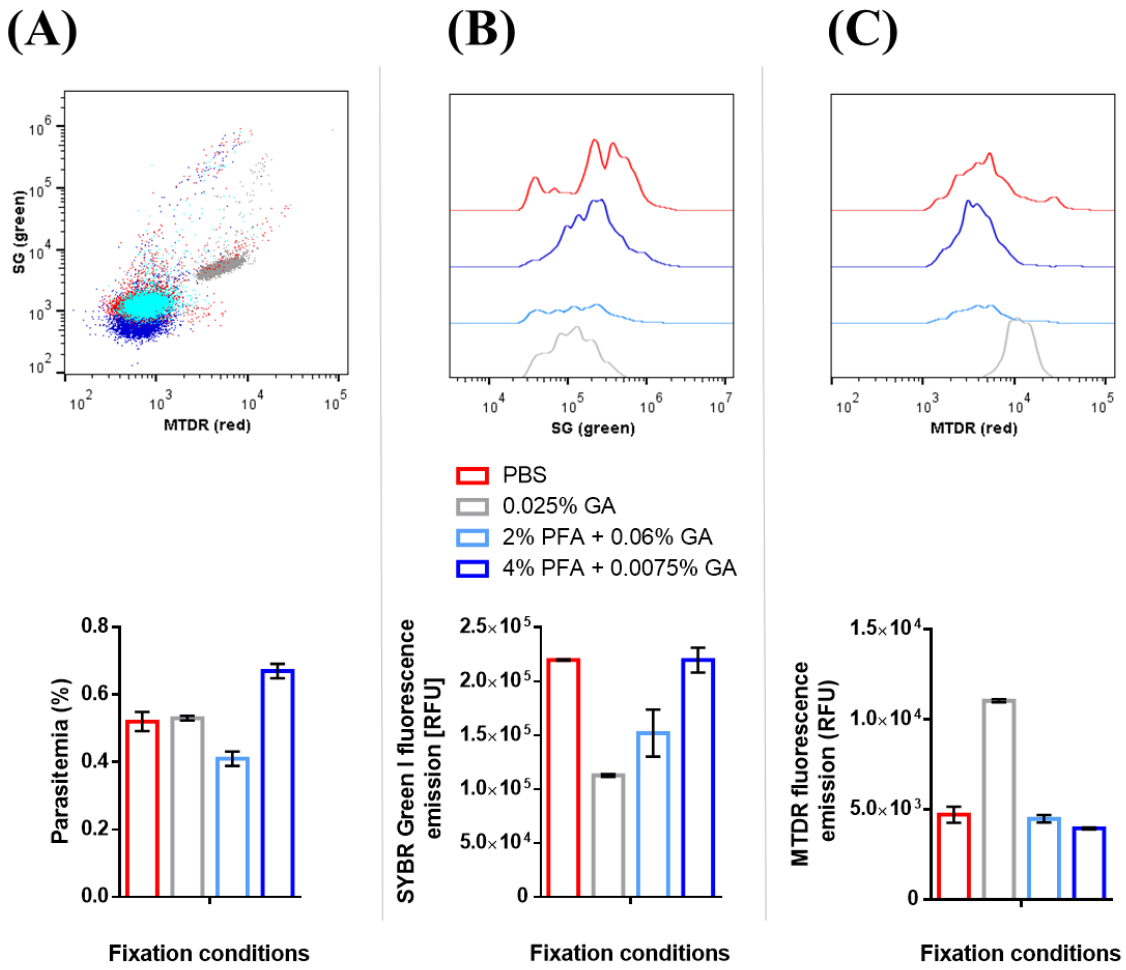

Figure IV.9 – ΔΨm adapted to field conditions: parasitemia and fluorescence emission disturbances. (A) MTDR and SG fluorescence emission, parasitemia (percentage of green fluorescence emitting events within the RBC population, see Gate II and III in Figure IV.8); (B) SG fluorescence emission only and its GM; and (C) MTDR fluorescence emission only and its GM of 4% PFA + 0.0075% GA, 2% PFA + 0.06% GA, 0.025% GA, and PBS (3D7, 250nM MTDR, 0.5x SG, events retrieved from Gate III, within 100,000 events recorded). Error bars represent SEM. ΔΨm, mitochondrial membrane potential. MTDR, Mitotracker™ Deep Red FM. SG, SYBR™ Green I. GM, geometric mean. 4% PFA + 0.0075% GA, 4% paraformaldehyde with 0.075% glutaraldehyde, dark blue. 2% PFA + 0.06%, 2% paraformaldehyde with 0.06% glutaraldehyde, light blue. 0.025% GA, 0.025% glutaraldehyde, gray. PBS, phosphate buffer saline, red.

Parasite viability is quantified in the ΔΨm assay by the geometric mean (GM) difference in both green and red fluorescence (SG, DNA presence; MTDR, mitochondrial integrity, respectively). The GM of fluorescence emission observed in PBS-treated samples (unfixed control) resemblances the most with the 4% PFA + 0.075% GA fixation procedure. Therefore, 4% PFA + 0.075% GA fixative was adopted during further optimizations.

b) ΔΨm assay under fixation conditions

The fixation procedure using 4% PFA + 0.0075% GA was selected to further test the interference of fixation in the ΔΨm assay ability to detect ΔΨm variations. The ΔΨm was induced with 500nM of ATQ for 6h in a trophozoite-stage (22-26hpi) synchronized parasite culture. One assay with two biological replicas and 4 technical replicas each was performed, and results are presented in Figure IV.10. As shown in Figure IV.10, ATQ induces a loss of retention of MTDR within parasite mitochondria in unfixed samples, triggered by the ΔΨm collapse. In opposition, 4% PFA + 0.0075% GA-fixed samples, do not show any difference in its red fluorescence emission between ATQ and RPMI-treated cells, resulting in the absence of a detected ΔΨm collapse by this method. The 4% PFA + 0.0075% GA fixation hamper ΔΨm collapse detection. However, such a fixation procedure could still be applied if the purpose is only to detect mitochondria, and not its viability (e.g. [124]).

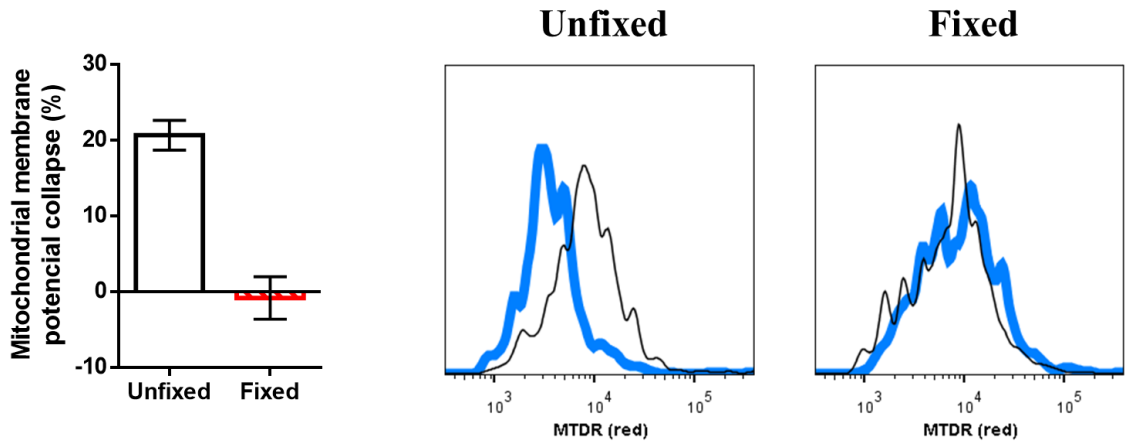

Figure IV.10 – Fixation interference on the ΔΨm collapse assessment. ΔΨm collapse (%) and red fluorescence emission of the ATQ-treated samples (3D7, 250nM) unfixed (PBS) and fixed MTDR, 0.5x SG, 4% PFA + 0.0075% GA, events retrieved from Gate III, within 100,000 events recorded. Error bars represent SEM. ΔΨm, mitochondrial membrane potential. MTDR, Mitotracker™ Deep Red FM. PBS, phosphate buffer saline, unfixed, black bar. Fixed, red bar. ATQ, atovaquone, blue line. RPMI, black line.

IV.2. CHARACTERIZATION OF THE ACTIVITY OF A NEWLY SYNTHESIZED ANTIMALARIAL CANDIDATE

Ru2 is a candidate antimalarial drug of organo-ruthenium compound nature. Organometallic compounds are a growing tendency in new potential therapeutic drugs. Ruthenium complexes, specifically, are one of the good examples of improved therapeutic formulas[125], with an increasing application in antimalarial treatments[126–128]. Combining metallic compounds with formerly used antimalarial agents have also been proved to be a promising solution for resistant strains[129–131].

Ru2 was synthesized by Milheiro *et al.* [132] and antimalarial activity assays revealed that it has very potent activity against *P. falciparum*. We then further investigated the mechanism of action of Ru2 using the optimized ΔΨm assay described above.

IV.2.1. Effect of Ru2 in *Plasmodium falciparum* membrane potential ΔΨm

Parasite viability after drug pressure was measure by the newly developed ΔΨm assay (see III.2.1.2. and optimized conditions). Giemsa-stained Ru2 treated *P. falciparum* show decreased cellular volume and rounded cell morphology[‡‡‡] (Figure IV.11-B). The results obtained on microscopical observations of Ru2-treated parasites agree with the following flow cytometry results.

Different concentrations of Ru2 corresponding to 10x, 100x and 1000x the IC_{50} were used to evaluate Ru2 impact in the mitochondrial membrane potential ΔΨm of the parasites. The impact was assessed at 3, 6, and 12 hours after treatment. ATQ was used as a control[§§§], at a concentration of 100x the correspondent IC_{50} during 6h[114,133]. The ΔΨm collapse and parasitemia were evaluated. Results of four independent assays, each with 2-3 biological replicas, and 4 technical replicas are presented in Figure IV.11-A. Positive and negative controls were performed in parallel with Ru2: as expected[114], 100x IC_{50} of ATQ during 6h of treatment induced a decrease of ± 20% of the ΔΨm. Validating assay conditions.

[‡‡‡] Gate II adapted to include events in a lower FSC area.
[§§§] ATQ is an antimalarial drug used in the optimization process, that can effectively collapse the ΔΨm of parasites, in conditions already verified (see IV.1.4. in Results and Discussion).

Considering the "incubation period" and "concentration", Ru2 showed a progressive impact on ΔΨm collapse more dependent on the incubation period, rather than the dosage applied (Figure IV.11-A). In our work Ru2 effect on *P. falciparum* was described by two parameters: ΔΨm collapse and parasitemia decrease. All conditions of incubation time and Ru2 concentration allowed the detection of a significant ΔΨm collapse in treated parasites. However, just a few conditions tested caused a parasitemia decrease.

The 10x IC_{50} Ru2 treatment induces ΔΨm collapse of about 20% but does not interfere with the parasitemia in neither 3h nor 6h of treatment (Figure IV.11-A, light orange bars). The 3h treatment with 100x IC_{50} Ru2 can induce a detectable impact on the ΔΨm, but still has no impact on the parasitemia (Figure IV.11-A, medium orange bar at 3h). The same does not happen for longer incubation periods, where the parasitemia starts to show a slight decrease after 6h and almost complete eradication of parasites after 12h (Figure IV.11-A, medium orange bars at 6h and 12h). The 1000x IC_{50} Ru2 decreases parasitemia in a time-dependent manner. Treatment with the higher concentration of Ru2 can affect parasitemia within 3h, reducing parasite population almost totally at 12h (Figure IV.11-A, dark orange bars)

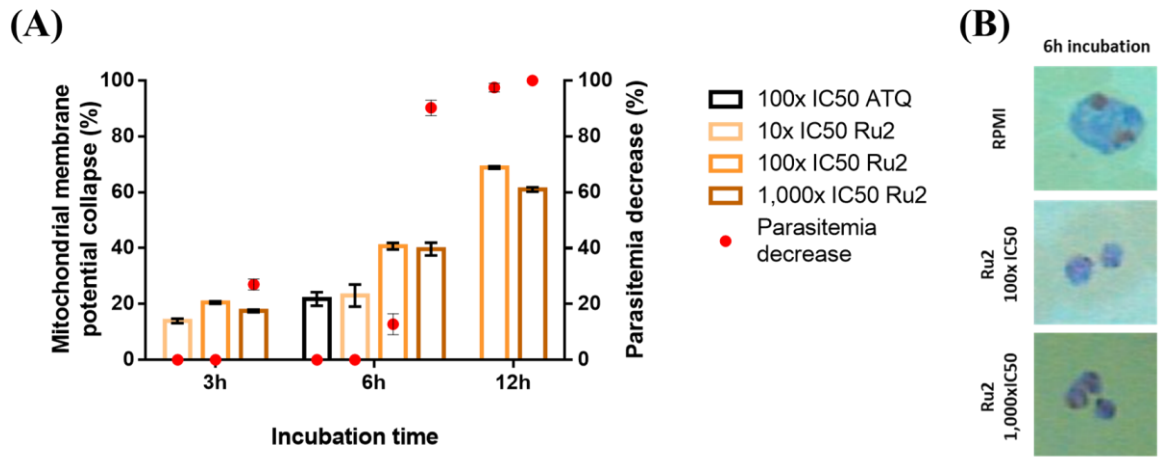

Figure IV.11 – Impact of RU2 in *Plasmodium falciparum* membrane potential ΔΨm and viability. (A) ΔΨm collapse (bars) and parasitemia decrease (red dots) of Ru2 treated parasites for 3, 6 and 12h with 10x, 100x and 1,000x IC_{50} Ru2, and for 6h with 100x IC_{50} ATQ (3D7, 250nM MTDR, 0.5x SG, 100,000 recorded events). Error bars represent SEM. (B) Microscopical observation of Giemsa-stained smears (1,000x magnification, oil immersion) obtained after 6h with 100x and 1,000x IC_{50} Ru2 treatment, and RPMI (negative control). ΔΨm, mitochondrial membrane potential; ATQ, atovaquone; MTDR, Mitotracker™ Deep Red FM; SG, SYBR™ Green I.

Within these results, there are two different patterns obtained from Ru2-treated samples: i) ΔΨm collapse with no parasitemia decrease; ii) ΔΨm collapse with a significant parasitemia decrease. The pattern i) is seen in lower concentrations and smaller incubation periods, whereas the ii) in opposite conditions. The two patterns differ in parasite population maintenance. Where parasitemia has decreased radically (pattern ii), the measured ΔΨm collapse may be a consequence of a very pronounced cellular death, instead of a primary effect of Ru2 in parasite mitochondria. On the contrary, a significant ΔΨm collapse without parasitemia decrease (pattern i) reassures that mitochondrial dysfunction has been induced by Ru2 treatment and did not result from a complete membrane disintegration of a dying cell. Therefore, a correct assessment of parasite viability after Ru2 treatment is only achieved in conditions where pattern i) is represented.

Cellular morphology of Ru2-treated parasites is highly suggestive of stressed parasites[134–136]. The ΔΨm collapse is one of the first signs of stress-induced death in *P. falciparum* parasites[102,134]. Hence, the loss of viability detected in parasites treated with relatively mild conditions (low dose of Ru2, during short periods, 3h) could be an early sign of stress-induced death. Ru2 showed to be a very fast-acting drug (ΔΨm collapse detected after a 3h-treatment), a behavior that differs from a typical mitochondrion targeting drugs, like ATQ with is a slow-acting drug[120]. Thus, the mitochondria may not be the primary target of this antimalarial candidate, but the victim of secondary toxicity caused during Ru2 treatment.

IV.2.2. The stage-specific efficacy of Ru2 against *Plasmodium falciparum*

After observing that, incubation with 10x IC_{50} of Ru2 for 3h and/or 6h impacted parasite viability before destroying parasite integrity, we further investigated the mode of action of Ru2. To determine whether the efficacy of the compound was stage-specific, we first synchronized *P. falciparum* 3D7 cultures to obtain rings (3-9hpi) and trophozoites (22-28hpi). Parasites were then incubated with 10x IC_{50} of Ru2 for periods of 3 or 6h (as in IV.2.1.), and ΔΨm assessed by flow cytometry (as in III.4.1.2.). Results of one assay, with three biological replicas and four technical replicas each, are presented in Figure IV.12.

The 10x IC_{50} Ru2 concentration applied for 3h does not induce drastic morphological alterations (Figure IV.12-B) or change in parasitemia (Annex IX) either in rings or trophozoite-stages. These conditions do not appear to induce abrupt cell death. Hence, allowing the evaluation of earlier and stage-specific effects of Ru2 on *P. falciparum* parasites. Results revealed the previously reported (see IV.2.1.) time-dependent effect of Ru2 in ΔΨm collapse. Overall results do not suggest the stage-specific affect a single life cycle stage. However, at 6h incubation, Ru2 presents a significative ($p < 0.05$) effect towards trophozoite-stage parasites (Figure IV.12-A).

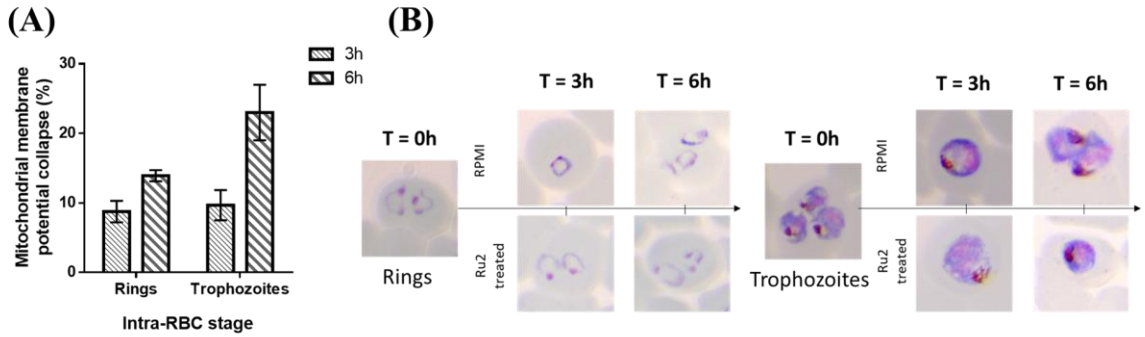

Figure IV.12 – Stage-specific parasite viability (ΔΨm and parasitemia) after Ru2 treatment. (A) ΔΨm collapse (%) of 10x IC_{50} Ru2 treated rings (3-9hpi) and trophozoites (22-28hpi) for 3h and 6h (3D7, 250nM MTDR, 0.5x SG, 100,000 recorded events). Error bars represent SEM. (B) Schematic representation of 10x IC_{50} Ru2 treatment applied to rings and trophozoites for 3h and 6h, with Giemsa-stained images (1,000x magnification, in an oil immersion objective) at time 0 (T=0h), 3 (T=3h), and 6 (T=6h) of RPMI- (top), and Ru2-treated (bottom) parasites.

The fast onset of ΔΨm collapse in both intra-RBC stages, suggests the impairment of the redox balance[137]. Organoruthenium compounds induce oxidative stress on *P. falciparum* parasites[138] and interact with DNA by intercalation and methylation[139]. Organoruthenium complexes inhibit numerous enzymes that participate in the parasite redox balance, namely the thioredoxin reductase[140,141] and cysteine proteases, like falcipain[142]. By inducing oxidative stress, Ru2 is creating significant damage to the cell, either by lipid peroxidation, oxidation of proteins, or DNA damage[143]. One of the consequences of this attack is the loss of the mitochondrial membrane integrity by lipid peroxidation. Such a result, induces the release of cytochrome c, collapsing the ΔΨm and irreversibly compromising the cell viability[144,145].

IV.2.3. The cytocidal activity of Ru2 against *Plasmodium falciparum*

The cytocidal activity determination of the antimalarial candidate aimed to assess the extension and reversibility of the mitochondrial damage, earlier quantified by the ΔΨm assay. Through the interpretation of the Ru2-induced ΔΨm collapse outcomes, it is possible to reveal the impact of Ru2 in parasite survival. Such findings will allow further elucidating in its potential as an antimalarial candidate.

Parasites were treated with 10x the IC_{50} during 3 and 6h, washed to remove the drug and returned to standard culture conditions (as in III.4.2.) until completing one life cycle (48h) and three life cycles (96h). Results from two independent assays, each with 2-3 biological replicas, and four technical replicas each are presented in Figure IV.13. The gating strategy applied to flow cytometry results is described in Figure III.3. Ru2 treatment has a time-dependent effect in trophozoites ($p < 0.05$) but not in ring-stage parasites. At 48h after resuming growth, 3 and 6h-treated rings reached a 40% decrease in parasitemia (Figure IV.13-A), whereas trophozoites achieved 30% when submitted to 3h of Ru2, and 40% when submitted to 6h of Ru2. After 96h post-treatment, rings suffered a 95% decrease in parasitemia (with 3h or 6h of treatment, Figure IV.13-A). On the other hand, trophozoites suffered a decrease in parasitemia of 70% and 90% for the 3 and 6h treatment periods, respectively ($p < 0.05$).

Giemsa-stained images of iRBCs (Figure IV.13-B) at 48h post-treatment showed parasites with vacuolated and hyaline cytoplasm, lacking a nuclear structure, and with few reminiscent hemozoin crystals. On the contrary, at 96h, parasites presented unrecognizable cellular structures, both on rings and trophozoites.

Flow cytometry results suggest that there is not an immediate death process after Ru2 treatment, but that only after three reinvasion cycles the drug pressure becomes completely effective in parasitemia extinction. However, morphological findings suggest that both 3 and 6h of treatment can trigger mechanisms of cell death (visible after 48h, Figure IV.13-B, T48), resulting in the parasitic cell destruction (visible after 96h, Figure IV.13-B, T96). The lower decrease recorded at 48h (Figure IV.13-A) post-treatment is most probably due to the presence of “crisis forms” (a feature of apoptosis)[134,146], occurring during the first reinvasion cycle, and stained by the SG. Hence, emitting green fluorescence and giving

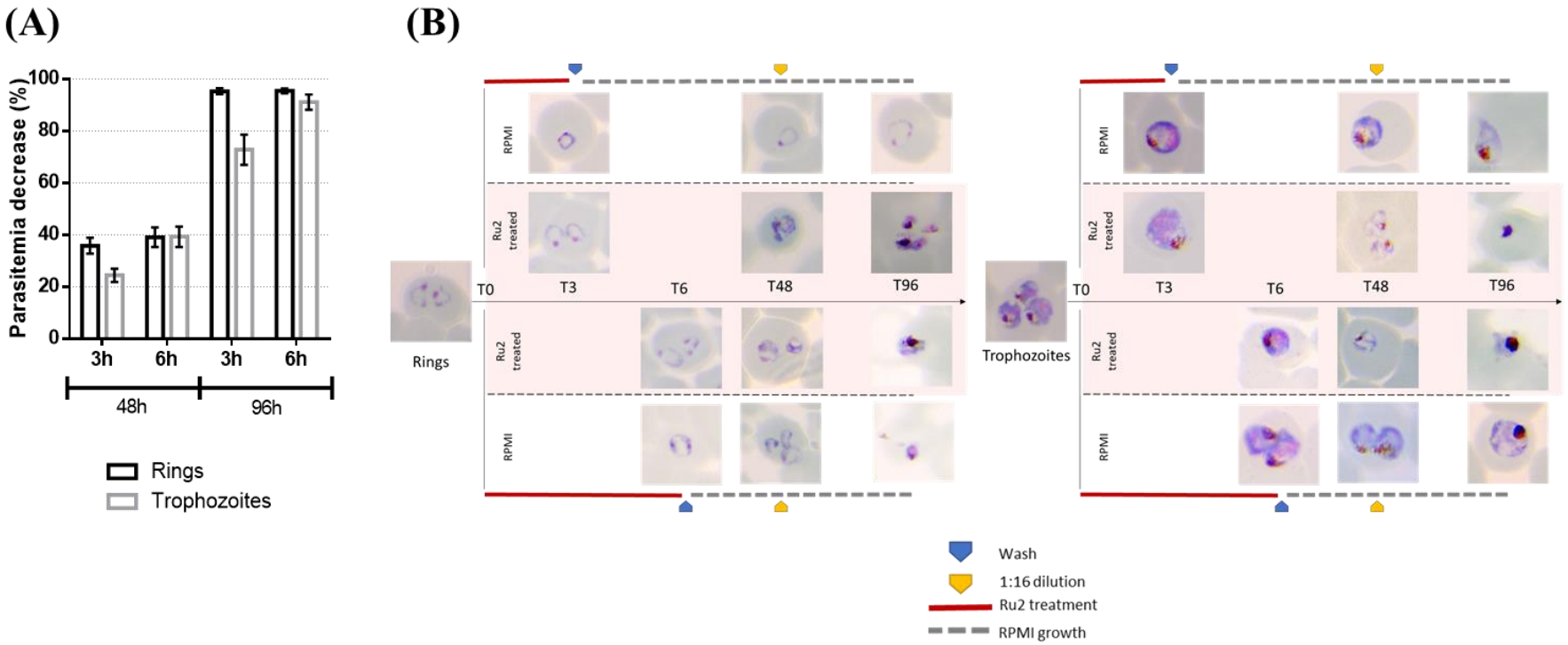

Figure IV.13 – Stage-specific Ru2 cytocidal activity after 3h and 6h of treatment. (A) Parasitemia decrease of 10x IC_{50} Ru2-treated rings (3-9hpi) and trophozoites (22-28hpi) for 3h and 6h, measured after 48h post-treatment and 96h post-treatment. Error bars represent SEM. (B) Schematic representation of 10x IC_{50} Ru2 treatment applied to rings and trophozoites for 3h and 6h, with Giemsa-stained images (1,000x magnification, in an oil immersion objective) at 0h (T0), 3h (T3), 6h (T6), 48h (T48), and 96h (T96) post-treatment of RPMI- (white area), and Ru2-treated (beige area) parasites.

signals in the flow cytometry determinations. These already unviable parasites, after two more reinvasion cycles, have enough time to deteriorate, reducing the SG fluorescence[147].

The fast-acting mechanism of Ru2 (see IV.2.2.) was also reflected in parasite survival. Especially true for ring-stage parasites, where regardless of the damage extension caused by Ru2 to mitochondria, it always triggered the same level of death response. Yet, trophozoites showed slightly lower susceptibility to Ru2 in this cytocidal activity assay.

CHAPTER V

Conclusions

Conclusions

1.

a) Overall, the MTDR and SG fluorescence assay has proven to be a viable flow cytometry assay for *P. falciparum* iRBCs recognition.

b) The implementation of a dual staining strategy:

    a. enhances the technique resolution and ability to accurately single-out iRBCs;

    b. identifies and distinguishes stage-specific parasites and their viability.

c) Field condition adaptation of the ΔΨm assay has yet to be completed, due to the incomplete optimization of the fixation procedure.

2.

a) Ru2 has revealed to be an effective antimalarial candidate in *in vitro* conditions, showing:

    a. a fast-acting drug pattern, capable of destroying the mitochondrial integrity when using 10x its IC_{50} for 3h.

    b. to bear a multi-stage action, collapsing ΔΨm of both rings and trophozoites equally.

b) The damages caused by Ru2 in parasite mitochondria are probably irreversible, jeopardizing parasite survival.

CHAPTER VI

Future Developments

Future Developments

1.

a) In the future, the implemented methodology should also be tested for its ability to detect dormant artemisinin-resistant parasites. From this detection, an earlier diagnosis of treatment failure could be done and followed by a treatment plan more adequate.

b) This methodology could also be evaluated on its efficacy with other specimens, besides cell cultures, like field-collected human blood and animal model blood samples, so much to help implement this protocol in field conditions, as also to widen the future applications of this method.

c) The optimization of the field conditions introduction to the ΔΨm (viability) assay is yet to be achieved. Although there were close resemblances between the fluorescence emission of fixed and unfixed conditions, the ΔΨm collapse could not be detected after the fixation process. In the future, other fixation strategies should be tested in its ability to maintain the viability assessment or adapted to achieve this purpose.

2.

a) Ru2 impact on *P. falciparum* could have resulted from a stress oxidative environment induction inside the parasitic cell. The quantification of oxidative stress induced by Ru2 is still yet to be accomplished.

b) Ru2 impact should also be studied in other *P. falciparum* life stages, like gametocytes or ookinetes, to assess its efficacy in a transmission-blocking approach.

REFERENCES

1. Scholar, E. in *xPharm: The Comprehensive Pharmacology Reference* 1–5 (Elsevier, 2007). doi:10.1016/B978-008055232-3.60932-8

2. Murray, C. J., Rosenfeld, L. C., Lim, S. S., Andrews, K. G., Foreman, K. J., Haring, D., Fullman, N., Naghavi, M., Lozano, R. & Lopez, A. D. Global malaria mortality between 1980 and 2010: a systematic analysis. *The Lancet* **379,** 413–431 (2012).

3. World Health Organization. *World malaria report 2018*. (World Health Organization, 2018). at <http://www.who.int/malaria/publications/world-malaria-report-2018/en/>

4. Peatey, C. L., Chavchich, M., Chen, N., Gresty, K. J., Gray, K.-A., Gatton, M. L., Waters, N. C. & Cheng, Q. Mitochondrial Membrane Potential in a Small Subset of Artemisinin-Induced Dormant Plasmodium falciparum Parasites In Vitro. *J. Infect. Dis.* **212,** 426–434 (2015).

5. Chen, N., LaCrue, A. N., Teuscher, F., Waters, N. C., Gatton, M. L., Kyle, D. E. & Cheng, Q. Fatty Acid Synthesis and Pyruvate Metabolism Pathways Remain Active in Dihydroartemisinin-Induced Dormant Ring Stages of Plasmodium falciparum. *Antimicrobial Agents and Chemotherapy* **58,** 4773–4781 (2014).

6. Tucker, M. S., Mutka, T., Sparks, K., Patel, J. & Kyle, D. E. Phenotypic and Genotypic Analysis of In Vitro-Selected Artemisinin-Resistant Progeny of Plasmodium falciparum. *Antimicrob Agents Chemother* **56,** 302–314 (2012).

7. Nogueira, F. & Rosário, V. E. do. Métodos para avaliação da atividade antimalárica nas diferentes fases do ciclo de vida do Plasmodium. *Revista Pan-Amazônica de Saúde* **1,** 109–124 (2010).

8. Tiendrebeogo, R. W., Adu, B., Singh, S. K., Dodoo, D., Dziegiel, M. H., Mordmüller, B., Nébié, I., Sirima, S. B., Christiansen, M. & Theisen, M. High-throughput tri-colour flow cytometry technique to assess Plasmodium falciparum parasitaemia in bioassays. *Malaria Journal* **13,** 412 (2014).

9. Amaratunga, C., Neal, A. T. & Fairhurst, R. M. Flow Cytometry-Based Analysis of Artemisinin-Resistant Plasmodium falciparum in the Ring-Stage Survival Assay. *Antimicrobial Agents and Chemotherapy* **58,** 4938–4940 (2014).

10. Ekland, E. H., Schneider, J. & Fidock, D. A. Identifying apicoplast-targeting antimalarials using high-throughput compatible approaches. *The FASEB Journal* (2011). doi:10.1096/fj.11-187401

11. Silvie, O., Mota, M. M., Matuschewski, K. & Prudêncio, M. Interactions of the malaria parasite and its mammalian host. *Current Opinion in Microbiology* **11,** 352–359 (2008).

12. Guerrant, R. L., Walker, D. H. & Weller, P. F. *Tropical infectious diseases: principles, pathogens & practice*. (Elsevier Churchill Livingstone, 2006).

13. Thu, A. M., Phyo, A. P., Landier, J., Parker, D. M. & Nosten, F. H. Combating multidrug-resistant Plasmodium falciparum malaria. *FEBS J.* **284,** 2569–2578 (2017).

14. World Health Organization. *Guidelines for the treatment of malaria*. (World Health Organization, 2015). at <https://apps.who.int/iris/handle/10665/162441>

15. Institute for Health Metrics and Evaluation (IHME). *Findings from the Global Burden of Disease Study 2017*. (IHME, 2018).

16. Cowman, A. F. & Crabb, B. S. Invasion of Red Blood Cells by Malaria Parasites. *Cell* **124,** 755–766 (2006).

17. Mota, M. M. & Rodriguez, A. Invasion of mammalian host cells by Plasmodium sporozoites. *Bioessays* **24,** 149–156 (2002).

18. Mota, M. M., Pradel, G., Vanderberg, J. P., Hafalla, J. C. R., Frevert, U., Nussenzweig, R. S., Nussenzweig, V. & Rodríguez, A. Migration of Plasmodium Sporozoites Through Cells Before Infection. *Science* **291,** 141–144 (2001).

19. Arnot, D. E. in *Encyclopedia of Malaria* (eds. Hommel, M. & Kremsner, P. G.) 1–9 (Springer New York, 2013). doi:10.1007/978-1-4614-8757-9_43-1

20. Radfar, A., Méndez, D., Moneriz, C., Linares, M., Marín-García, P., Puyet, A., Diez, A. & Bautista, J. M. Synchronous culture of Plasmodium falciparum at high parasitemia levels. *Nature Protocols* **4,** 1899–1915 (2009).

21. Bannister, L. H., Hopkins, J. M., Fowler, R. E., Krishna, S. & Mitchell, G. H. A Brief Illustrated Guide to the Ultrastructure of Plasmodium falciparum Asexual Blood Stages. *Parasitology Today* **16,** 427–433 (2000).

22. Hopkins, J., Fowler, R., Krishna, S., Wilson, I., Mitchell, G. & Bannister, L. The plastid in Plasmodium falciparum asexual blood stages: a three-dimensional ultrastructural analysis. *Protist* **150,** 283–295 (1999).

23. Dooren, G. G. van, Marti, M., Tonkin, C. J., Stimmler, L. M., Cowman, A. F. & McFadden, G. I. Development of the endoplasmic reticulum, mitochondrion and apicoplast during the asexual life cycle of Plasmodium falciparum. *Molecular Microbiology* **57,** 405–419 (2005).

24. Bannister, L. H., Hopkins, J. M., Margos, G., Dluzewski, A. R. & Mitchell, G. H. Three-Dimensional Ultrastructure of the Ring Stage of Plasmodium falciparum: Evidence for Export Pathways. *Microscopy and Microanalysis* **10,** 551–562 (2004).

25. Magowan, C., Brown, J. T., Liang, J., Heck, J., Coppel, R. L., Mohandas, N. & Meyer-Ilse, W. Intracellular structures of normal and aberrant Plasmodium falciparum malaria parasites imaged by soft x-ray microscopy. *PNAS* **94,** 6222–6227 (1997).

26. TimVickers, B. _falciparum jpg: D. M., Carlos Moneriz and José M. Bautistaderivative work: *Intraerythrocytic blood stages of Plasmodium falciparum in culture.* (2010). at <https://commons.wikimedia.org/wiki/File:Blood_stages_of_P._falciparum_over_48h.jpg>

27. Learngaramkul, P., Petmitr, S., Krungkrai, S. R., Prapunwattana, P. & Krungkrai, J. Molecular Characterization of Mitochondria in Asexual and Sexual Blood Stages of Plasmodium falciparum. *Molecular Cell Biology Research Communications* **2,** 15–20 (1999).

28. Krungkrai, J., Prapunwattana, P. & Krungkrai, S. R. Ultrastructure and function of mitochondria in gametocytic stage of Plasmodium falciparum. *Parasite* **7,** 19–26 (2000).

29. Ginsburg, H. in *Recent Advances in Malaria* 219–290 (2016). doi:10.1002/9781118493816.ch9

30. Gisselberg, J. E., Dellibovi-Ragheb, T. A., Matthews, K. A., Bosch, G. & Prigge, S. T. The Suf Iron-Sulfur Cluster Synthesis Pathway Is Required for Apicoplast Maintenance in Malaria Parasites. *PLOS Pathogens* **9,** e1003655 (2013).

31. Cottet-Rousselle, C., Ronot, X., Leverve, X. & Mayol, J.-F. Cytometric assessment of mitochondria using fluorescent probes. *Cytometry A* **79,** 405–425 (2011).

32. Painter, H. J., Morrisey, J. M., Mather, M. W. & Vaidya, A. B. Specific role of mitochondrial electron transport in blood-stage Plasmodium falciparum. *Nature* **446,** 88–91 (2007).

33. Lane, K. D., Mu, J., Lu, J., Windle, S. T., Liu, A., Sun, P. D. & Wellems, T. E. Selection of Plasmodium falciparum cytochrome B mutants by putative PfNDH2 inhibitors. *PNAS* **115,** 6285–6290 (2018).

34. Cowell, A. N. & Winzeler, E. A. The genomic architecture of antimalarial drug resistance. *Brief Funct Genomics* **18,** 314–328 (2019).

35. Blasco, B., Leroy, D. & Fidock, D. A. Antimalarial drug resistance: linking Plasmodium falciparum parasite biology to the clinic. *Nature Medicine* **23,** 917–928 (2017).

36. Li, Q. & Hickman, M. R. *Pharmacokinetics and Pharmacodynamics of Antimalarial Drugs Used in Combination Therapy*. (Bentham Science Publishers, 2015).

37. Hyde, J. E. Mechanisms of resistance of Plasmodium falciparum to antimalarial drugs. *Microbes and Infection* **4,** 165–174 (2002).

38. Kublin, J. G., Dzinjalamala, F. K., Kamwendo, D. D., Malkin, E. M., Cortese, J. F., Martino, L. M., Mukadam, R. A. G., Rogerson, S. J., Lescano, A. G., Molyneux, M. E., Winstanley, P. A., Chimpeni, P., Taylor, T. E. & Plowe, C. V. Molecular Markers for Failure of Sulfadoxine-Pyrimethamine and Chlorproguanil-Dapsone Treatment of Plasmodium falciparum Malaria. *J Infect Dis* **185,** 380–388 (2002).

39. Antoine, T., Fisher, N., Amewu, R., O'Neill, P. M., Ward, S. A. & Biagini, G. A. Rapid kill of malaria parasites by artemisinin and semi-synthetic endoperoxides involves ROS-dependent depolarization of the membrane potential. *J Antimicrob Chemother* **69,** 1005–1016 (2014).

40. Korsinczky, M., Chen, N., Kotecka, B., Saul, A., Rieckmann, K. & Cheng, Q. Mutations in Plasmodium falciparum cytochrome b that are associated with atovaquone resistance are located at a putative drug-binding site. *Antimicrob. Agents Chemother.* **44,** 2100–2108 (2000).

41. Hawley, S. R., Bray, P. G., Mungthin, M., Atkinson, J. D., O'Neill, P. M. & Ward, S. A. Relationship between Antimalarial Drug Activity, Accumulation, and Inhibition of Heme Polymerization in Plasmodium falciparum In Vitro. *Antimicrob Agents Chemother* **42,** 682–686 (1998).

42. Peel, S. A., Bright, P., Yount, B., Handy, J. & Baric, R. S. A strong association between mefloquine and halofantrine resistance and amplification, overexpression, and mutation in the P-glycoprotein gene homolog (pfmdr) of Plasmodium falciparum in vitro. *Am. J. Trop. Med. Hyg.* **51,** 648–658 (1994).

43. Sanchez, C. P. & Lanzer, M. Changing ideas on chloroquine in Plasmodium falciparum. *Current Opinion in Infectious Diseases* **13,** 653–658 (2000).

44. Lanners, H. N. Effect of the 8-aminoquinoline primaquine on culture-derived gametocytes of the malaria parasitePlasmodium falciparum. *Parasitol Res* **77,** 478–481 (1991).

45. Dahl, E. L. & Rosenthal, P. J. Multiple Antibiotics Exert Delayed Effects against the Plasmodium falciparum Apicoplast. *Antimicrobial Agents and Chemotherapy* **51,** 3485–3490 (2007).

46. Dharia, N. V., Plouffe, D., Bopp, S. E. R., González-Páez, G. E., Lucas, C., Salas, C., Soberon, V., Bursulaya, B., Kochel, T. J., Bacon, D. J. & Winzeler, E. A. Genome scanning of Amazonian

Plasmodium falciparum shows subtelomeric instability and clindamycin-resistant parasites. *Genome Res* **20,** 1534–1544 (2010).

47. Olliaro, P. L., Haynes, R. K., Meunier, B. & Yuthavong, Y. Possible modes of action of the artemisinin-type compounds. *Trends in Parasitology* **17,** 122–126 (2001).

48. Nosten, F. Waking the Sleeping Beauty. *J Infect Dis* **202,** 1300–1301 (2010).

49. Miotto, O., Almagro-Garcia, J., Manske, M., Macinnis, B., Campino, S., Rockett, K. A., Amaratunga, C., Lim, P., Suon, S., Sreng, S., Anderson, J. M., Duong, S., Nguon, C., Chuor, C. M., Saunders, D., Se, Y., Lon, C., Fukuda, M. M., Amenga-Etego, L., Hodgson, A. V. O., Asoala, V., Imwong, M., Takala-Harrison, S., Nosten, F., Su, X.-Z., Ringwald, P., Ariey, F., Dolecek, C., Hien, T. T., Boni, M. F., Thai, C. Q., Amambua-Ngwa, A., Conway, D. J., Djimdé, A. A., Doumbo, O. K., Zongo, I., Ouedraogo, J.-B., Alcock, D., Drury, E., Auburn, S., Koch, O., Sanders, M., Hubbart, C., Maslen, G., Ruano-Rubio, V., Jyothi, D., Miles, A., O'Brien, J., Gamble, C., Oyola, S. O., Rayner, J. C., Newbold, C. I., Berriman, M., Spencer, C. C. A., McVean, G., Day, N. P., White, N. J., Bethell, D., Dondorp, A. M., Plowe, C. V., Fairhurst, R. M. & Kwiatkowski, D. P. Multiple populations of artemisinin-resistant Plasmodium falciparum in Cambodia. *Nat. Genet.* **45,** 648–655 (2013).

50. Ashley, E. A., Dhorda, M., Fairhurst, R. M., Amaratunga, C., Lim, P., Suon, S., Sreng, S., Anderson, J. M., Mao, S., Sam, B., Sopha, C., Chuor, C. M., Nguon, C., Sovannaroth, S., Pukrittayakamee, S., Jittamala, P., Chotivanich, K., Chutasmit, K., Suchatsoonthorn, C., Runcharoen, R., Hien, T. T., Thuy-Nhien, N. T., Thanh, N. V., Phu, N. H., Htut, Y., Han, K.-T., Aye, K. H., Mokuolu, O. A., Olaosebikan, R. R., Folaranmi, O. O., Mayxay, M., Khanthavong, M., Hongvanthong, B., Newton, P. N., Onyamboko, M. A., Fanello, C. I., Tshefu, A. K., Mishra, N., Valecha, N., Phyo, A. P., Nosten, F., Yi, P., Tripura, R., Borrmann, S., Bashraheil, M., Peshu, J., Faiz, M. A., Ghose, A., Hossain, M. A., Samad, R., Rahman, M. R., Hasan, M. M., Islam, A., Miotto, O., Amato, R., MacInnis, B., Stalker, J., Kwiatkowski, D. P., Bozdech, Z., Jeeyapant, A., Cheah, P. Y., Sakulthaew, T., Chalk, J., Intharabut, B., Silamut, K., Lee, S. J., Vihokhern, B., Kunasol, C., Imwong, M., Tarning, J., Taylor, W. J., Yeung, S., Woodrow, C. J., Flegg, J. A., Das, D., Smith, J., Venkatesan, M., Plowe, C. V., Stepniewska, K., Guerin, P. J., Dondorp, A. M., Day, N. P. & White, N. J. Spread of Artemisinin Resistance in Plasmodium falciparum Malaria. *N Engl J Med* **371,** 411–423 (2014).

51. Dondorp, A. M., Yeung, S., White, L., Nguon, C., Day, N. P. J., Socheat, D. & von Seidlein, L. Artemisinin resistance: current status and scenarios for containment. *Nat. Rev. Microbiol.* **8,** 272–280 (2010).

52. White, N. J. Qinghaosu (Artemisinin): The Price of Success. *Science* **320,** 330–334 (2008).

53. Breglio, K. F., Rahman, R. S., Sá, J. M., Hott, A., Roberts, D. J. & Wellems, T. E. Kelch Mutations in Plasmodium falciparum Protein K13 Do Not Modulate Dormancy after Artemisinin Exposure and Sorbitol Selection In Vitro. *Antimicrobial Agents and Chemotherapy* **62,** (2018).

54. Hott, A., Casandra, D., Sparks, K. N., Morton, L. C., Castanares, G.-G., Rutter, A. & Kyle, D. E. Artemisinin-Resistant Plasmodium falciparum Parasites Exhibit Altered Patterns of Development in Infected Erythrocytes. *Antimicrobial Agents and Chemotherapy* **59,** 3156–3167 (2015).

55. Gray, K.-A., Gresty, K. J., Chen, N., Zhang, V., Gutteridge, C. E., Peatey, C. L., Chavchich, M., Waters, N. C. & Cheng, Q. Correlation between Cyclin Dependent Kinases and Artemisinin-Induced Dormancy in Plasmodium falciparum In Vitro. *PLOS ONE* **11,** e0157906 (2016).

56. Duvalsaint, M. & Kyle, D. E. Phytohormones, Isoprenoids, and Role of the Apicoplast in Recovery from Dihydroartemisinin-Induced Dormancy of Plasmodium falciparum. *Antimicrobial Agents and Chemotherapy* **62,** (2018).

57. Kennedy, K., Cobbold, S. A., Hanssen, E., Birnbaum, J., Spillman, N. J., McHugh, E., Brown, H., Tilley, L., Spielmann, T., McConville, M. J. & Ralph, S. A. Delayed death in the malaria parasite Plasmodium falciparum is caused by disruption of prenylation-dependent intracellular trafficking. *PLOS Biology* **17,** e3000376 (2019).

58. Shears, M. J., MacRae, J. I., Mollard, V., Goodman, C. D., Sturm, A., Orchard, L. M., Llinás, M., McConville, M. J., Botté, C. Y. & McFadden, G. I. Characterization of the Plasmodium falciparum and P. berghei glycerol 3-phosphate acyltransferase involved in FASII fatty acid utilization in the malaria parasite apicoplast. *Cellular Microbiology* **19,** e12633 (2017).

59. Wein, S., Maynadier, M., Ba, C. T. V., Cerdan, R., Peyrottes, S., Fraisse, L. & Vial, H. Reliability of Antimalarial Sensitivity Tests Depends on Drug Mechanisms of Action. *Journal of Clinical Microbiology* **48,** 1651–1660 (2010).

60. Noedl, H., Wongsrichanalai, C., Scott Miller, R., Saw Aye Myint, K., Looareesuwan, S., Sukthana, Y., Wongchotigul, V., Kollaritsch, H., Wiedermann, G. & Wernsdorfer, W. H. Plasmodium falciparum:

effect of anti-malarial drugs on the production and secretion characteristics of histidine-rich protein II. *Experimental Parasitology* **102,** 157–163 (2002).

61. Desakorn, V., Dondorp, A. M., Silamut, K., Pongtavornpinyo, W., Sahassananda, D., Chotivanich, K., Pitisuttithum, P., Smithyman, A. M., Day, N. P. J. & White, N. J. Stage-dependent production and release of histidine-rich protein 2 by Plasmodium falciparum. *Trans. R. Soc. Trop. Med. Hyg.* **99,** 517–524 (2005).

62. Noedl, H., Wernsdorfer, W. H., Miller, R. S. & Wongsrichanalai, C. Histidine-Rich Protein II: a Novel Approach to Malaria Drug Sensitivity Testing. *Antimicrobial Agents and Chemotherapy* **46,** 1658–1664 (2002).

63. Butterworth, A. S., Robertson, A. J., Ho, M.-F., Gatton, M. L., McCarthy, J. S. & Trenholme, K. R. An improved method for undertaking limiting dilution assays for in vitro cloning of Plasmodium falciparum parasites. *Malaria Journal* **10,** 95 (2011).

64. Gamboa, D., Ho, M.-F., Bendezu, J., Torres, K., Chiodini, P. L., Barnwell, J. W., Incardona, S., Perkins, M., Bell, D., McCarthy, J. & Cheng, Q. A Large Proportion of P. falciparum Isolates in the Amazon Region of Peru Lack pfhrp2 and pfhrp3: Implications for Malaria Rapid Diagnostic Tests. *PLOS ONE* **5,** e8091 (2010).

65. Pasini, E. M., van den Ierssel, D., Vial, H. J. & Kocken, C. H. A novel live-dead staining methodology to study malaria parasite viability. *Malaria Journal* **12,** 190 (2013).

66. Woodrow, C. J., Wangsing, C., Sriprawat, K., Christensen, P. R., Nosten, F., Rénia, L., Russell, B. & Malleret, B. Comparison between Flow Cytometry, Microscopy, and Lactate Dehydrogenase-Based Enzyme-Linked Immunosorbent Assay for Plasmodium falciparum Drug Susceptibility Testing under Field Conditions. *Journal of Clinical Microbiology* **53,** 3296–3303 (2015).

67. Manandhar, M. S. & Van Dyke, K. Detailed purine salvage metabolism in and outside the free malarial parasite. *Exp. Parasitol.* **37,** 138–146 (1975).

68. Nsanzabana, C., Djalle, D., Guérin, P. J., Ménard, D. & González, I. J. Tools for surveillance of anti-malarial drug resistance: an assessment of the current landscape. *Malaria Journal* **17,** 75 (2018).

69. Varela, M. L., Razakandrainibe, R., Aldebert, D., Barale, J. C. & Jambou, R. Cytometric measurement of in vitro inhibition of Plasmodium falciparum field isolates by drugs: a new approach for re-invasion inhibition study. *Malaria Journal* **13,** 110 (2014).

70. Reilly, H. B., Wang, H., Steuter, J. A., Marx, A. M. & Ferdig, M. T. Quantitative dissection of clone-specific growth rates in cultured malaria parasites. *International Journal for Parasitology* **37,** 1599–1607 (2007).

71. World Health Organization. In vitro micro-test (mark III) for the assessment of the response of plasmodium falciparum to chloroquine, mefloquine, quinine, amodiaquine, sulfadoxine/ pyrimethamine and artemisinin (archived). (2001). at <https://www.who.int/malaria/publications/atoz/ctd_mal_97_20_Rev_2_2001/en/>

72. Chotivanich, K., Tripura, R., Das, D., Yi, P., Day, N. P. J., Pukrittayakamee, S., Chuor, C. M., Socheat, D., Dondorp, A. M. & White, N. J. Laboratory Detection of Artemisinin-Resistant Plasmodium falciparum. *Antimicrobial Agents and Chemotherapy* **58,** 3157–3161 (2014).

73. Srinivas, S. D. & Puri, S. K. Time course of in vitro maturation of intra-erythrocytic malaria parasite: a comparison between Plasmodium falciparum and Plasmodium knowlesi. *Memórias do Instituto Oswaldo Cruz* **97,** 901–903 (2002).

74. Rieckmann, K. H., Campbell, G. H., Sax, L. J. & Mrema, J. E. Drug sensitivity of plasmodium falciparum. An in-vitro microtechnique. *Lancet* **1,** 22–23 (1978).

75. Schuck, D. C., Ribeiro, R. Y., Nery, A. A., Ulrich, H. & Garcia, C. R. S. Flow cytometry as a tool for analyzing changes in Plasmodium falciparum cell cycle following treatment with indol compounds. *Cytometry* **79A,** 959–964 (2011).

76. Grimberg, B. T., Erickson, J. J., Sramkoski, R. M., Jacobberger, J. W. & Zimmerman, P. A. Monitoring Plasmodium falciparum Growth and Development by UV Flow Cytometry Using an Optimized Hoechst-Thiazole Orange Staining Strategy. *Cytometry A* **73,** 546–554 (2008).

77. Contreras, C. E., Rivas, M. A., Domínguez, J., Charris, J., Palacios, M., Bianco, N. E. & Blanca, I. Stage-specific activity of potential antimalarial compounds measured in vitro by flow cytometry in comparison to optical microscopy and hypoxanthine uptake. *Memórias do Instituto Oswaldo Cruz* **99,** 179–184 (2004).

78. Janse, C. J. & Van Vianen, P. H. in *Methods in Cell Biology* (eds. Darzynkiewicz, Z., Robinson, J. P. & Crissman, H. A.) **42,** 295–318 (Academic Press, 1994).

79. Caramello, P., Lucchini, A., Savoia, D. & Gioannini, P. Rapid diagnosis of malaria by use of fluorescent probes. *Diagnostic Microbiology and Infectious Disease* **17,** 293–297 (1993).

80. Molecular Probes, Inc. SYBR® Green I Nucleic Acid Gel Stain. (2006). at <https://assets.thermofisher.com/TFS-Assets/LSG/manuals/mp07567.pdf>

81. Jang, J. W., Kim, J. Y., Yoon, J., Yoon, S. Y., Cho, C. H., Han, E. T., An, S. S. A. & Lim, C. S. Flow Cytometric Enumeration of Parasitemia in Cultures of Plasmodium falciparum Stained with SYBR Green I and CD235A. *The Scientific World Journal* (2014). doi:10.1155/2014/536723

82. Dery, V., Duah, N. O., Ayanful-Torgby, R., Matrevi, S. A., Anto, F. & Quashie, N. B. An improved SYBR Green-1-based fluorescence method for the routine monitoring of Plasmodium falciparum resistance to anti-malarial drugs. *Malaria Journal* **14,** 481 (2015).

83. Johnson, J. D., Dennull, R. A., Gerena, L., Lopez-Sanchez, M., Roncal, N. E. & Waters, N. C. Assessment and Continued Validation of the Malaria SYBR Green I-Based Fluorescence Assay for Use in Malaria Drug Screening. *Antimicrobial Agents and Chemotherapy* **51,** 1926–1933 (2007).

84. Karl, S., Wong, R. P., St Pierre, T. G. & Davis, T. M. A comparative study of a flow-cytometry-based assessment of in vitro Plasmodium falciparum drug sensitivity. *Malar J* **8,** 294 (2009).

85. Evers, A., Heppner, S., Leippe, M. & Gelhaus, C. An efficient fluorimetric method to measure the viability of intraerythrocytic Plasmodium falciparum. *Biological Chemistry* **389,** 1523–1525 (2008).

86. Silva, G. N. S., Schuck, D. C., Cruz, L. N., Moraes, M. S., Nakabashi, M., Gosmann, G., Garcia, C. R. S. & Gnoatto, S. C. B. Investigation of antimalarial activity, cytotoxicity and action mechanism of piperazine derivatives of betulinic acid. *Tropical Medicine & International Health* **20,** 29–39 (2015).

87. Bouillon, A., Gorgette, O., Mercereau-Puijalon, O. & Barale, J.-C. Screening and evaluation of inhibitors of Plasmodium falciparum merozoite egress and invasion using cytometry. *Methods Mol. Biol.* **923,** 523–534 (2013).

88. Campo, J. J., Aponte, J. J., Nhabomba, A. J., Sacarlal, J., Angulo-Barturen, I., Jiménez-Díaz, M. B., Alonso, P. L. & Dobaño, C. Feasibility of Flow Cytometry for Measurements of Plasmodium falciparum Parasite Burden in Studies in Areas of Malaria Endemicity by Use of Bidimensional Assessment of YOYO-1 and Autofluorescence. *Journal of Clinical Microbiology* **49,** 968–974 (2011).

89. Guy, R., Liu, P., Pennefather, P. & Crandall, I. The use of fluorescence enhancement to improve the microscopic diagnosis of falciparum malaria. *Malaria Journal* **6,** 89 (2007).

90. Totino, P. R., Magalhães, A. D., Silva, L. A., Banic, D. M., Daniel-Ribeiro, C. T. & Ferreira-da-Cruz, M. de F. Apoptosis of non-parasitized red blood cells in malaria: a putative mechanism involved in the pathogenesis of anaemia. *Malaria Journal* **9,** 350 (2010).

91. Jiménez-Díaz, M. B., Mulet, T., Gómez, V., Viera, S., Alvarez, A., Garuti, H., Vázquez, Y., Fernández, A., Ibáñez, J., Jiménez, M., Gargallo-Viola, D. & Angulo-Barturen, I. Quantitative measurement of Plasmodium-infected erythrocytes in murine models of malaria by flow cytometry using bidimensional assessment of SYTO-16 fluorescence. *Cytometry Part A* **75A,** 225–235 (2009).

92. Fu, Y., Tilley, L., Kenny, S. & Klonis, N. Dual labeling with a far red probe permits analysis of growth and oxidative stress in P. falciparum-infected erythrocytes. *Cytometry Part A* **77,** 253–263 (2010).

93. Kawamoto, F. Rapid diagnosis of malaria by fluorescence microscopy with light microscope and interference filter. *The Lancet* **337,** 200–202 (1991).

94. Ochola, L., Vounatsou, P., Smith, T., Mabaso, M. & Newton, C. The reliability of diagnostic techniques in the diagnosis and management of malaria in the absence of a gold standard. *Lancet Infectious Diseases* **6,** 582–588 (2006).

95. Zhang, J., Li, N., Siddiqui, F. A., Xu, S., Geng, J., Zhang, J., He, X., Zhao, L., Pi, L., Zhang, Y., Li, C., Chen, X., Wu, Y., Miao, J., Cao, Y., Cui, L. & Yang, Z. In vitro susceptibility of Plasmodium falciparum isolates from the China-Myanmar border area to artemisinins and correlation with K13 mutations. *International Journal for Parasitology: Drugs and Drug Resistance* **10,** 20–27 (2019).

96. Joshi, B. P., Mohanakrishnan, D., Mittal, G., Kar, S., Pola, J. K., Golakoti, N. R., Nanubolu, J. B., D., R. B., S., S. S. K. & Sahal, D. Synthesis, mechanistic and synergy studies of diarylidenecyclohexanone derivatives as new antiplasmodial pharmacophores. *Med Chem Res* **27,** 2312–2324 (2018).

97. Smeijsters, L. J. J. W., Zijlstra, N. M., Franssen, F. F. J. & Overdulve, J. P. Simple, fast, and accurate fluorometric method to determine drug susceptibility of Plasmodium falciparum in 24-well suspension cultures. *Antimicrobial Agents and Chemotherapy* **40,** 835–838 (1996).

98. Vianen, P. H. van, Engen, A. van, Thaithong, S., Keur, M. van der, Tanke, H. J., Kaay, H. J. van der, Mons, B. & Janse, C. J. Flow cytometric screening of blood samples for malaria parasites. *Cytometry* **14,** 276–280 (1993).

99. Janse, C. J., van Vianen, P. H., Tanke, H. J., Mons, B., Ponnudurai, T. & Overdulve, J. P. Plasmodium species: Flow cytometry and microfluorometry assessments of DNA content and synthesis. *Experimental Parasitology* **64,** 88–94 (1987).

100. Malleret, B., Claser, C., Ong, A. S. M., Suwanarusk, R., Sriprawat, K., Howland, S. W., Russell, B., Nosten, F. & Rénia, L. A rapid and robust tri-color flow cytometry assay for monitoring malaria parasite development. *Scientific Reports* **1,** 1–10 (2011).

101. Troiano, L., Ferraresi, R., Lugli, E., Nemes, E., Roat, E., Nasi, M., Pinti, M. & Cossarizza, A. Multiparametric analysis of cells with different mitochondrial membrane potential during apoptosis by polychromatic flow cytometry. *Nature Protocols* **2,** 2719–2727 (2007).

102. Green, D. R. & Reed, J. C. Mitochondria and Apoptosis. *Science* **281,** 1309–1312 (1998).

103. Mathur, A., Hong, Y., Kemp, B. K., Barrientos, A. A. & Erusalimsky, J. D. Evaluation of fluorescent dyes for the detection of mitochondrial membrane potential changes in cultured cardiomyocytes. *Cardiovasc. Res.* **46,** 126–138 (2000).

104. Shoji, K. F. & Debure, L. in *CD95: Methods and Protocols* (ed. Legembre, P.) 49–62 (Springer New York, 2017). doi:10.1007/978-1-4939-6780-3_6

105. Hayat, M. A. *Stem Cells and Cancer Stem Cells,Volume 3: Stem Cells and Cancer Stem Cells, Therapeutic Applications in Disease and Injury:* (Springer Science & Business Media, 2011).

106. ThermoFisher Scientific. Mitochondrion-Selective Rhodamines and Rosamines. *Probes for Mitochondria—Section 12.2* at <https://www.thermofisher.com/uk/en/home/references/molecular-probes-the-handbook/probes-for-organelles/probes-for-mitochondria.html>

107. Russell, B., Chalfein, F., Prasetyorini, B., Kenangalem, E., Piera, K., Suwanarusk, R., Brockman, A., Prayoga, P., Sugiarto, P., Cheng, Q., Tjitra, E., Anstey, N. M. & Price, R. N. Determinants of In Vitro Drug Susceptibility Testing of Plasmodium vivax. *Antimicrobial Agents and Chemotherapy* **52,** 1040–1045 (2008).

108. Molecular Probes, Inc. MitoTracker® Mitochondrion-Selective Probes. (2018). at <https://assets.thermofisher.com/TFS-Assets/LSG/manuals/mp07510.pdf>

109. Pathak, A. K., Shiau, J. C., Thomas, M. B. & Murdock, C. C. Cryogenically preserved RBCs support gametocytogenesis of Plasmodium falciparum in vitro and gametogenesis in mosquitoes. *Malaria Journal* **17,** 457 (2018).

110. Trager, W. & Jensen, J. B. Human malaria parasites in continuous culture. *Science* **193,** 673–675 (1976).

111. Lambros, C. & Vanderberg, J. P. Synchronization of Plasmodium falciparum Erythrocytic Stages in Culture. *The Journal of Parasitology* **65,** 418–420 (1979).

112. Ginsburg, H., Krugliak, M., Eidelman, O. & Ioav Cabantchik, Z. New permeability pathways induced in membranes of Plasmodium falciparum infected erythrocytes. *Molecular and Biochemical Parasitology* **8,** 177–190 (1983).

113. Ginsburg, H., Kutner, S., Zangwil, M. & Cabantchik, Z. I. Selectivity properties of pores induced in host erythrocyte membrane by Plasmodium falciparum. Effect of parasite maturation. *Biochimica et Biophysica Acta (BBA) - Biomembranes* **861,** 194–196 (1986).

114. Biagini, G. A., Viriyavejakul, P., O'neill, P. M., Bray, P. G. & Ward, S. A. Functional characterization and target validation of alternative complex I of Plasmodium falciparum mitochondria. *Antimicrob. Agents Chemother.* **50,** 1841–1851 (2006).

115. Zhao, B., Zhang, D., Li, C., Yuan, Z., Yu, F., Zhong, S., Jiang, G., Yang, Y.-G., Le, X. C., Weinfeld, M., Zhu, P. & Wang, H. ATPase activity tightly regulates RecA nucleofilaments to promote homologous recombination. *Cell Discovery* **3,** 1–15 (2017).

116. Khoury, D. S., Cromer, D., Best, S. E., James, K. R., Sebina, I., Haque, A. & Davenport, M. P. Reduced erythrocyte susceptibility and increased host clearance of young parasites slows Plasmodium growth in a murine model of severe malaria. *Scientific Reports* **5,** 1–7 (2015).

117. Jenkins, B. J., Daly, T. M., Morrisey, J. M., Mather, M. W., Vaidya, A. B. & Bergman, L. W. Characterization of a Plasmodium falciparum Orthologue of the Yeast Ubiquinone-Binding Protein, Coq10p. *PLOS ONE* **11,** e0152197 (2016).

118. Sigala, P. A., Crowley, J. R., Hsieh, S., Henderson, J. P. & Goldberg, D. E. Direct Tests of Enzymatic Heme Degradation by the Malaria Parasite Plasmodium falciparum. *J. Biol. Chem.* **287,** 37793–37807 (2012).

119. Srivastava, I. K., Rottenberg, H. & Vaidya, A. B. Atovaquone, a broad spectrum antiparasitic drug, collapses mitochondrial membrane potential in a malarial parasite. *J. Biol. Chem.* **272,** 3961–3966 (1997).

120. Nixon, G. L., Moss, D. M., Shone, A. E., Lalloo, D. G., Fisher, N., O'Neill, P. M., Ward, S. A. & Biagini, G. A. Antimalarial pharmacology and therapeutics of atovaquone. *J Antimicrob Chemother* **68,** 977–985 (2013).

121. Scarpelli, P. H., Tessarin-Almeida, G., Viçoso, K. L., Lima, W. R., Borges-Pereira, L., Meissner, K. A., Wrenger, C., Raffaello, A., Rizzuto, R., Pozzan, T. & Garcia, C. R. S. Melatonin activates FIS1, DYN1, and DYN2 Plasmodium falciparum related-genes for mitochondria fission: Mitoemerald-GFP as a tool to visualize mitochondria structure. *Journal of Pineal Research* **66,** e12484 (2019).

122. Moon, S., Lee, S., Kim, H., Freitas-Junior, L. H., Kang, M., Ayong, L. & Hansen, M. A. E. An Image Analysis Algorithm for Malaria Parasite Stage Classification and Viability Quantification. *PLOS ONE* **8,** e61812 (2013).

123. Jogdand, P. S., Singh, S. K., Christiansen, M., Dziegiel, M. H., Singh, S. & Theisen, M. Flow cytometric readout based on Mitotracker Red CMXRos staining of live asexual blood stage malarial parasites reliably assesses antibody dependent cellular inhibition. *Malaria Journal* **11,** 235 (2012).

124. Ling, L., Mulaka, M., Munro, J., Dass, S., Mather, M. W., Riscoe, M. K., Llinás, M., Zhou, J. & Ke, H. Genetic ablation of the mitochondrial ribosome in Plasmodium falciparum sensitizes the human malaria parasite to antimalarial drugs targeting mitochondrial functions. *bioRxiv* 2020.01.14.906198 (2020). doi:10.1101/2020.01.14.906198

125. Zhang, C. X. & Lippard, S. J. New metal complexes as potential therapeutics. *Curr Opin Chem Biol* **7,** 481–489 (2003).

126. Navarro, M., Gabbiani, C., Messori, L. & Gambino, D. Metal-based drugs for malaria, trypanosomiasis and leishmaniasis: recent achievements and perspectives. *Drug Discovery Today* **15,** 1070–1078 (2010).

127. Rylands, L., Welsh, A., Maepa, K., Stringer, T., Taylor, D., Chibale, K. & Smith, G. S. Structure-activity relationship studies of antiplasmodial cyclometallated ruthenium(II), rhodium(III) and iridium(III) complexes of 2-phenylbenzimidazoles. *European Journal of Medicinal Chemistry* **161,** 11–21 (2019).

128. Stringer, T., Quintero, M. A. S., Wiesner, L., Smith, G. S. & Nordlander, E. Evaluation of PTA-derived ruthenium(II) and iridium(III) quinoline complexes against chloroquine-sensitive and resistant

strains of the Plasmodium falciparum malaria parasite. *Journal of Inorganic Biochemistry* **191,** 164–173 (2019).

129. Sánchez-Delgado, R. A., Navarro, M., Pérez, H. & Urbina, J. A. Toward a novel metal-based chemotherapy against tropical diseases. 2. Synthesis and antimalarial activity in vitro and in vivo of new ruthenium- and rhodium-chloroquine complexes. *J. Med. Chem.* **39,** 1095–1099 (1996).
130. Rajapakse, C. S. K., Martínez, A., Naoulou, B., Jarzecki, A. A., Suárez, L., Deregnaucourt, C., Sinou, V., Schrével, J., Musi, E., Ambrosini, G., Schwartz, G. K. & Sánchez-Delgado, R. A. Synthesis, characterization, and in vitro antimalarial and antitumor activity of new ruthenium(II) complexes of chloroquine. *Inorg Chem* **48,** 1122–1131 (2009).
131. Adams, M., Kock, C. de, Smith, P. J., Land, K. M., Liu, N., Hopper, M., Hsiao, A., Burgoyne, A. R., Stringer, T., Meyer, M., Wiesner, L., Chibale, K. & Smith, G. S. Improved antiparasitic activity by incorporation of organosilane entities into half-sandwich ruthenium(II) and rhodium(III) thiosemicarbazone complexes. *Dalton Trans.* **44,** 2456–2468 (2015).
132. Milheiro, S. A., Gonçalves, J., Lopes, R., Madureira, M., Lobo, L., Lopes, A., Nogueira, F., Fontinha, D., Prudêncio, M., Piedade, F., Pinto, S., Florindo, P. & Moreira, R. Half- Sandwich cyclopentadienylruthenium(II) Complexes: A New Antimalarial Chemotype. (2020). doi:10.26434/chemrxiv.12155178.v1
133. Schuck, D. C., Ferreira, S. B., Cruz, L. N., da Rocha, D. R., Moraes, M. S., Nakabashi, M., Rosenthal, P. J., Ferreira, V. F. & Garcia, C. R. Biological evaluation of hydroxynaphthoquinones as anti-malarials. *Malar J* **12,** 234 (2013).
134. López, M. L., Vommaro, R., Zalis, M., de Souza, W., Blair, S. & Segura, C. Induction of cell death on Plasmodium falciparum asexual blood stages by Solanum nudum steroids. *Parasitology International* **59,** 217–225 (2010).
135. Deponte, M. & Becker, K. Plasmodium falciparum – do killers commit suicide? *Trends in Parasitology* **20,** 165–169 (2004).
136. Engelbrecht, D., Durand, P. M. & Coetzer, T. L. On Programmed Cell Death in Plasmodium falciparum: Status Quo. *J Trop Med* **2012,** (2012).
137. Nepveu, F. & Turrini, F. Targeting the redox metabolism of Plasmodium falciparum. *Future Medicinal Chemistry* **5,** 1993–2006 (2013).

138. Macedo, T. S., Colina-Vegas, L., Paixão, M. D., Navarro, M., Barreto, B. C., Oliveira, P. C. M., Macambira, S. G., Machado, M., Prudêncio, M., D'alessandro, S., Basilico, N., Moreira, D. R. M., Batista, A. A. & Soares, M. B. P. Chloroquine-containing organoruthenium complexes are fast-acting multistage antimalarial agents. *Parasitology* **143,** 1543–1556 (2016).

139. Andersson, J., Li, M. & Lincoln, P. AT-Specific DNA Binding of Binuclear Ruthenium Complexes at the Border of Threading Intercalation. *Chemistry – A European Journal* **16,** 11037–11046 (2010).

140. Luo, Z., Yu, L., Yang, F., Zhao, Z., Yu, B., Lai, H., Wong, K.-H., Ngai, S.-M., Zheng, W. & Chen, T. Ruthenium polypyridyl complexes as inducer of ROS-mediated apoptosis in cancer cells by targeting thioredoxin reductase. *Metallomics* **6,** 1480–1490 (2014).

141. McCarty, S. E., Schellenberger, A., Goodwin, D. C., Fuanta, N. R., Tekwani, B. L. & Calderón, A. I. Plasmodium falciparum Thioredoxin Reductase (PfTrxR) and Its Role as a Target for New Antimalarial Discovery. *Molecules* **20,** 11459–11473 (2015).

142. P. Fricker, S. Cysteine proteases as targets for metal-based drugs. *Metallomics* **2,** 366–377 (2010).

143. Rhoads, D. M., Umbach, A. L., Subbaiah, C. C. & Siedow, J. N. Mitochondrial Reactive Oxygen Species. Contribution to Oxidative Stress and Interorganellar Signaling. *Plant Physiology* **141,** 357–366 (2006).

144. Ott, M., Gogvadze, V., Orrenius, S. & Zhivotovsky, B. Mitochondria, oxidative stress and cell death. *Apoptosis* **12,** 913–922 (2007).

145. Ott, M., Robertson, J. D., Gogvadze, V., Zhivotovsky, B. & Orrenius, S. Cytochrome c release from mitochondria proceeds by a two-step process. *PNAS* **99,** 1259–1263 (2002).

146. Meslin, B., Barnadas, C., Boni, V., Latour, C., De Monbrison, F., Kaiser, K. & Picot, S. Features of Apoptosis in Plasmodium falciparum Erythrocytic Stage through a Putative Role of PfMCA1 Metacaspase-Like Protein. *J Infect Dis* **195,** 1852–1859 (2007).

147. Sundriyal, S., Malmquist, N. A., Caron, J., Blundell, S., Liu, F., Chen, X., Srimongkolpithak, N., Jin, J., Charman, S. A., Scherf, A. & Fuchter, M. J. Development of Diaminoquinazoline Histone Lysine Methyltransferase Inhibitors as Potent Blood-Stage Antimalarial Compounds. *ChemMedChem* **9,** 2360–2373 (2014).

148. Ponnudurai, T., Leeuwenberg, A. D. & Meuwissen, J. H. Chloroquine sensitivity of isolates of Plasmodium falciparum adapted to in vitro culture. *Trop Geogr Med* **33,** 50–54 (1981).

149. Talman, A. M., Blagborough, A. M. & Sinden, R. E. A Plasmodium falciparum Strain Expressing GFP throughout the Parasite's Life-Cycle. *PLoS One* **5,** (2010).

APPENDICES AND ANNEXES

Appendix I

Private consent for voluntary blood donation to be used as an additive in *Plasmodium falciparum* cell cultures

DESDE 1902

SANITATEM QUAERENS IN·TROPICOS

INSTITUTO DE HIGIENE E MEDICINA TROPICAL

UNIVERSIDADE NOVA DE LISBOA

DOAÇÃO DE ERITROCITOS HUMANOS PARA SEREM USADOS COMO ADITIVO EM MEIO DE CULTURA *IN VITRO* DE *Plasmodium falciparum*

Por favor, leia com atenção a seguinte informação. Se achar que algo está incorreto ou que não está claro, não hesite em solicitar mais informações junto do investigador que lhe entregou este formulário. Se concordar com a proposta que lhe foi feita, queira assinar este documento.

Instituição Promotora| Instituto de Higiene e Medicina Tropical IHMT, Universidade Nova de Lisboa

Investigadores para contacto| Fátima Nogueira, Investigadora Auxiliar (fnogueira@ihmt.unl.pt; telefone +351 213652626; ext 361).

Parte dos trabalhos de investigação em malária que realizamos no nosso laboratório exige cultivar os parasitas (*Plasmodium falciparum*) *in vitro*. Um dos exemplos de aplicação das culturas *in vitro* de parasitas da malaria é a pesquisa de novos medicamentos, sendo o primeiro passo testar a atividade das moléculas *in vitro*, em cultura, de forma a selecionar aquelas mais eficazes contra o parasita, para depois prosseguir os estudos em animais e finalmente no homem. A realização de outros estudos mais abrangentes, como conhecer melhor a biologia do parasita também estão baseados em culturas *in vitro* de *Plasmodium falciparum*.

A cultura apenas é possível com a adição de eritrócitos humanos ao meio de cultura, não existindo substituto.

O objetivo desta dadiva é obter eritrócitos humanos para adicionar à cultura de parasitas.

O sangue que consentir doar para este fim será processado da seguinte forma:

1. o dador acompanhado do Investigador dirige-se ao laboratório do IHMT;

2. após ler e assinar este consentimento, um técnico de diagnóstico e terapêutica do laboratório efetua a colheita de 10 a 15 mL de sangue venoso;
3. o tubo de colheita apenas é rotulado com a data de colheita e o seu nome nunca aparece associado a este tubo;
4. o seu sangue é centrifugado e os glóbulos brancos (leucócitos), plasma e eritrócitos (ou glóbulos vermelhos) são separados por centrifugação;
5. o plasma e os glóbulos brancos são descartados e destruídos. O tubo com os seus glóbulos vermelhos (que se mantém rotulado apenas com a data da colheita e onde não aparece o seu nome), são conservados no frigorífico;
6. os seus glóbulos vermelhos são usados para adicionar às culturas de parasitas nos 15 dias seguintes à colheita.

A partir dos seus glóbulos vermelhos, não será extraído, armazenado ou analisado o seu material ou informação genética (os glóbulos vermelhos não têm núcleo). Também não serão armazenados, analisados ou usados, sucedâneos (derivados ou partes) do seu sangue para além dos glóbulos vermelhos e estes apenas são usados para cultivar parasitas da malaria (como referido) e em nenhuma circunstância serão usados com fins comerciais.

A sua participação é voluntária e não envolve qualquer tipo de compensação monetária. Não existem riscos ou desconfortos previsíveis para além daqueles associados à extração de 10 ou 15 mL de sangue venoso por profissional de saúde autorizado e em condições controladas do laboratório do IHMT.

Deste procedimento foi dado conhecimento ao Conselho de Ética do IHMT.

AGRADECEMOS A SUA COLABORAÇÃO

Assinatura do(a) Investigador(a)_____

Declaro ter lido e compreendido este documento, bem como as informações verbais que me foram fornecidas pela pessoa que acima assina. Desta forma, aceito doar sangue e a sua utilização para este fim, confiando nas garantias de confidencialidade e anonimato que me são dadas pelo investigador.

Nome:_____

Assinatura:_____

Data: …… /…… /……..

ESTE DOCUMENTO É COMPOSTO DE 1 PÁGINA E FEITO EM DUPLICADO:

UMA VIA PARA A INVESTIGADOR, OUTRA PARA O DOADOR.

Annex I

REAGENTS AND SOLUTIONS

RPMI complete medium:

a) 1l of autoclaved Milli-Q H_2O.
b) Add progressively 10.44g of RPMI (Gibco), 5.94g of HEPES (Sigma), 5g of Albumax (Gibco), and 0.1g of hypoxanthine (Sigma).
c) After the addition of all the solutes, homogenize the mixture in a stirrer for 30min.
d) In the end, pH is set to 7.4 with 2g of $NaHCO_3$ at 5% (Sigma).
e) Then, filter the RPMIc medium with a vacuum filter, PES 0.2µm, 500mL of capacity (VWR®, Pennsylvania), to a sterile bottle.
f) Finishing filtration, submit the bottle to a sterility test.
g) Keep the medium at 4°C.

Thawing solutions:

Three types of successive gradients of sodium chloride concentrations applied in the thawing of cryopreserved *P. falciparum* samples protocol (see III.1.1.):

a) 12% NaCl solution in sterile Milli-Q H_2O.
b) 1.6% NaCl solution in sterile Milli-Q H_2O.
c) Salt-dextrose solution: 0.2% dextrose with 0.9% NaCl in sterile Milli-Q H_2O.

Giemsa 20%:

a) For 100mL of Giemsa 20%: add 20mL of Giemsa's Azur eosin methylene blue solution (Sigma) to 80mL of buffered water.
    i. For the preparation of buffered water: add a tablet (Sigma) to 1l of Milli-Q H_2O.
b) The solution is homogenized and filtered with filter paper to a sterile bottle.
c) The final 20% working solution is conserved at 4°C.

Phosphate Buffer Saline (PBS):

a) Addition of 1 tablet of PBS (VWR) to 100mL of Milli-Q H_2O.
b) The solution is transferred to a bottle, sealed (and autoclaved for sterile PBS).
c) PBS solution is conserved at 4°C.

D-sorbitol 5%:

a) Dilute 50g of D-sorbitol in 1l of Milli-Q H_2O.
b) Homogenize the solution and autoclave it.
c) Keep the final concentration of D-sorbitol 5% at 4°C.

Flow cytometer sheath fluid:

a) Add 100ml of autoclaved Milli-Q H_2O to 50g of Sodium Azide, homogenize and conserve at 4°C.
b) Add 5mL of the previously prepared solution to 1l of autoclaved Milli-Q H_2O.

Fluorescent probes:

Mitotracker™ Deep Red FM

Mitotracker™ Deep Red FM (Invitrogen™) was acquired as a lyophilized product and prepared as recommended[108]. The reagent was dissolved in 100% DMSO to a final concentration of 919µM and stored as stock solutions in DMSO at 100µM and 5µM. Stock solutions were kept at -20°C, protected from the light. Treatment levels of DMSO were below 0.5%.

SYBR™ Green I

SYBR™ Green I (Invitrogen™) was acquired as a lyophilized product and prepared as recommended[80]. The reagent was dissolved in 100% DMSO to a final concentration of 20x, stored as stock solutions in PBS at 1x, and conserved at -20°C, protected from the light. Treatment levels of DMSO were below 0.5%.

Annex II

BIOLOGICAL MATERIAL

3D7 and 3D7HT-GFP Plasmodium falciparum strains

The 3D7 *P. falciparum* strain derives from the NF54 isolate after limited dilutions and defines itself by being chloroquine-sensitive[148]. On the other hand, the 3D7HT-GFP is the product of a 3D7 genetic recombinant constructed by the integration of GFP under control of the EF1 promoter into the *Pf47* gene. The 3D7HT-GFP strain is capable of constitutively expressing GFP throughout the parasite life cycle[149]. The 3D7 strain belongs to a cryopreserved collection of the UEI Malaria Laboratory (IHMT) and the 3D7HT-GFP (MRA-1029, MR4, ATCC® Manassas Virginia) was obtained through BEI Resources, NIAID, NIH, contributed by[149].

Uninfected RBC

In vitro culture of *P. falciparum* employs its intra-RBC stages. Therefore, it is mandatory for the preparation of fresh uRBC for new cycles of invasion of the parasites in culture. The UEI Malaria Laboratory (IHMT) uses venous whole blood samples from volunteer donors (preferably from the blood type 0 Rh +) to prepare its uRBCs, for research purposes. Written informed consent is signed by blood donors (Appendix I) agreeing in donating their blood for this investigation purpose and confirming that they did not have taken any antimalarial drug treatment or any other drug recently. The protocol for the preparation of uRBC is described below:

a) Collection of the volunteer donor venous blood to a 9mL K3 EDTA-tube S-Monovette® (STARSDET AG & Co. KG, Nümbrecht).
b) After a correct homogenization, the whole blood is transferred to a centrifuge tube and centrifuged at 2,000rpm for 5min.
c) Discard plasma and buffy coat, and the remaining RBCs are washed with PBS five times. To fully remove the buffy coat, horizontal movements must be done perpendicular to the surface of the erythrocytic mass. Wash steps centrifugations

also performed at 2,000rpm for 5min. During this procedure, attention should be taken to the macroscopic look of the supernatant to assess the need for more washes.

d) At the final wash step, instead of PBS, it is added RPMIc medium to the RBCs.
e) After the last centrifugation, the volume of the RMPIc medium must allow a 50% RBC solution.
f) Lastly, this solution goes to identified sterile bottles.
g) The 50% RBC solution in the RPMIc medium is conserved at 4°C for 15 days.

Annex III

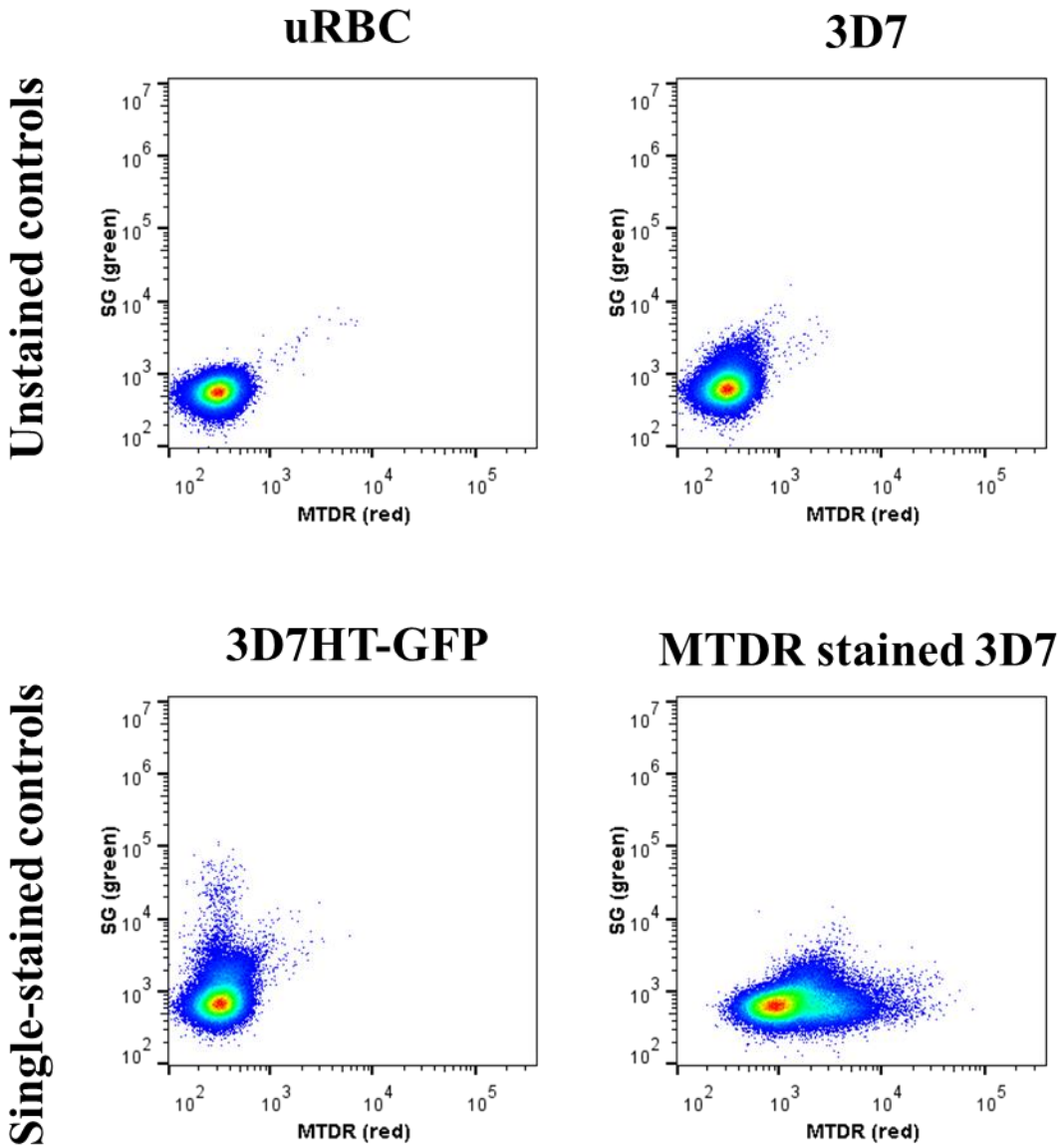

Figure A.I – Unstained and single-stained controls for green and red fluorescence in 3D7HT-GFP strains stained with MTDR. Green and red fluorescence flow cytometry plots of unstained uRBC and iRBC (3D7) samples, and single stained iRBC samples for GFP (3D7HT-GFP) and MTDR (250nM). uRBC, uninfected RBC, from a Gate II. iRBC, infected RBC, from a Gate III. GFP, green fluorescence protein. MTDR, Mitotracker™ Deep Red FM. Unstained and single-stained controls prove the unnecessity for compensation.

Annex IV

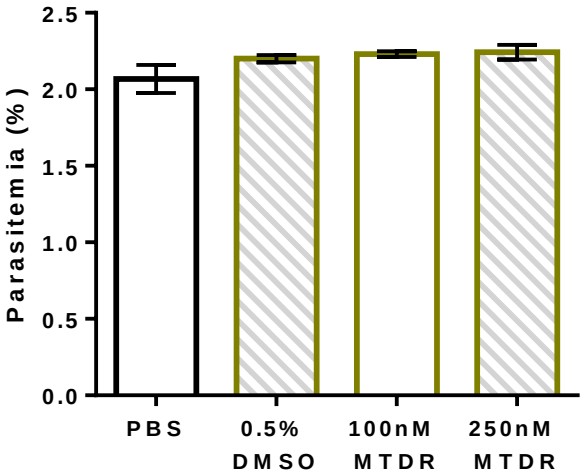

Figure A.II – Absence of interference of the DMSO concentration in Mitotracker™ Deep Red FM working staining solutions. Parasitemia retrieved by flow cytometry after incubation with PBS (negative control), 0.5% DMSO (DMSO concentration present in 250nM of MTDR), 100nM, and 250nM of MTDR (3D7, 0.5x SG, 100,000 recorded events). Parasitemia was calculated from the percentage of green fluorescence emitting events within the RBC population. The DMSO present in MTDR working staining concentration does not interfere in parasite viability, maintaining parasitemia percentage equal to the negative control (PBS).

Annex V

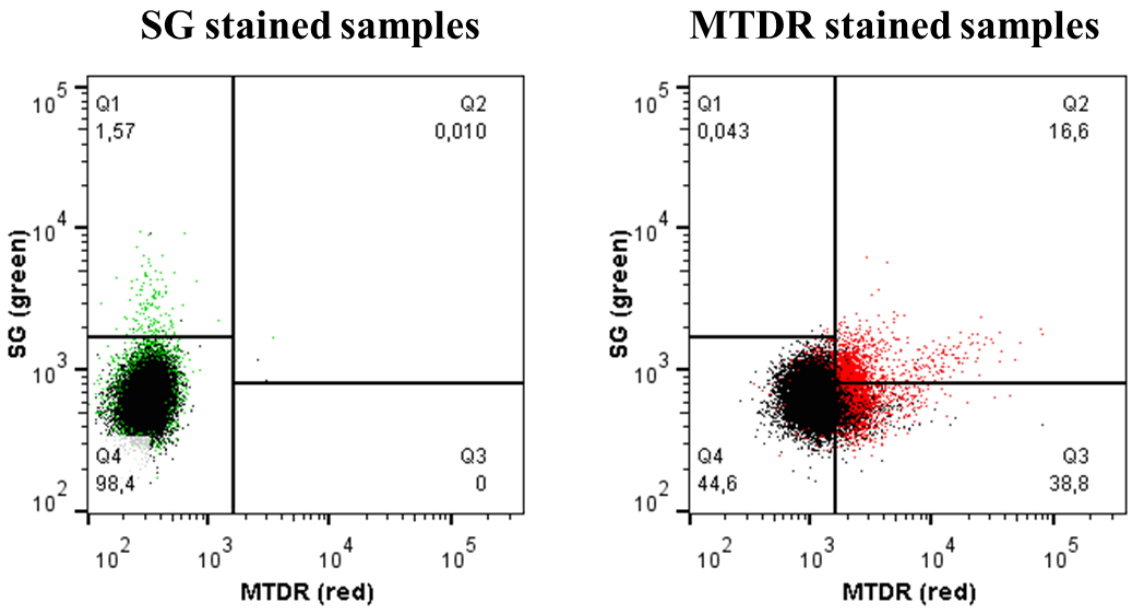

Figure A.III – Single-stained controls for green and red fluorescence in 3D7 strains stained with MTDR. Green and red fluorescence flow cytometry plots of single-stained uRBC (black) and iRBC (3D7, colored) samples, for SG (0.5x) and MTDR (250nM). Events retrieved from Gate II, within100,000 events recorded. uRBC, uninfected RBC. iRBC, infected RBC. SG, SYBR™ Green I. MTDR, Mitotracker™ Deep Red FM. Single-stained controls prove the unnecessity for compensation.

Annex VI

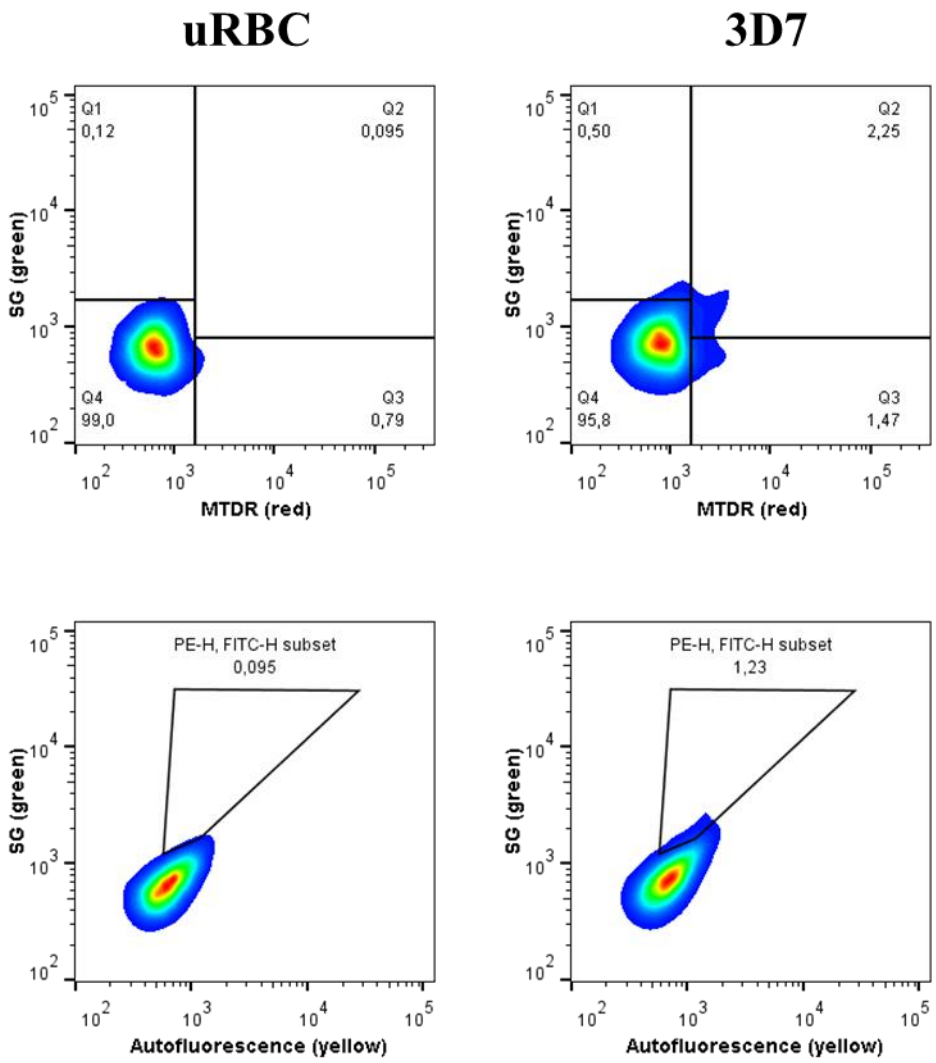

Figure A.IV – Resolution in the green/red and the green/yellow flow cytometry plots in the identification of the infected RBC population. 3D7 strains stained with 0.5x SG (Events retrieved from Gate II, within 100,000 events recorded). uRBC, uninfected RBC. SG, SYBR™ Green I. MTDR, Mitotracker™ Deep Red FM.

Annex VII

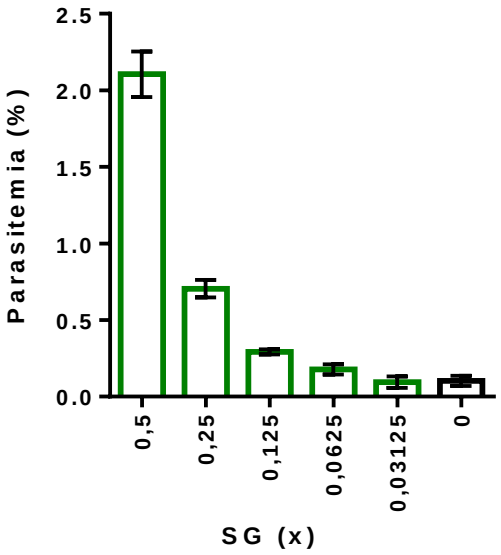

Figure A.V – SYBR™ Green I able to identify infected RBC at different concentrations. Parasitemia retrieved from SG stained 3D7 infected RBCs at 0.5, 0.25, 0.125, 0.0625, 0.03125, and 0x SG (10,000 events recorded). SG, SYBR™ Green I. Parasitemia was calculated from the percentage of green fluorescence emitting events within the RBC population.

Annex VIII

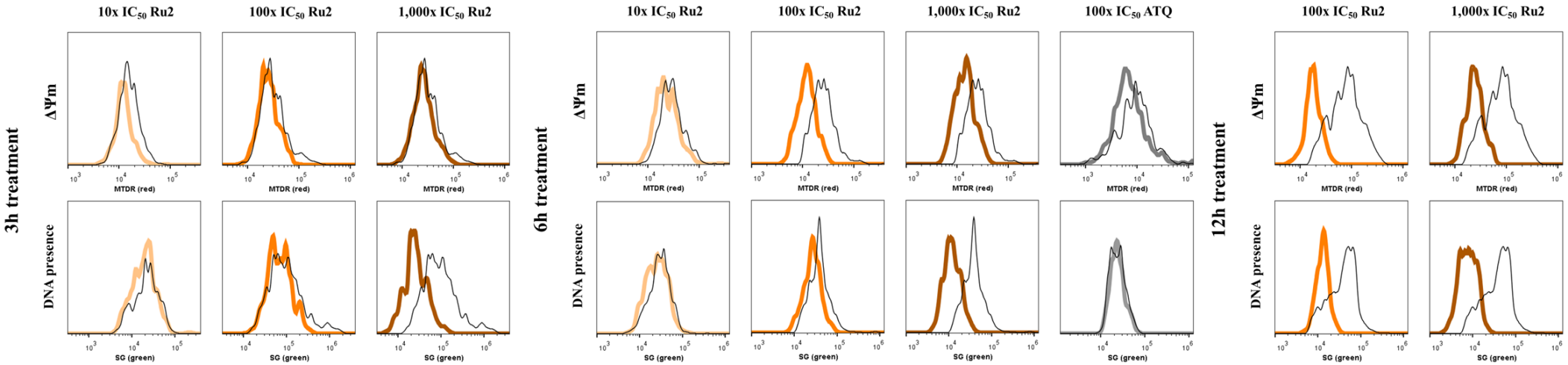

Figure A.VI – Parasite viability (ΔΨm and DNA presence) after Ru2 treatment. Green fluorescence emission (SG, DNA presence) and Red fluorescence emission (MTDR, ΔΨm) of 10x, 100x, and 1000x IC_{50} Ru2 treated parasites for 3h, 6h, and 12h, and 100x IC_{50} ATQ treated parasites for 6h (3D7, 250nM MTDR, 0.5x SG, events retrieved from Gate III, within 100,000 events recorded). ΔΨm, mitochondrial membrane potential. SG, SYBR™ Green I. MTDR, Mitotracker™ Deep Red FM. Ru2-treated parasites, thick (light/medium/dark) orange line. ATQ-treated parasites, thick gray line. RPMI-treated parasites, thin black line.

Annex IX

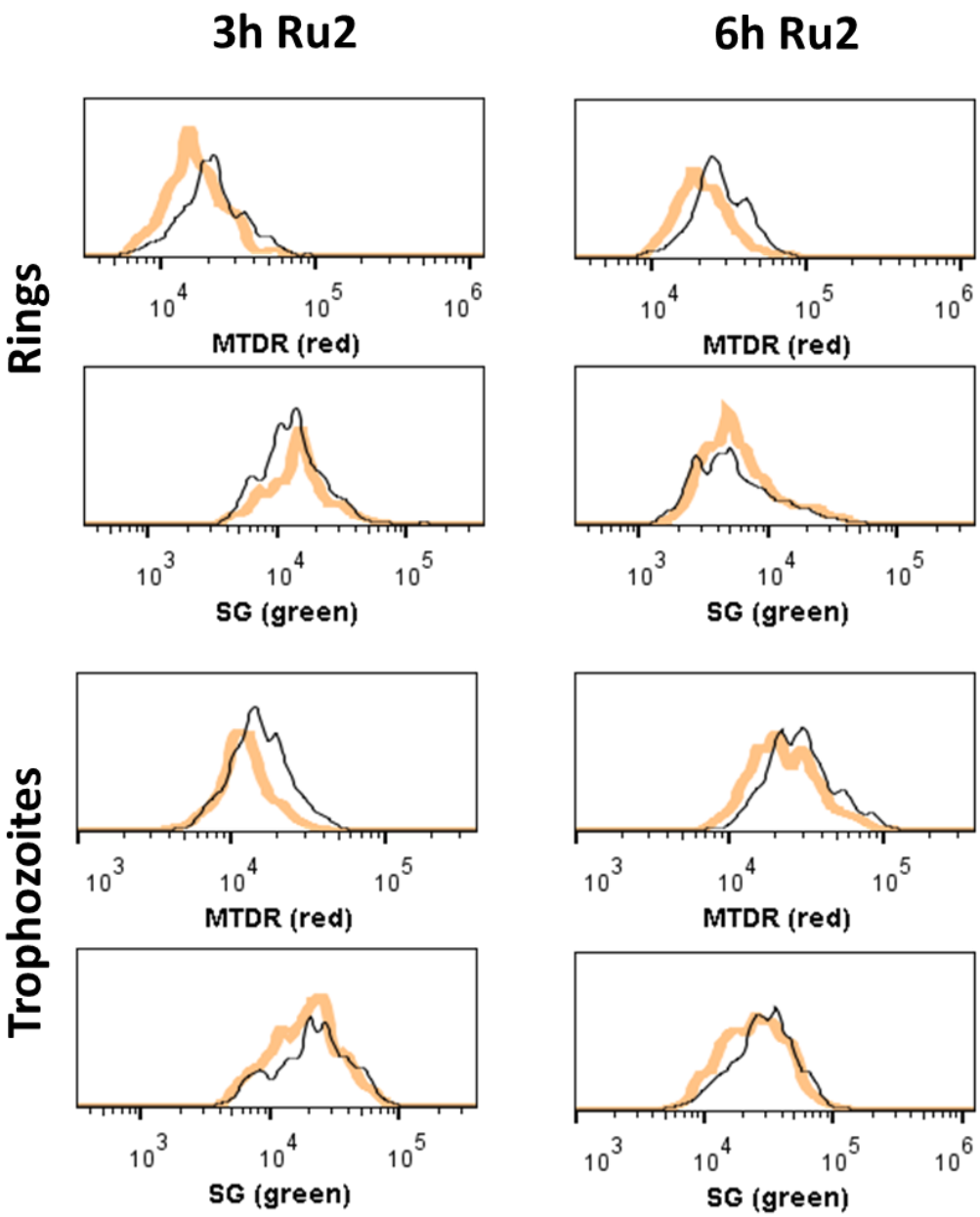

Figure A.VII – Stage-specific parasite viability (ΔΨm and DNA presence) after Ru2 treatment. Green fluorescence emission (SG, DNA presence) and Red fluorescence emission (MTDR, ΔΨm) of 10x IC50 Ru2-treated rings and trophozoites for 3h, and 6h (3D7, 250nM MTDR, 0.5x SG, events retrieved from Gate III, within 100,000 events recorded). ΔΨm, mitochondrial membrane potential. SG, SYBR™ Green I. MTDR, Mitotracker™ Deep Red FM. Ru2-treated parasites, thick orange line. RPMI-treated parasites, thin black line.

Annex X

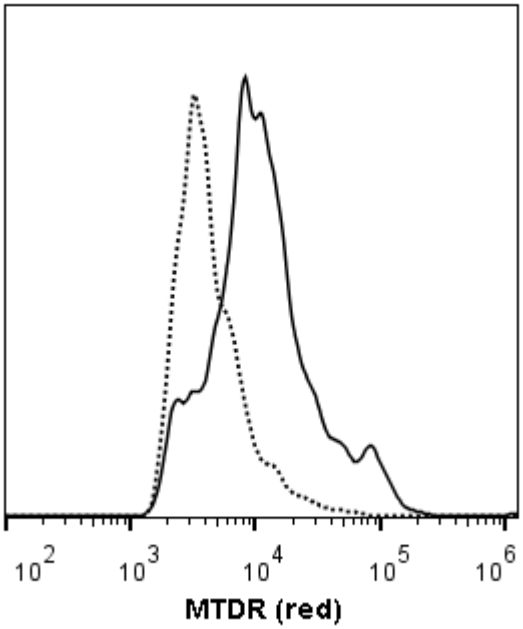

Figure A.VIII – MTDR fluorescence emission evolution within 6h of trophozoite development. MTDR fluorescence histogram of 20-24hpi trophozoite-stage parasite at t=0h (dotted line) and after 6h (solid line) of growth in RPMIc medium (3D7, 250nM MTDR, 0.5x SG; events retrieved from Gate III, within 100,000 events recorded). MTDR, Mitotracker™ Deep Red FM